ATRIAL REVERSE REMODELING IN HYPERTENSIVE SUBSTRATE

Shivshankar Thanigaimani. MS.

Centre for Heart Rhythm Disorders
Royal Adelaide Hospital

&

School of Medicine
The University of Adelaide

A thesis submitted to The University of Adelaide

in fulfillment of the requirements of the degree of

Doctor of Philosophy (Medicine & Surgery)

July 2014

ABSTRACT

Hypertension is a major independent risk factor for atrial fibrillation (AF). Despite various clinical and experimental studies on atrial remodeling in hypertensive substrates, pre-clinical experimental studies involving the prevention and treatment of electrical and structural changes secondary to hypertension remain limited. Many antihypertensive drugs have been shown to reduce AF recurrence in patients with hypertension. Additionally, recent work suggests that anti-fibrotic drug, Tranilast, has beneficial effects in preventing AF. This thesis focuses on the electrophysiological and structural effects with anti-fibrotic and anti-hypertensive therapies in hypertensive large animal model.

Chapter 1 details the theoretical mechanisms involved in the initiation and maintenance of AF and various conditions that contributes to abnormal atrial substrate formation. Importantly, studies involving reverse remodeling of various substrates and possible prevention of pathological atrial remodeling are also discussed.

Chapter 2 details the histological, anatomical and molecular changes in the hypertensive atria. We demonstrated that hypertension resulted in structural remodeling through increased myocyte hypertrophy, endomysial and interstitial fibrosis and inflammation along with increased septal thickness, which was contributed by increased CTGF and TGF-$ß_1$ and reduced connexin43 expressions. Further, we showed that anti-hypertensive treatments could reverse all these pathological changes. This highlights the important

role of aggressive blood pressure lowering therapy in patients with AF and hypertension.

Chapter 3 illustrates the reverse electrical remodeling of hypertensive substrate using anti-hypertensive therapies. Significant improvement in conduction abnormalities and reduction in susceptibility to AF were seen with anti-hypertensive treatments. This further affirms the importance of blood pressure control in patients with hypertension and AF.

Chapter 4 details the histological, anatomical and molecular changes leading to the prevention of remodeling process in hypertensive atria. Tranilast (anti-fibrotic) treatment resulted in prevention of atrial structural remodeling by preventing myocyte hypertrophy, endomysial and interstitial fibrosis, inflammation, septal thickness and altered CTGF, TGF-$ß_1$ and connexin43 expression levels.

Chapter 5 illustrates the prevention of atrial electrical remodeling in hypertensive atria with tranilast treatment during the development of high blood pressure. The results showed a reduced susceptibility to AF by preventing conduction slowing and heterogeneity seen with hypertension. Importantly, the beneficial effects seen in chapter 4 & 5 with tranilast treatment were independent of blood pressure levels.

Chapter 6 examines the fibrillatory electrograms in hypertensive atria. Complex fractionated atrial electrograms (CFAE) and dominant frequency (DF) are thought to

represent substrate sites in AF. A novel index of spatio-temporal stability (STS) was used in this study. We found that STS of CFAE was able to better predict AF termination than absolute mean fractionation values.

DECLARATION

I certify that this work contains no material which has been accepted for the award of any other degree or diploma in my name, in any university or other tertiary institution and, to the best of my knowledge and belief, contains no material previously published or written by another person, except where due reference has been made in the text. In addition, I certify that no part of this work will, in the future, be used in a submission in my name, for any other degree or diploma in any university or other tertiary institution without the prior approval of the University of Adelaide and where applicable, any partner institution responsible for the joint-award of this degree.

I give consent to this copy of my thesis when deposited in the University Library, being made available for loan and photocopying, subject to the provisions of the Copyright Act 1968. The author acknowledges that copyright of published works contained within this thesis resides with the copyright holder(s) of those works.

I also give permission for the digital version of my thesis to be made available on the web, via the University's digital research repository, the Library Search and also through web search engines, unless permission has been granted by the University to restrict access for a period of time.

ACKNOWLEDGEMENT

I would like to thank Professor Prashanthan Sanders, my primary supervisor for his guidance and support during my doctoral candidature. I also would like to thank Dr. Dennis Lau, my co-supervisor for his immense support. I am also thankful to my co-supervisors Dr. Anthony G. Brooks and Dr. Pawel Kuklik for their support and supervision over the duration of my candidature in particular with understanding statistical methods and analysis. Both my supervisor and co-supervisors helped me develop my research and scientific writing skills. I learned extensively from their meticulous supervision. I am grateful to all my mentors for helping me develop competitive research skills. I am also grateful for the scholarship support from the University of Adelaide and Peter Hetzel Electrophysiological Scholarship during my doctoral degree.

I appreciate the research environment provided by Centre for Heart Rhythm disorders members. I would like to also acknowledge Dr. Rajiv Mahajan, Dr. Anand Ganesan and Dr. Kurt Roberts Thomson for their constructive inputs to this work. I am also thankful to Dr. Srinivasan Govindarajan for his assistance with MRI scans and analysis.

I am very grateful to Dr. Mohan Rao and Dr. Timothy Kuchel who taught me the surgical procedures involved with this study. I am also thankful to the members of LARIF: Dr. Susan Porter, Ms. Loren Mathews, Ms. Carol Hewitt, Ms. Samantha

Herzog and Mr. Maurice Malycha. This study would have been impossible without their significant contribution.

Finally, I would like to thank my father: Thanigaimani Balaraman; mother: Lourdes Juliet Thanigaimani and my brother: Prabhu Shankar for their immense support during all these years. I am very grateful to my friends Raghuveeran Anbalagan, Vimal Ganesh and Walter Clint Fernando for their encouragement and support during the exciting times of my candidature. Last, but not least, I was blessed with the understanding and immense support from my fiancée, Dr. Saranya Hariharan during my doctoral studies.

PUBLICATIONS AND COMMUNICATIONS TO LEARNED SOCIETIES

Chapter 2 & 3:

Conference proceedings: Shivshankar Thanigaimani, Dennis H. Lau, Anthony G. Brooks, Pawel Kuklik, Rajiv Mahajan, Timothy Kuchel and Prashanthan Sanders. Reverse remodeling of the atrial substrate in hypertensive ovine model: Implications of conventional anti-hypertensive drugs. Cardiac society of Australia and New Zealand, Gold coast, Australia. Heart Lung and Circulation. 2013. Vol 22; Page – S99..

Conference proceedings: Shivshankar Thanigaimani, Dennis H. Lau, Anthony G. Brooks, Pawel Kuklik, Rajiv Mahajan, Timothy Kuchel and Prashanthan Sanders. Reverse remodeling of the atrial substrate in a hypertensive ovine model: A chronic pharmacological intervention study. 34th Annual scientific sessions of the Heart rhythm society, Denver, CO, USA. Heart Rhythm. 2013. (May supplement) Page – 236.

Chapter 4 & 5:

Conference proceedings: Shivshankar Thanigaimani, Anthony G. Brooks, Rajiv Mahajan, Pawel Kuklik, Darragh Twomey, Rajeev Pathak, Darren Kelly, Prashanthan Sanders, Dennis H. Lau. Tranilast has similar efficacy as anti-hypertensive drugs in prevention of atrial remodeling during hypertension. 35th Annual scientific sessions of

the Heart rhythm society, California, San Francisco, USA. Heart Rhythm. 2014 (May supplement)..

Chapter 6:

Conference proceedings: Shivshankar Thanigaimani, Dennis H. Lau, Anthony G. Brooks, Pawel Kuklik, Anand Ganesan and Prashanthan Sanders. Spatio temporal differences in bipolar electrogram characteristics: Shannon entropy and frequency domain as predictive parameters of AF termination. Cardiac society of Australia and New Zealand. Gold coast, Australia. Hear Lung and Circulation. 2013. Vol 22; Page – S100.

Conference proceedings: Shivshankar Thanigaimani, Dennis H. Lau, Pawel Kuklik, Anthony G. Brooks, Anand Ganesan and Prashanthan Sanders. Differences in bipolar electrogram characteristics during AF initiation and pre-termination: Comparing Shannon entropy with time and frequency domain measures. 34th Annual scientific sessions of the Heart rhythm society, Denver, CO, USA. Heart Rhythm. 2013. (May supplement) Page – 254.

Conference proceedings: Shivshankar Thanigaimani, Pawel Kuklik, Anthony Brooks, Anand Ganesan, Rajiv Mahajan, Julia Kim, Prashanthan Sanders, and Dennis H. Lau. Dominant frequency rather than electrogram fractionation plays a role in atrial

fibrillation initiation in hypertensive atria. Faculty of Health sciences Postgraduate research conference (2012). University of Adelaide.

Conference proceedings: Shivshankar Thanigaimani, Pawel Kuklik, Anthony Brooks, Anand Ganesan, Rajiv Mahajan, Julia Kim, Prashanthan Sanders, and Dennis H. Lau, . Time and frequency domain analysis of atrial electrograms during the initiation and pre-termination of atrial fibrillation in hypertensive sheep with remodeled atria. 2012. The 5th Asia pacific heart rhythm society scientific sessions in conjunction with 8th Asia pacific atrial fibrillation symposium. Journal of Arrhythmia. 2012. Vol 28; Supplement.10; Page 704.

Conference proceedings: Shivshankar Thanigaimani, Dennis H. Lau, Pawel Kuklik, Anand Ganesan, Julia Kim, Rajiv Mahajan, Anthony Brooks, and Prashanthan Sanders. Spatio-temporal profile of dominant frequency and complex fractionated atrial electrograms during atrial fibrillation in sheep with induced hypertension. 33rd Annual scientific sessions of the Heart rhythm society, Massachusetts, USA. Heart Rhythm 2012. Vol 9, No 5 (May supplement) Page – S333.

1 ATRIAL REMODELING: IMPLICATIONS FOR ATRIAL FIBRILLATION

1.1 Introduction

Atrial fibrillation (AF) is an abnormal rhythmicity of the heart that is most commonly seen in clinical practice. AF occurs mostly in older population increasing from 0.5% to 9% between less than 55 years and >80 years of age respectively [1]. In addition, over the next 50 years, a 2.5 fold increase in the number of AF patients is predicted due to aging population in the US [1]. Until recently, various risk factors have been described to perpetuate AF; such as aging [1], congestive heart failure [2], myocardial infarction [3], hypertension [4], mitral valve stenosis [5], mitral regurgitation [6], obesity [7] and sleep apnea [8]. The association of the above substrates with atrial remodeling has been well established in both animal models and/or humans.

Atrial fibrillation is associated with a 5-8 fold increased risk of stroke and a reduced survival rates in these subset of patients [9, 10]. This also indicates that nearly 15% of all strokes are attributable to AF [11]. Independent of any stroke history, AF has also been shown to be associated with dementia [12]. In addition, frequent clinical symptoms like palpitations, fatigue, dyspnea, light headedness and chest discomfort are also shown to significantly increase the morbidity rates in AF patients [13, 14]. In contrast to the belief that AF increases the mortality rates in patients with co-

existing cardiovascular conditions, recent epidemiological data suggest that AF can independently increase the mortality rates by 1.5 to 1.9 fold [15]. A recent review suggests an upward trend in AF related hospitalizations from 1996 to 2006 with AF prevalence likely to double by year 2050. [16]. This burden will account for at least 1% of healthcare expenditure across multiple countries.

Data from the Framingham heart study has shown various independent risk factors for AF development during a long term follow up. Major risk factors included aging, congestive heart failure, myocardial infarction, valvular heart disease, diabetes and hypertension [5, 17]. In addition to the established risk factors, other known conditions such as hypertrophic cardiomyopathy, sick sinus syndrome, atrial septal defect and end stage renal failure have also been shown to be associated with AF [18-20]. Further, myocarditis, pericardial diseases, thyrotoxicosis, pulmonary pathology and severe infection are recognized as precipitators of AF [21-23]. More recently, obesity, sleep apnea, smoking and alcohol consumption have also been shown as new risk factors for AF development [8, 24-27]. With increased recognition of the underlying mechanisms and substrates for AF, a recent white paper has suggested that the term ‘lone AF’ should be avoided [28].

This review will discuss: 1) Basic theoretical mechanisms of AF; 2) Atrial remodeling in substrates predisposed to AF; 3) Reverse remodeling and possible prevention of atrial remodeling in various AF substrates.

1.2 Mechanisms of AF

1.2.1 Early glimpses of AF:

The first ever accounted atrial fibrillation was around 2000BC in the Yellow emperor's classic of Internal Medicine [14]. It was after several thousands of years that the pathology appeared in the scientific literature in 1700s when William Withering treated a patient who had "weak irregular pulse" with *Digitalis purpurea* and observed the regularity in rhythm which he described as "fuller and more regular pulse" [14]. Though the irregular rate and rhythm was observed visually, there were no actual measurements of electrical activity to demonstrate atrial fibrillation until 1874 when Edme Felix Alfred Vulpian observed irregular atrial electrical activity in dog hearts and termed it as "*fremissement fibrillaire*" [29]. During nineteenth century, Jean-Baptiste de Senac observed dilated, irregularly fibrillating atria in mitral stenosis patients [21]. Nothnagel performed graphical techniques to demonstrate the association of fibrillating atrium and pulse pattern and termed it as "Delirium cordis" [30]. He stated, "In this form of arrhythmia, the heartbeats follow each other in complete irregularity. At the same time, the height and tension of the individual pulse waves are continuously changing"[30]. In 1899, Cushny made a vital observation linking 'fibrillating atrium' and 'pulse pattern' together before which it was considered as separate entities. He compared the pulse curves in delirium cordis to that in dogs with induced "auricular" fibrillation and demonstrated similarity in the pulse curve patterns [22]. In 1904, Sir James McKenzie

demonstrated the correlation between the loss of waves in jugular venous pulse to the loss of atrial contraction observed in delirium cordis which was concomitant with Cushny's work [23].

The most imperative finding that made the field of atrial fibrillation as extensive as it is today is the invention of string galvanometer by Willem Einthoven in early 20th century [24]. In 1902, he published the first recorded electrogram in *Festschrift* book [25]. Following this, in 1909, Sir Thomas Lewis was the first to describe AF on an ECG pattern as fine diastolic oscillations associated with varying QRS complex intervals [31].

1.2.2 Initial AF theories:

After the first ECG based description of AF was published, three major theories were put forward using a number of experimental models to explain the mechanism of AF.

1.2.2.1 Multiple Heterotopous centers theory:

Engleman demonstrated that muscle fibers were able to generate pulsatile activity individually when they were stimulated either electrically or chemically (Potassium infusion) [32]. Based on these observations, Winterberg proposed that since muscle fibres are sprinted transmurally through the myocardium making connections with each myocytes, there is a possibility that any of these fibres could get stimulated

electrically or chemically and behave as a source of focal activity. And also, since many fibres could possibly be stimulated at a single point of time, multiple focal activity can co-exist to induce a fibrillating atrium [32].

1.2.2.2 Single tachysystolic theory:

Winterberg observed rapid atrial contractile activity under vagal influence with which he claimed that a single focus in the atrium discharging at a rapid rate of 3000-3500 per minute is responsible for this kind of arrhythmia [33]. This hypothesis was later replaced by *Circus movement theory* proposed by Lewis, in which he describes atrial fibrillation as a single circuit rapid re-entrant wave in an atrial tissue that lacks the ability to execute a homogenous excitation thereby resulting in fibrillatory conduction [34].

1.2.2.3 Multi circuit re-entry theory:

Mines and Garrey combined the concepts of '*Multiple Heterotopous centres theory'* and '*Circus movement theory'* to propose that both multiple focus and circuit re-entry were present simultaneously in a fibrillating atrium [35]. For the first time, this theory explained the concept of re-entry by claiming that size of the circuit was fixed and the re-entry was due to shortening of the refractory period in the myocytes. Therefore, myocytes tends to depolarize again even before the previous action potential had returned to its resting state. This will lead to multiple discharges from

the atrial tissue that can maintain the fibrillating atrium [35]. With this concept, Mines put forward the ingredients of re-entrant circuit as follows; Conduction slowing, shortened refractory period and the length of muscle fibre being greater than the excitation wave.

Following this, Garrey challenged the concept of '*Multiple Heterotopous centers theory'* and '*Single tachysystolic theory'* individually. He cut the fibrillating atrium in to small pieces and observed that the cut pieces continued to fibrillate. Therefore, he argued against the single focus theory. As the fibrillating pieces did not last for longer periods compared to the whole fibrillating atrium, he consequently argued against the multiple focal activity as well [36].

1.2.2.4 Multiple wavelet theory:

Moe *et al* proposed the 'Multiple wavelet theory' based on the concepts of 'Multiple circuit re-entry theory' [37]. According to this theory, fibrillating atrium was maintained as a result of many independent wavelets circulating around the refractory tissue. Contrary to its basic concept, in this theory, the circuits were not fixed in space and did not have to be essentially a complete circuit. Instead, there were open circuits and the waves propagated through the atrial tissue until they encountered a refractory tissue to quench themselves or shaped in to new daughter wavelets if the propagated wave encountered an inexcitable tissue. Thus, maintenance of atrial fibrillation depends on the maximum number of wavelets in the

atrial tissue present at any one point of time. This was experimentally demonstrated by Allessie *et al* where they employed a canine model to map acetylcholine induced AF [38]. They estimated that around 4 to 6 wavelets were required to maintain a fibrillating atrium and the termination of AF was heralded by decrease in the number of wavelets. In 1977, Allessie *et al* studied the centre of the re-entrant circuit using multiple intracellular and extracellular electrodes and observed that the circuit centre was not an inexcitable tissue due to anatomical obstacle rather it is an excitable tissue that remained refractory due to the centripetal force accelerated by the circular paths [39]. Another contrasting feature of this theory based on the circus movement theory is that the circuit length is being determined by the electrophysiological properties of the tissue (conduction velocity, refractory period and sensitivity to the stimulus) rather than the anatomical structures [39]. Based on this concept, multiple re-entry circuits were possible to co-exist in the absence of an anatomical obstacle which led to the '*leading circle theory*' [39, 40]. Multiple wavelet theory became robust after the works of Cox *et al*, where he performed mapping of atrial fibrillation during an open chest surgery and made surgical lines of block (MAZE procedure) which terminated chronic atrial fibrillation due to inability of multiple wavelets to sustain [41].

1.2.2.5 Localized focal triggered activity:

In 1947, Scherf demonstrated that a single focus is capable of initiating atrial tachycardia by application of aconitine in atrial appendage which he was able to

isolate by clamping the appendage. He also injected aconitine into sinus node and was able to induce atrial tachycardia and further terminate or re-initiate it by cooling or warming the locus [42]. Since, in this case, arrhythmia was initiated and maintained by a single focus, *circus movement theory* was contradicted. In 1972, thoracic veins were demonstrated to initiate AF [43]. A landmark finding was by Haissaguerre *et al* when they described the initiation of ectopic beats from pulmonary veins [11]. Myocardial cells from the pulmonary vein sleeves exhibited abnormal automaticity and triggered activity following rapid atrial pacing [44]. Though the presence of specialized conduction tissues in the myocardial sleeves of pulmonary vein could possibly be the initiating source of focal ectopy, the mechanism is not yet fully known. To date, pulmonary vein ablation has been the cornerstone treatment method for atrial fibrillation. Following this discovery, several loci such as superior vena cava, coronary sinus, ligament of Marshall, crista terminalis, left atrial posterior wall, septal and valvular regions have been demonstrated to act as focal initiators of AF [45-50].

1.2.2.6 Mother wave hypothesis:

Ortiz *et al* mapped the conversion of atrial flutter into atrial fibrillation where he noted that line of functional block and areas of slow conduction in re-entrant circuit were the determinant factors for conversion of one rhythm to the other [51]. If a propagated re-entrant wave encounters a long line of functional block, it goes around the line of block and together with an area of slow conduction; it forms a stable

circuit to develop in to an atrial flutter. If the encountered line of functional block is not long enough, the re-entrant circuit takes only a short time to circulate around the block, thus making the circuit shorter and hence unstable. These shortened circuits if encountered with variably exciting tissue would aggravate the instability of the waves which will degrade into AF. In addition, these shortened circuits could get stabilized again by passing through a refractory tissue and slow area of conduction leading to sustenance of AF [51]. A single mother wave was proposed to explain this phenomenon which warrants further investigations under clinical conditions.

1.2.2.7 Rotors and focal triggers

Multiple theories exist and yet it is not clear if AF mechanism is different in different substrates. Recently, Narayan *et al* proposed that localized electrical rotors and focal sources are vital in sustaining AF [52]. They further demonstrated that ablation of focal impulse and rotor modulation could improve the outcomes through CONFIRM trial. In spite of a number of plausible mechanisms proposed through various studies, a clear understanding of AF mechanism is yet to be determined.

1.3 Atrial remodeling due to AF: Mechanisms by which AF perpetuates itself

Though AF can be initiated by the underlying cardiovascular conditions, its level of detrimental effects significantly depend on the duration of episode even in the

absence of any cardiovascular conditions. According to epidemiological data, 25% of paroxysmal AF progress to chronic condition over a period of 8 years follow up [53]. Investigators thought that existence of AF related remodeling can in turn support the persistent of arrhythmia. This is based on the concept of 'AF begets AF' as elegantly shown by Wijiffels *et al* using chronically instrumented goat model of tachypacing induced AF [54].

1.3.1 Electrical remodeling

1.3.1.1 Atrial refractory period

Wijiffels *et al* showed that the susceptibility to AF increased with longer maintenance of atrial pacing in a goat model [54]. In addition, atrial effective refractory periods were found to be abbreviated with maladaptation to pacing cycle length [54]. This concept was again accomplished in a canine model by Morillo *et al* [55]. Following this, various researchers confirmed these findings experimentally in both humans and animal models [56-65]. These findings were first performed in humans by Attuel *et al* and observed loss of rate adaptation during atrial arrhythmias [66]. Misier *et al* showed that loss of adaptation occurs in lone atrial fibrillation as well [67]. Following this, Kamalvand *et al* showed that ERP heterogeneity and its dispersion across the atrial myocytes could provide as a substrate for AF [68]. Goette *et al* & Daoud *et al* noted an abbreviated ERP with shorter durations of rapid atrial

pacing which demonstrates that even shorter episodes of atrial arrhythmia was enough to compose changes to electrophysiology of the myocytes.

1.3.1.2 Atrial conduction

In the goat model of rapid atrial pacing, Wijiffels *et al* noticed fibrillatory conduction with an associated changes in ERP whilst the chronic condition required longer exposure of rapid atrial pacing [54]. However, they did not distinguish a change in conduction velocity across Buchmann's bundle in the first 24 hours. On the other hand, Fareh *et al* demonstrated an increase in conduction slowing and/or block and shorter ERP in AF sites with a combined mapping of AF induction and ERP in a canine model of rapid atrial pacing [59]. In the activation patterns, they noticed conduction block which was thought to be due to ERP heterogeneity paving the way for re-entry. Stabilization of the pathological ERP was followed by conduction slowing. Given the invasiveness of measuring conduction velocity; investigators usually apply P-wave duration and electrogram fractionation as surrogates. Kumagai *et al* noticed prolonged P-wave duration and fractionated electrical activity within the right atrium in cardioverted patients [64]. Morton *et al* showed that tachyarrhythmia lead to initial changes of ERP followed by gradual changes in conduction velocity in an ovine model [62].

1.3.1.3 Sinus node recovery time

Sinus node recovery time has been shown to prolong during atrial fibrillation. Several investigators have demonstrated significant prolongation of recovery time [56, 64, 65, 69-71]. This was also observed during short duration of atrial pacing in humans [72]. This increased duration required by the sinus node to repolarize leads to dispersion in the ERP and could initiate ectopic beats [73]. Nonetheless, the mechanism by which sinus node recovery time contributes to arrhythmia maintenance is not clearly understood.

1.3.2 Structural remodeling

Atrial dilatation is one of the common structural abnormalities observed in AF patients. Certainly, it can be a cause or consequence of atrial fibrillation. A prospective study by Sanfilipo *et al* studied the atrial volumes in lone AF patients in comparison to normal controls and demonstrated that dilatation is a consequence of arrhythmia rather than being a cause [74]. Chen *et al* studied the electrophysiology of normal and dilated atrium in AF patients to show the association of ERP dispersion and prolonged conduction time with atrial dilatation [75]. Molecular aspects of atrial dilatation were studied and a number of factors characteristic to structural abnormality were further observed. They include disorganization of Z band material due to the depletion of sarcomeres which was replaced with

accumulation of glycogen, disorganization of sarcoplasmic reticulum, hypertrophy, myolysis and dispersion of nuclear chromatin [76-80].

In addition, accumulation of fibrous tissue in the extracellular space and abnormalities in the coupling of gap junction proteins have been observed with structural remodeling in neonatal rat cultured cardiomyocytes [81]. Increased fibrous tissue was shown to be associated with a corresponding increase in Angiotensin II activity that acts downstream to the formation of fibrous tissue [81]. Despite a number of gap junction proteins being recently discovered, connexin 40 and 43 are the predominant gap junctions that are involved in the conduction homogeneity of the atrial myocytes through electrical coupling. Connexin 40 and 43 undergo heterodimeric coupling to conduct the electrical impulse of the propagating wavefront. Abnormal coupling or uncoupling of connexin 40 and 43 would lead to conduction heterogeneity which would provide as a substrate for arrhythmia development. In addition, connexin40 deficiency has been demonstrated to be associated with atrial conduction disturbances in a mice model and therefore could perpetuate arrhythmia [82]. Conduction heterogeneity has been suggested to be due to altered connexin distribution in a goat model of pacing induced persistent AF [83]. In humans, reduced connexin43 expression, heterogeneous distribution of connexin40 along with augmented fibrosis has been shown to be associated with structural remodeling of the atria in AF patients, and thus aid in initiation and/or self perpetuation of reentry and AF [77].

1.3.3 Ion channel remodeling

Electrophysiological properties of myocytes are largely dependent on ion channel function that can affect action potential duration. Therefore, the above discussed electrical and structural remodelling of the atrium could possibly be due to abnormalities in these ion channels. Higher susceptibility of arrhythmias in atria as compared to ventricles could be due to their differential ion channel expressions as evident with the shape of their respective action potential curves. In addition, atrial specific ion channels are being targeted to potentially cardiovert AF patients [84]. Further, studies on ion channels tend to investigate expression levels rather than its functional activity. Changes in the expression levels could not be exclusively speculated to be accountable for remodelling since the expression levels does not directly implicate the activity of a protein. For example, mModifications like single nucleotide polymorphisms (SNP) and post-translational modifications could significantly affect the ratio of expression levels to the functional activity of a protein.

To date, patch clamp studies and gene expression studies have given us a fair idea of the involvement of ion channels in the formation of an action potential. Some of the important ion channels and their role in action potential duration (APD) are tabulated below;

Reference	Ion channel	Role in APD	Changes during AF

[85]	Depolarizing sodium current (I_{Na})	Upstroke of action potential	↔
[85-88]	L-type calcium current (ICa_L)	Plateau phase	↓
[85, 86, 89, 90]	Transient outward potassium current (Ito)	Repolarization	↓
[89]	Sustained outward potassium current (IK_{sus})	Repolarization	↓
[91]	Ultra rapid, rapid and slow delayed rectifier (IK_{ur}, IK_r, IK_s)	Repolarization	↓
[85, 86, 92]	Inward rectifying potassium current (IK_1)	Maintenance of action potential plateau	↑
[85, 92, 93]	Acetylcholine activated inward rectifying potassium current	Maintenance of action potential plateau	↑↓

Alterations in sodium, calcium and potassium channels are considered to be largely responsible for the electrophysiological changes in myocytes as reflected by rate adaptation during atrial remodeling. Some of the major calcium dependent factors that interact with calcium channels during remodeling are Calcium/Calmodulin kinase II (CaMKII), calcineurin and ryanodine receptors (RyR). CaMKII has been shown to induce hypertrophy in cardiomyocytes through the activation of myocyte enhancer factor 2 (MEF2) *in vivo* [94]. Calcineurin is a calmodulin dependent phosphatase that aids in cardiac hypertrophy through a different transcription factor, NFAT (Nuclear Factor Activated T cell) [95]. Despite the fact that CaMKII and calcineurin have a common precursor (RyR), it is suggested that both proteins act in a separate signaling pathway since calcineurin is less efficient in activating MEF2

which is actively initiated by CaMKII [94]. Further, enhanced CaMKII activity leading to increased RyR2-dependent Ca^{2+} sparks has been suggestive of its role in AF susceptibility [96]. In contrast, calcineurin has been shown to induce hypertrophy in patients with atrial tachyarrhythmia which further contributes to structural remodeling [97]. This confirms that both calmodulin and calcineurin acts in different pathways despite having a common precursor as initiated by the ryanodine receptors (RyR) on the sarcoplasmic reticulum. This series of interactions in the ion channel related proteins could partly be a mechanistic function underlying atrial ion channel remodeling.

1.4 Atrial remodeling in substrates predisposed to AF

1.4.1 Hypertension

Hypertension is the most common predisposing factor for AF. It accounts for more number of AF than any other risk factors due to its high prevalence in nearly 28.6% of the US population and 972 million people in the world [26, 98]. It is responsible for 14% of AF incidence whilst increasing the risk of AF by 1.5- and 1.4 fold in women and men respectively [26]. Data from the Framingham study has shown that a 5mm increase in left atrial size, as seen in hypertension and atrial stretch, results in 39% increased risk of developing AF [26]. Co-existence of hypertension and atrial fibrillation has also been shown to escalate the risk of other cardiovascular related morbidity and mortality rates [12].

Hypertension is the most accounting risk factor with vast established clinical features predictive to AF development. Prior to direct electrophysiological studies in humans, indirect clinical characteristics were used to predict AF development in hypertensive patients. Key aspects include left atrial enlargement, left ventricular hypertrophy, increased P-wave duration and reduced diastolic mitral flow [13, 99, 100]. Increased P wave duration in patients with essential hypertension was suggested to be a feature of conduction slowing [9, 13]. In 1983, Loaldi *et al* observed an increased atrial ectopies in essential hypertensive patients that was assessed through 24 hour ambulatory electrocardiographic monitoring [10]. Later, in 1998, Haissegeure *et al* demonstrated that a majority of focal ectopic triggers originated from pulmonary veins [11]. Studies by Lau *et al* and Kistler *et al* in a hypertensive ovine model showed an increased conduction slowing and conduction heterogeneity, increased P-wave duration, increased atrial refractoriness, increased atrial fibrosis, increased inflammatory infiltrates, bi-atrial enlargement and reduced diastolic mitral flow during short term and long term exposure to hypertension[101, 102]. In small animals, choisy *et al* reported on the association of hypertension in the atrial substrate development involving left atrial fibrosis and unchanged atrial effective refractory period [103]. Lau *et al* further confirmed this results with a significant atrial electrical and structural remodeling in ageing spontaneously hypertensive rats [104]. They also showed that hypertension had a compounding effect on the pathophysiology of atrial substrate formation despite ageing.

In clinical setting, direct inter-relation of hypertension and AF was studied to demonstrate that hypertensive patients with history of AF had significantly higher C reactive protein levels and increased P wave dispersion which are indicative of underlying inflammation in the atrial electrophysiological remodeling [105]. Medi *et al* characterized the electrophysiological and electro-anatomical properties of chronically treated systemic hypertensive patients to demonstrate global conduction slowing and increased AF vulnerability which could be attributed to hypertension *per se* [106].

Atrial fibrillation is initiated through various proposed mechanisms such as intra atrial re-entry, abnormal automaticity and triggered activity influenced by various electrophysiological factors. Abnormal automaticity occurs mainly due to abnormal diastolic membrane depolarization that leads to premature firing of the action potential. This could possibly be caused by calcium release from ryanodine receptors within the atrial myocytes. This is further favored by β-adrenergic stimulation or decreased vagal activity [107]. This could, in part, be one of the reasons for the relationship of AF to β-adrenergic receptor coordinated disorders, e.g., Hypertension. The functional aspects of electrophysiological factors and action potential morphology of the atria differs from that of the ventricular myocytes due to differences in the kinetics of ionic currents [108]. Studies determining the direct atrial electrophysiological effects of β-adrenergic receptor blockers on the susceptibility towards AF could shed more light on this theory.

Peripheral resistance being an important determinant of blood pressure majorly depends on vascular tone which again is directly dependent on the contraction of vascular smooth muscles. The contraction of vascular smooth muscle depends on the actin myosin interaction in the vascular smooth muscle cells which in turn depends on the intracellular calcium concentration. Calcium channels in vascular smooth muscle cell are voltage gated and are in a close co-ordination with potassium channels. Therefore calcium and potassium channels orchestrate together to maintain the membrane potential. Efflux of potassium causes hyperpolarization of vascular smooth muscle cell membrane and result in the closure of L-type voltage gated calcium channel and hence decrease the intracellular calcium concentrations [109]. This action leads to vasodilation but aids the maintenance of hyperpolarized state of the membrane. Hyperpolarization activated inward current is shown to act as a source of AF by increasing the ectopic activity [110]. In pathological conditions, L-type calcium channel density is increased in the smooth muscle cells as demonstrated in spontaneously hypertensive rats [111]. In contrast, the potassium channel activity is also increased but without any effect on the closure of calcium gated channels. This is thought to be a mechanism leading to impairment of vascular tone that can be reversed with antihypertensive treatment [109].

Since other underlying cardiovascular and pathophysiological conditions also contribute to AF, electrophysiological studies performed after treatment of hypertension would give further insights into the reversal of atrial substrate during hypertension and could be a more optimized approach to avoid other compounding

cardiovascular effects and determine the direct correlation between hypertension and AF, thereby reverse remodeling.

1.4.2 Congestive heart failure

Nearly 40% of congestive heart failure patients are diagnosed with AF under clinical conditions [112]. Chronic rapid pacing induced heart failure is used in this area of research ever since it was described in 1962 [113]. Increased interstitial fibrosis, cellular hypertrophy and degeneration were observed in a feline model of spontaneous cardiomyopathy and these structural abnormalities were suggested to initiate arrhythmias [114]. Power *et al* showed supporting evidence in an ovine model of heart failure with an additional data on ERP being inversely correlated to LA area [115]. Li *et al* extended the evidence with histological correlation where they demonstrated a marked increase in atrial fibrosis which attributed to the conduction heterogeneity albeit ERP was unaltered [2]. They further demonstrated that ERP changes were seen only with rapid atrial pacing and therefore suggested varying mechanisms involved in different AF substrates. These results construct an understanding that AF in heart failure is predominantly due to conduction heterogeneity rather than ERP.

Sanders *et al* performed electro-anatomical mapping technique to demonstrate atrial dilatation, areas of low voltage and scarring in patients with CHF and AF and compared to controls [116]. These spontaneous scarring as evidenced by areas of

low voltage may indicate underlying fibrosis. In addition, all pacing sites showed an increased refractoriness and conduction abnormalities along with functional block along crista terminalis. The increased propensity of atrial fibrillation in spite of an increased atrial refractoriness indicate that AF inducibility in congestive heart failure patients is principally related to structural remodeling and conduction properties rather than rate related remodeling which was previously understood from studies by Li *et al* [2].

1.4.3 Mitral stenosis

Mitral stenosis continues to be the most common risk factor for atrial fibrillation in developing countries [117]. Mitral stenosis patients have been demonstrated to have bi-atrial enlargement even without a history of atrial fibrillation [118]. Recently, John *et al* studied the electrophysiological features of rheumatic mitral stenosis patients undergoing mitral commissurotomy and demonstrated a prolonged refractoriness in both atria, significant increase in left atrial conduction time and prolongation in corrected sinus node recovery time [118]. Other electrical changes include a site specific conduction abnormality at crista terminalis and electro-anatomical evidence of low voltage areas in both left (LA) and right atrium (RA) signifying the underlying structural remodeling.

1.4.4 Aging

Aging is an important contributor for AF development with the prevalence increasing from 2.3% to 5.9% in individuals older than 40 and 65 years of age respectively [119]. The investigators also showed that 70% of AF patients were between 65 and 85 years of age. In 1986, Spach & Dolber demonstrated that aging was associated with dissimilarities in extracellular waveforms that were due to electrical uncoupling of the side-to-side connection between the fibres. The authors suggested that these electrophysiological consequences could sustain re-entry [120]. Further, aging has been shown to be associated with electrical and structural remodeling including conduction slowing/heterogeneity, impairment of sinus node function and increased ERP [121]. In addition, aging has also been shown to be associated with increased complex electrograms occurring near low voltage areas and thereby slowing conduction. These features are suggested to be due to the underlying myocardial architecture since complex electrograms were predominantly seen along the posterior and high septal RA regions [122].

1.4.5 Myocardial ischemia

Myocardial infarction has been shown to be an important risk factor for AF with a relative risk of 3.6 [123]. New onset AF is seen in up to 22% of patients presenting with acute coronary syndrome. Experimental studies showed that atrial ischemia induced by atrial artery occlusion resulted in local conduction slowing with re-entry

contributing to AF [124]. A canine model of right coronary artery occlusion was used to demonstrate atrial refractoriness shortening with loss of rate adaptation although atrial arrhythmia was not evaluated in this study [125]. Miyauchi *et al* demonstrated an increased monophasic action potential duration and amplitude resulting in increased heterogeneity and AF inducibility after 8 weeks following permanent occlusion of left anterior descending coronary artery in a canine model [126]. In a sheep myocardial infarction model, atrial refractoriness was unaltered [3]. Specifically, ischemia secondary to left circumflex artery balloon occlusion resulted in greater conduction slowing and heterogeneity and higher AF vulnerability with longer AF durations compared to animals with left anterior descending artery occlusion or control.

1.4.6 Obesity

Obesity has been suggested to be an important and modifiable risk factor for AF. This increased risk of AF in obese patients appears to be mediated by left atrial dilatation as demonstrated in a Framingham heart study [27]. Wanahita *et al* showed in a meta-analysis that obesity increased the risk of developing AF by 49% in the general population in parallel with increasing body mass index [127]. Recently, Abed *et al* demonstrated the association of obesity with increased susceptibility to AF through electro-structural remodeling in an ovine model [7]. Despite an unchanged ERP, other electrophysiological factors such as conduction velocity slowing and increased heterogeneity were seen along with increase in left atrial

volume, inflammatory infiltration and lipidosis. They further showed that these changes were associated with an altered pro-fibrotic cytokine levels. In humans, Munger *et al* demonstrated a reduction in atrial refractoriness in the left atrium and in the proximal and distal pulmonary veins along with an increased left atrial volume and pressure in obese AF patients than in AF patients with normal body mass index [128]. Increased pericardial fat may be a potential mechanism by which obesity can increase AF vulnerability. Wong *et al* showed that presence of pericardial fat was increasingly associated with AF severity and poor ablation outcomes [129]. Recently, Venteclef *et al* demonstrated a paracrine effect of pericardial fat in promoting myocardial fibrosis through secretion of adipokines leading to abnormal atrial substrate [130]. Direct infiltration of adipocytes into atrial myocardium has also been suggested to increase fibrosis and may further explain increased AF in obesity [131].

1.4.7 Obstructive sleep apnea

Gami *et al* demonstrated a close association between obstructive sleep apnoea (OSA) and AF with an adjusted odds ratio of 2.19 in developing AF compared to high risk patients with multiple cardiovascular diseases [8]. OSA has also been suggested to be an independent risk factor for incident AF in patients over 65 years of age [132]. Further, an association of sleep disordered breathing has been shown in relatively young AF patients (56±12 years) with increased odds ratio of 3.04 in comparison to normal age and sex matched controls [133]. Potential mechanisms underlying this

association can be seen from experimental studies. Ghias *et al* demonstrated the increased AF inducibility due to augmented neural activity from ganglionic plexi adjacent to right pulmonary veins in a canine model of sleep apnoea [134]. Iwazaki *et al* suggested that forced inspiration in obese rats could have induced acute LA distension related to diastolic dysfunction which could precipitate arrhythmogenic substrate during OSA episodes [135]. Linz *et al* demonstrated in a pig model that OSA was associated with increased spontaneous AF and atrial oxidative stress along with activation of pro-fibrotic pathways in the atria [136]. They further showed that sympathetic renal denervation reduced the spontaneous AF triggers by reduction of sympathetic activity although oxidative stress was unaltered. Renal denervation also led to a reduction in postapneic blood pressure and prevention of ERP shortening displaying an anti-arrhythmic effect and importance of autonomic disbalance in OSA related AF [137].

1.4.8 Atrial septal defect

Atrial septal defect (ASD) results in chronic right atrial volume overload [138]. Due to volume overload, the atrium is more prone to dilatation and stretch. A study by Gatzoulis *et al* showed that 19% of patients with atrial septal defect have been noted with AF which persists even after the surgical intervention [139]. Electrophysiological findings showed an increase in right atrial ERP and conduction delay in ASD patients compared to control patients [140]. Similar study on left atria showed dilatation and scarring seen in low voltage areas and were correlated with

conduction heterogeneity and unaltered ERP [141]. These electrical and structural changes can be due to volume overload and atrial stretch in ASD leading to AF.

1.4.9 Atrial stretch

Atrial stretch ultimately leading to atrial dilatation is encountered in many clinical conditions during AF development [13, 142] that is associated with pressure and volume overload in atrial myocytes. In 1955, Fraser *et al* showed that atrial dilatation is correlated with an increased risk of AF [143]. After two decades, Probst *et al* showed that dilatation was a consequence of AF and not its cause [144]. There were a number of studies showing an increased left atrial dimension in AF patients [74, 145-149]. A cohort study in lone AF patients showed no increase in atrial size leading to a postulation that atrial dimension increased with longer durations of AF [150, 151].

Varying observations of atrial refractoriness have been reported in an acute volume overload animal models [152-155]. Nevertheless, most Langendorff models have shown significant abbreviations of refractoriness and reduction in monophasic action potential duration, conduction slowing, increased intra-atrial conduction block and spatial conduction heterogeneity [156, 157]. However, several investigators have shown that atrial refractoriness is either unchanged or increased in different animal models [158, 159]. Conflicting results on atrial conduction and fibrosis were observed in chronic stretch models [6, 160].

In humans, Calkins *et al* demonstrated an unchanged ERP with simultaneous atrial and ventricular pacing while the same group published a contrary result after modifying the pacing protocol [161, 162]. Kalman and Sparks speculated these differences were due to different pacing protocol, degree of atrial pressure overload causing stretch and its autonomic effect as employed in different studies [142]. This theory was supported by results of Tse and co-workers where the investigators demonstrated a significant ERP abbreviation by enhancing autonomic blockade and attenuated response by reducing the pressure overload with calcium channel blockade [163]. Several investigators have demonstrated an increased ERP, conduction abnormalities and areas of low voltage using electro-anatomic mapping in various chronic stretch models [116, 118, 141]. Other acute studies showed an increase in ERP and heterogeneity with an increased atrial pressure [164, 165]. Therefore, it could be possible that increased ERP dispersion in the atriacan be arrhythmogenic independent of absolute ERP changes. Major factors underlying stretch related atrial remodeling could potentially include;

- Initiation of after-depolarization through mechano-electric feedback [166-168];
- Stretch activated channels and proteins [169-171];
- Calcium loading [157, 163];
- Autonomic innervations [163]; and
- Increased atrial size and conduction abnormalities that may promote re-entry [156, 157, 163, 165, 166].

All these mechanisms warrant more research to enable putative management of stretch regulated AF.

1.4.10 Aortic stiffness

A prospective data from community based observational cohort in Framingham showed that pulse pressure is an important yet modifiable risk factor for incident AF. They further demonstrated that the association between pulse pressure and AF was stronger even after adjusting for other predictive factors of AF such as left atrial enlargement, left ventricular mass and fractional shortening [172]. Central pulse wave analysis is a clinically validated, non-invasive, reproducible assessment method for aortic stiffness [173]. Lau *et al* demonstrated that lone AF patients with highest levels ($\geq 75^{th}$ percentile) of peripheral and central pulse pressures and augmentation pressure had a significantly higher AF recurrence rate following catheter ablation [174]. Further, hypertensive patients with pre-existing AF have been demonstrated to have higher heart-to-femoral pulse wave velocity indicative of an increased arterial stiffness in these subset of patients [175]. However, Reiffel *et al* showed that arterial stiffness index could not be used to predict the risk of AF in hypertensive patients since AF is suggested to be more complex than the immediate secondary effects of elevated atrial pressures and stretch [176].

1.4.11 Smoking

Smoking has been shown to be associated with a 2 fold increased risk of incident AF in a population based cohort study [177]. Although smoking is not associated with hospitalization, it was closely associated with an increased mortality rate in older adults (70±9 years) with AF [178]. Further, data from a large Danish cohort showed that smoking was linked with high risk of thromboembolism and death after adjusting for stroke risk stratification in AF patients [179]. Interestingly, as a paradox effect, a 8 year follow up study showed that smokers had lesser arrhythmias following coronary artery bypass graft as compared to non smokers which is suggested to be due to reduced hyper adrenergic stimulation in smokers following the stress of surgery [180].

1.4.12 Alcohol

Alcohol consumption even at moderate levels has been shown to be associated with atrial fibrillation in a large meta-analysis performed with 7 different prospective studies on Swedish men and women [181]. This association was also seen with heavy alcohol consumption in Japanese individuals [182]. Data from the Framingham heart study suggests little association between long-term moderate alcohol consumption and AF risk, however, a significantly increased risk were seen among subjects consuming >36 g/day [183]. Nevertheless, results from the LIFE study showed that up to 10 drinks per week appeared to be safe with regard to the

risk of AF in hypertensive patients with left ventricular hypertrophy [184]. In addition, Overvad *et al* showed that high alcohol consumption could worsen prognosis in patients with AF [185]. Interestingly, Mandyam *et al* suggested that alcohol consumption could precipitate AF through vagal triggers since these features were seen in the same patients [186].

1.5 Reverse remodeling of atrial substrate

The substrates leading to AF can be contributed by a diverse range of conditions as discussed in the previous section. Fortunately, the electrical and structural changes seen in atrial remodeling could be reversed. Reverse remodeling has been shown in human AF as well as in animal models of pacing induced AF and heart failure. [61, 187-193]. Everett *et al* reported on reverse electrical remodeling in a canine model of chronic AF with mitral regurgitation within 7 to 14 days following conversion to sinus rhythm although the vulnerability to AF persisted due to the underlying structural abnormalities [193]. Likewise, Ausma *et al* has shown that recovery in structural remodeling was a slow process and more difficult than electrical remodeling following cessation of tachy-pacing [192]. Rate related remodeling was shown to be reversed in a canine model of tachypacing with the ERP returning to its baseline after maintaining the atrium in sinus rhythm [57]. This was confirmed in humans where several minutes of induced AF was sufficient to shorten the ERP that recovered to its baseline normal values after AF had terminated for approximately 8 minutes [63].

Fan *et al* showed that mitral stenosis patients at the time of commissurotomy following cardioversion had a significantly abbreviated ERP that markedly increased at 3 month post commisurotomy follow up [194]. Likewise, Soylu *et al* who showed a reduction in ERP dispersion following correction of mitral stenosis [195]. The above studies were further supported by John *et al* where the reversal of atrial substrate in mitral stenosis patients was demonstrated after commissurotomy with reduced P wave duration, improved bipolar voltage and conduction velocity although atrial refractoriness was unchanged [118]. In obese individuals, weight reduction with intensive risk factor management has been shown to result in a reduction of AF burden and symptom severity in conjunction with reverse cardiac remodeling in obese patients [188].

With regard to the hypertensive substrate for AF, the jury is still out on the best anti-hypertensive agent for reverse atrial remodeling. A prospective, randomized trial in 6614 hypertensive patients aged between 70–84 years (systolic blood pressure ≥ 180 mm Hg, diastolic ≥ 105 mm Hg) showed that conventional antihypertensive drugs such as atenolol (50 mg), metoprolol (100 mg), pindolol (5 mg), or hydrochlorothiazide (25 mg) plus amiloride (2·5 mg) daily or newer drugs such as enalapril (10 mg) or lisinopril (10 mg), or felodipine (2·5 mg) or isradipine (2–5 mg) daily resulted in significant reduction in the incidence of AF [196]. However, conflicting data exists regarding the efficacy of different class of anti-hypertensive agents [197-201]. Several secondary prevention trials have reported that inhibitors of the renin angiotensin system may not reduce the risk of arrhythmia recurrence in AF

patients [197, 198]. Further, several randomized studies have shown differing results with respect to AF frequency in patients with hypertension and paroxysmal AF treated with non-dihydropyridine calcium channel blockers and angiotensin receptor blockers [199-201]. Molecular data regarding the reversal mechanism is not available from any of the above studies though stretch activated channels (SAC) have been studied elsewhere, highlighting their role of mechano-electric feedback that can promotes AF [202, 203]. Kimura *et al* illustrated the effects of mineralocorticoid receptor antagonist, eprelenone, at non antihypertensive dose, in reduction of hypertrophy, fibrosis and AF inducibility in Dahl salt-sensitive rats without affecting the blood pressure levels suggesting a role of MR associated with Rac1-oxidative stress/inflammatory axis [204]. Though most clinical trials focus on the occurrence and recurrence of paroxysmal and/or persistent AF with antihypertensive treatment, clear electrophysiological and molecular mechanisms involving these treatments are not known and are yet to be elucidated.

1.6 Prevention of atrial remodeling

The substrate for AF has been shown to be reversible with secondary prevention treatment as discussed earlier. Further, there are evidence that the abnormal atrial substrates can also be prevented. Fibrosis is one of the key substrates for remodeling of the atrium since it causes non-uniform conduction that may sustain re-entry. Pirfenidone, an anti-fibrotic drug has been shown to exert anti-fibrotic and renoprotective effects by inhibiting TGFβ-Smad2/3 signaling, improvement of

MMP9/TIMP1 balance, and suppression of fibroblast proliferation in addition to significant attenuation of blood pressure levels in Dahl salt-sensitive hypertensive rats [205]. It is also shown in a mice model to be beneficial in treating hypertension induced myocardial fibrosis by inhibiting NLRP3-induced inflammation and fibrosis [206]; hypertension induced cardiac hypertrophy by inhibiting angiotensin II [207]; and preventing cardiac remodeling [208]. Further, it has been demonstrated to prevent the fibrous tissue formation in a canine model of heart failure [209]. Electrophysiological data showed a significant reduction in conduction heterogeneity and reversal of conduction slowing which was in keeping with histological experiments. Molecular analysis revealed the reversal of major proteins involved in fibrosis mechanisms; most importantly TGF-$\beta_1$which is the signaling mediator of fibrosis formation. Yamazaki *et al* showed that pirfenidone inhibits angiotensin II in cardiac hypertrophy [210]. This was in line with previous studies since angiotensin and TGF-β_1 both act in the fibrosis pathway [211].

Tranilast, another anti-fibrotic drug has also been shown to prevent abnormal atrial remodeling. Tranilast has been demonstrated of its effect on pro-fibrotic and inflammatory cytokines and extracellular matrix protein synthesis albeit in different organ systems and experimental substrates.[212-215]. Importantly, in a canine tachypacing model, tranilast treatment reduced atrial fibrosis as well as increased ERP and improved conduction properties contributing to reduced AF susceptibility [216]. Several other agents have also been shown to prevent atrial remodeling in different experimental substrates. For example, omega-3 fatty acid has been shown

to be beneficial in preventing atrial remodeling in a ovine model of heart failure induced by intracoronary doxorubicin infusion [217]. Further, Parikh *et al* showed that relaxin, an anti-fibrotic hormone suppressed AF in hypertensive rats by increasing conduction velocity through prevention of fibrosis and hypertrophy [218]. Beneficial effects of mineralocorticoid receptor antagonist, eprelenone in reducing AF susceptibility has also been shown to be associated with reduced fibrosis and myocyte hypertrophy in addition to reduced oxidative stress/inflammatory axis [204].

In hypertensive substrate, effective blood pressure control has been shown to be beneficial. In 2005, Fuenmayor *et al* demonstrated that effective control of blood pressures in patients with hypertensive heart disease shortened the inter-atrial conduction time. [219]. This was accompanied by significant reduction in arrhythmia from holter monitoring during follow up. A randomized clinical study also showed that treatment with telmisartan reduced the P-wave dispersion more effectively and prevented more AF episodes than ramipril in hypertensive patients [220]. Further, angiotensin receptor blockers have been suggested to prevent AF by improving LV haemodynamics, reducing atrial stretch, inhibiting angiotensin-II induced fibrosis and altering ion channel function [221].

1.7 Summary

Despite the continuing research efforts to date, the complex mechanisms underlying AF remain incompletely understood. Variable findings have been reported on atrial ionic and electrical remodeling in different substrates and species used. While basic studies have significantly advanced our understanding in last few decades in isolated substrate model, the interplay between different risk factors and its effects on atrial remodeling has not been thoroughly examined. Nevertheless, these information are otherwise different to delineate from human studies due to the co-existence of multiple risk factors in the same patient. In appears that most substrates contribute to AF by structural remodeling whereby atrial fibrosis appears to be the central common pathway.

2 CHARACTERISATION OF REVERSE STRUCTURAL REMODELING OF HYPERTENSIVE ATRIA WITH ANTI-HYPERTENSIVE TREATMENT: IMPLICATIONS FOR ATRIAL FIBRILLATION

2.1 Introduction

The co-existence of hypertension and AF has been shown to increase morbidity and mortality of patients [12]. Due to its high prevalence in general population, hypertension accounts for most number of AF patients around the world than any other risk factors [26, 98]. Hypertension also increases the risk of AF by 1.5- and 1.4 fold in women and men respectively [26]. Furthermore, a recent data suggests that in addition to hypertension, patients with systolic blood pressure within non hypertensive range were also independently associated with increased incident AF [222]. The Framingham study has further shown that a 5mm increase in left atrial size, as seen in hypertensive subjects, results in 39% increased risk of developing AF [26]. Importantly, hypertension has increased throughout both developed and developing countries over the last few decades in higher proportion of patients with uncontrolled hypertension despite the availability of better anti-hypertensive agents [223].

Hypertension has been shown to cause electrical and structural remodeling [4, 102]. Reverse remodeling has been shown in human AF as well as in animal models of pacing induced AF and heart failure. [61, 189, 193, 199, 224-227]. Previous studies have also demonstrated that reverse electrical remodeling occurs more readily than structural changes [192, 228]. In this study, we aim to characterize in detail reverse structural remodeling following treatment with amlodipine, atenolol and clamp removal in a large animal model of 'one-kidney, one-clamp' induced hypertension using cardiac magnetic resonance (CMR) imaging and histopathological examination of atrial tissues.

2.2 Methods

2.2.1 Study approval and guidelines

This study was approved by the *'University of Adelaide Animal Ethics Committee'* and '*SA Pathology Animal Ethics Committee'*. Guidelines from the "Australian code of practice for the care and use of animals for scientific purposes" 7th edition, 2004 adopted by the 'National health and medical research council' were followed for all the experimental procedures.

2.2.2 Animal housing & preparation

Male merino cross sheep were used for this study. All animals were held in group in open paddocks. Animals were placed in a 22°C temperature controlled room 24 hours pre-operative and until full recovery of 2-3 weeks post operatively for survival procedures. Food and water were provided *ad libidium*.

Before each surgical procedure, animals were given water intake only and taken off from food 24 hours prior to general anaesthesia procedure and followed by intravenous sodium thiopentone (10-15 mg/kg) for induction to facilitate endo-tracheal intubation. Isoflurane 2-4% in 100% oxygen at 4L/min was exercised for maintenance throughout the procedure. Lignocaine 2mg/kg was used as local anaesthetic during surgery. Non-invasive blood pressure, heart rate, pulse oximetry, end-tidal CO_2 and temperature were continuously monitored during the whole surgical procedure. Amoxycilin (1 ml/20kg) and Buprenorphine (0.005-0.01 ml/kg) were administered intramuscularly for three days following renal surgeries. General anaesthesia was performed prior to renal surgery, cardiac MR scans and terminal electrophysiology study.

2.2.3 'One-kidney, one-clip' Renovascular Hypertension model

Conventional 'one-kidney, one-clip' model was used as previously described [101]. In brief, animal was placed on left lateral recumbent position under general

anaesthesia. Nephrectomy was performed on the right kidney. Two finger breadths were allowed from lateral extent of the paraspinal muscles for making an incision from just beneath the rib cage for about six inches vertically. The perinephric fat and Gerota's fascia were carefully separated from the surface of the kidney. The ureter and renal vessels were separately ligatured and right kidney was removed following which the wound was closed in layers.

In this study, we performed both nephrectomy and renal artery occlusion on the same day. A vascular occluder clamp was used (heavy duty 8mm, DOCXS Biomedical Products, Ukiah, CA, USA) to facilitate blood pressure titration for hypertension development (maintained at 150-160 mmHg approximately) and reversal. Following nephrectomy, the sheep was placed onto the right lateral recumbent position. Blunt dissection was performed via similar incision as the right side to expose the renal artery without interrupting the perinephric fat and Gerota’s fascia on the left kidney. Vascular occluder clamp was placed around the left renal artery with the actuating tube connected to an external port. The port was placed subcutaneously and sutured to maintain in a stable position. During the surgical procedure, approximately 50% occlusion of renal artery was verified with flow transducer (Transonic Flowmeter TS-401 with precision flow probe, Transonic Systems Inc., NY, USA) and Doppler velocity (Acuson XP-128, 7 MHz probe, Siemens Medical Systems, PA, USA) under direct vision to provide guidance for subsequent vascular occluder inflation.

Heparin (5000 I.U) was given for two days post-operatively to prevent any thrombosis due to renal artery clamping. After surgical procedures, sheep were held in individual pen houses and monitored twice daily during recovery. After complete recovery, usually 2-3 weeks, sheep were sent back to paddocks. Induction of hypertension was initiated after 2-3 weeks of complete recovery from the surgery. Following renal surgeries, animals were subjected to non-invasive blood pressure procedure to ensure they are acclimatized to the technique. Measurements were taken thrice weekly at the same time of the day by the same handler with the animal in a metabolic crate. Non-invasive blood pressure levels were measured by placing the blood pressure cuff over the brachial artery of the forelimb in conscious animals (Datascope Passport 2, Datascope Corp., NJ, USA). All blood pressure measurements were done ≥3 times with the animal in a completely relaxed state following at least 5-10 minutes of standing in the metabolic crate.

2.2.4 Cardiac MR Imaging

All animals were under general anaesthesia as described above and were securely placed in a dorsal position for the cardiac magnetic resonance (CMR) scans. While the animals were under automated mechanical ventilation, breath holding was done to acquire ECG gated image. With no inter slice gap, a slice thickness of 6mm and 10mm through the atria and ventricles respectively were used. CMR (Siemens Sonata 1.5 Tesla MR imaging system, Siemens Medical Solutions, Erlangen, Germany) was used to assess the anatomic and functional characteristics of the

animals prior to terminal studies. All analyses were performed offline using Argus software (Leonardo workstation, Siemens Medical Solutions, Erlangen, Germany). The left atrial (LA) and ventricular (LV) volumes, LA and LV ejection fraction (LAEF & LVEF) and inter-ventricular thickness (IVS) were assessed.

2.2.5 Study Timeline

A total of 32 sheep were used for this study. Seven sheep were used as normotensive controls without undergoing any renal surgeries. All remaining 25 sheep underwent renal surgeries to develop high blood pressure for 12 weeks. At the end of 12th week, 7 hypertensive animals underwent terminal studies followed by heart removal for structural analyses. All remaining animals were grouped sequentially into three different blood pressure lowering groups, namely, Amlodipine (10mg daily orally), Atenolol (100mg daily orally) and Clamp removal group. Treatment was designated for 16 weeks after which all animals were subjected to terminal studies followed by heart removal for structural analyses (Figure 1).

2.2.6 Anatomical/ Structural Analysis

Animals were humanely killed (Sodium thiopentone 100g/sheep, 2-4% Isoflurane in 100% O_2) after terminal electrophysiological mapping studies. Right and left atrial appendage were dissected and stored appropriately for specific experimentation. In addition, left (LV), right (RV) ventricles and Inter-ventricular septum (IVS) were

weighed. Tissues were triplicated and stored; Fixed in 10% formalin solution and OCT cassettes (Slow freezing with Isopentane under liquid nitrogen) for histology and Immunohistochemistry analyses respectively.

2.2.6.1 Histology

All tissues were fixed in formalin for one week followed by serially diluted washing with alcohol and embedded in paraffin. The embedded tissue were mounted on the microtome and cut into 5µm thick slices. These slices were placed on the slides and stained with haematoxylin & eosin and Masson's trichrome. These stained slides were digitized using an automated nanozoomer. Digitized images of the slides were used to analyse myocyte hypertrophy, inter-myocyte distance, interstitial fibrosis and inflammatory infiltration. Myocyte hypertrophy and inter-myocyte distance (endomysial fibrosis) were measured in both epicardial and endocardial regions. The layers were marked during storage for differentiation and continued to be consistent throughout the analyses. Regions from borderline up to 300µm depth were considered for analyses of both layers. The assessor was blinded to the groups and types of myocardial layers prior to analyses of all histological parameters.

Mean cell diameters of approximately 30-35 transversely cut myocytes from 5 different fields were measured to determine hypertrophy [229]. Inter-myocyte distance was measured as closest distance between myocytes at a mean of 40 cell-cell distance at 5 different fields. Fibrosis was quantified at 5 random fields in each

slide using color differentiation as described previously [230]. ImageJ 1.47v (National Institute of Health, USA) was used for analysis. All quantified results were expressed in percentage relative to the whole tissue area.

2.2.6.2 Immunostaining

The frozen tissues were used to perform immunohistochemistry and determine the expression levels of Connexin43, connective tissue growth factor (CTGF) and Transforming growth factor ß1 (TGF-ß1). Rabbit polyclonal primary antibodies were purchased from Abcam laboratories, Cambridge, MA, USA. A primary antibody dilution of 1: 100 was used. Immuno-stained images were scanned at 20 x magnifications for blinded quantification using ImagePro Premium v9.1 (Media cybernetics, Rockville, MD, USA). All quantified results were expressed in percentage relative to the whole tissue area.

2.2.7 Statistical Analysis

All data were expressed in mean ± standard deviation. Analyses of differential effects of blood pressure lowering therapies on structural parameters were performed using analysis of variance (ANOVA). Sidak adjusted post-hoc tests were used to delineate the differences between specific groups. Statistical significance was taken as $P<0.05$.

2.3 Results

Thirty-six male merino cross sheep underwent the procedure successfully to develop renovascular hypertension (61±6 kg). Four sheep were excluded from the study as they developed heart failure and pulmonary oedema during the period of hypertension. Remaining animals developed renovascular hypertension in a timely fashion for a mean duration of 12±2 weeks.

2.3.1 Blood Pressure

All normotensive control animals showed blood pressure within normal range (115±7 mmHg) whilst all animals that underwent renal surgeries demonstrated a significantly increased blood pressure levels (157±7 mmHg) at 12 weeks. Sixteen weeks of Amlodipine, Atenolol and clamp removal treatment reduced SBP to 133±3 mmHg ($p<0.001$), 131±11 mmHg ($p=0.007$) and 125±7 mmHg ($p<0.001$) respectively showing significant reversal of hypertension.

2.3.2 Cardiac Functional and Morphological Assessment

As compared to normotensive controls, hypertensive group showed a significantly higher left atrial dilatation (EDV = 24±2 vs. 48±8 mL; $p=0.001$) and lower LA ejection fraction (32±3 vs. 13±5 %; $p=0.033$). These changes were unaltered after treatment in all the groups. Left ventricular volumes and ejection fraction did not

change in hypertension indicating that no animals suffered from heart failure (Table 1). Inter-ventricular septal thickness and left ventricular mass were significantly increased in hypertension as compared to controls. Pharmacological therapies but not clamp removal group reversed the inter-ventricular septal thickness and left ventricular mass. Right ventricular mass were unaffected in hypertension and treatment groups.

2.3.3 Histological Examination

2.3.3.1 Inflammatory Infiltration

Inflammation was significantly increased during hypertension compared to control group [LA – 5.1±0.5 vs. 3.3±0.5 %; p=0.001; RA – 5.8±0.9 vs. 3.5±0.3 %; p=0.001]. Increased inflammation as seen during hypertension was significantly reversed after treatment with amlodipine [LA – 3.1±0.7 %: p<0.001; RA – 3.8±0.8 %: p<0.001], atenolol [LA – 2.8±0.3 %: p<0.001; RA – 3.0±0.2 %: p<0.001] and clamp removal [LA – 3.3±0.5: p<0.001; RA – 4.4±0.7 %: p=0.015] groups (Figure 2). No significant differences in inflammation were seen between different anti-hypertensive groups.

2.3.3.2 Atrial Interstitial Fibrosis

Fibrosis was significantly increased in hypertensive animals as compared to control group [LA – 21.7±6.2 vs. 4.7±3.7 %; p<0.001; RA – 23.3±4.7 vs. 7.8±0.8 %;

p<0.001]. Fibrous tissue were significantly reversed after treatment with amlodipine [LA – 7.7±2.9 %: p<0.001; RA – 14.9±4.9 %: p=0.009], atenolol [LA – 5.1±1.9 %: p<0.001; RA – 11.5±2.7 %; p<0.001] and clamp removal [LA – 4.8±1.6 %: p<0.001; RA – 13.6±3.2 %: p=0.002] groups (Figure 3). No significant differences in fibrosis were seen between different anti-hypertensive groups.

2.3.3.3 Myocyte Size and Inter-myocyte Distance

Epicardial myocyte size (hypertrophy) was significantly increased during hypertension compared to control group in both the atrium (p<0.01) (Figure 4). This increased myocyte size in the epicardial region was significantly reversed after treatment with amlodipine, atenolol and clamp removal groups in both LA and RA (p<0.01). Epicardial inter-myocyte distance (endomysial fibrosis) was significantly increased during hypertension compared to controls in both the atrium (p<0.01). This was significantly reversed in LA after treatment with amlodipine (p=0.03) and atenolol (p=0.02) with a positive trend in clamp removal group (p=0.08). In RA, reversal was seen in amlodipine (p=0.05) and atenolol (p=0.01) although was not seen in clamp removal group (p=0.12).

Likewise, endocardial myocyte size was significantly increased during hypertension compared to control group (p<0.01). In LA, this increased myocyte size in the endocardial region showed a positive trend towards reversal with amlodipine (p=0.078) and atenolol (p=0.171) treatment but not significant. Significant reversal

of myocyte size was seen in LA of clamp removal (p=0.040). All treatment groups showed a significant reversal in the right atrium (p<0.01). Endocardial inter-myocyte distance was significantly increased during hypertension compared to controls (p<0.01). This was significantly reversed with amlodipine, atenolol and clamp removal groups in both atria (p<0.01) (Table 2) (Figure 5). Both hypertrophy and endomysial fibrosis did not show any difference between the treatment groups. Further, there were no differences in myocyte hypertrophy and endomysial fibrosis between epicardial and endocardial regions.

2.3.4 Immunostaining

2.3.4.1 Connexin43

Hypertensive animals had significantly increased connexin43 expression as compared to normotensive controls [LA – 1.1±0.4 vs. 2.9±0.3 %; p=0.003; RA – 1.3±0.3 vs. 3.7±0.7 %; p<0.001]. Reduced connexin43 expression as seen in hypertension were reversed after treatment with amlodipine [LA – 2.8±1.0 %: p=0.010; RA – 2.6±1.0: p=0.001], atenolol [LA – 3.0±0.3: p=0.006; RA – 3.7±0.4; p<0.001] and clamp removal [LA – 2.4±0.8: p=0.088; RA – 3.6±1.4; p=0.004] (Figure 6). Connexin43 expression levels did not show any difference between the treatment groups.

2.3.4.2 CTGF

Connective tissue growth factor (CTGF) expression was significantly increased in hypertensive animals as compared to normotensive controls [LA – 2.1±0.6 vs. 0.7±0.3; p<0.001; RA – 2.4±0.5 vs. 1.1±0.5 %; p<0.001]. Increased CTGF expression as seen in hypertension was significantly reversed to normotensive range after treatment with amlodipine [LA –1.1±0.2 %: p=0.003; RA – 1.1±0.4 %: p<0.001] and atenolol [LA – 1.2±0.3 %: p=0.015; RA – 1.4±0.3 %; p=0.016]. In clamp removal group, reversal of CTGF expression was seen only in LA (1.1±0.3 %; p=0.004) but not in RA (2.1±0.7 %; p=0.988] (Figure 7). CTGF expression levels did not show any difference between the treatment groups.

2.3.4.3 TGF-ß$_1$

TGF-ß$_1$ was highly expressed in hypertensive animals as compared to normotensive controls [LA – 3.5±0.7 vs. 2.0±0.8; p=0.026; RA – 3.6±0.3 vs. 2.5±0.5 %; p<0.001]. This increased TGF-ß$_1$expression levels were significantly reversed after treatment with amlodipine [LA – 1.9±0.8: p=0.024; RA – 2.0±0.4 %: p<0.001], atenolol [LA – 2.0±1.01: p=0.036; RA – 2.4±0.8 %: p=0.011] and clamp removal [LA – 2.0±0.5: p=0.017; RA – 2.0±0.3 %: p<0.001] groups (Figure 8). TGF-ß$_1$ expression levels did not show any difference between the treatment groups.

2.4 Discussion

This is the first study to characterize the reverse structural remodeling in large animal model of hypertension after treatment with anti-hypertensive drugs. Remarkable reduction in blood pressures and cardiac histological abnormalities were seen with 16 weeks treatment. Specifically;

- Hypertension causes structural remodeling through myocyte hypertrophy, increased interstitial fibrosis and inflammation. This was further seen along with increased septal hypertrophy, atrial dilatation and dysfunction.
- Structural changes at molecular level were seen including increased inflammatory and pro-fibrotic cytokines (CTGF and TGF-$ß_1$) and reduced connexin43 expressions.
- Anti-hypertensive treatments resulted in significant reverse structural remodeling by reversing inflammation, fibrosis and hypertrophy seen with reduced septal hypertrophy, inflammatory and pro-fibrotic cytokines and connexin expression.
- No significant differences between blood pressure lowering therapies were seen during reverse structural remodeling.

2.4.1 Structural Remodeling in Hypertensive Atria

Kistler *et al* developed chronic hypertension in large animal model with pre-natal corticosteroid exposure and showed evidence of structural remodeling in chronic hypertension with increase in hypertrophy, myolysis, mitochondrial and nuclear

enlargement along with increased collagen fibrils [102]. Lau *et al* developed hypertension model by nephrectomizing the right kidney and occluding the renal blood flow on the left renal artery. He showed that the substrate could develop in as early as 5 weeks from onset of hypertension and demonstrated the progression of structural remodeling with time [101, 231]. They showed a significant increase in atrial and ventricular hypertrophy, increased lymphocytic infiltration, inflammation and fibrosis even with short term hypertension [231]. In small animals, structural remodeling in spontaneously hypertensive rats has been demonstrated with increased interstitial fibrosis and inflammation [103, 104]. Our results are in keeping with the previous observations and in addition, we also showed that these structural remodeling in hypertension could be due to changes in connexins as well as inflammatory and pro-fibrotic cytokines in large animal model. Reduced connexin expression has been previously demonstrated to be involved in large and small animal models of hypertension and ventricular hypertrophy [232, 233]. In addition, CTGF has been reported to be an important candidate gene involved in hypertension [234]. ET-1 induced ECM accumulation occurs through CTGF promoter region due to which CTGF has been suggested to be a pharmacological approach for ET1 induced cardiovascular diseases [235]. Furthermore, CTGF and TGF- $ß_1$, through angiotensin-II induction, has been shown to be a downstream effector involved in NADPH oxidase – ROS – Rac1 pathway during fibrotic substrate formation in AF [211]. This pathway has been demonstrated to be inhibited by trimetazidine in pressure overloaded myocardial fibrosis [236]. These studies together explain the association of CTGF and TGF- $ß_1$ in development of fibrosis during hypertension.

2.4.2 Reverse structural remodeling in humans and other animal models

Reverse remodeling has been shown in human AF as well as in animal models of pacing induced AF and heart failure. [61, 189, 193, 199, 224-227]. Ausma *et al* has shown that recovery in structural remodeling was a slow process and more difficult than electrical remodeling following cessation of tachy-pacing [227]. In humans, John *et al* demonstrated that atrial electrophysiologic and electroanatomic abnormalities that result from chronic stretch due to MS reverses after MC [187]. Specifically to hypertension, clinical studies and systematic review have shown reduction in the risk of developing new-onset AF in at-risk with anti-hypertensive agents suggesting reverse remodeling [237, 238]. Our findings showed that anti-hypertensive treatment reversed structural remodeling which could at least, in part, be due to reduced hypertrophy, inflammation and interstitial and endomysial fibrosis. Atrial dilatation and function in all our treated groups were not reversed despite recovery in other structural abnormalities. It is likely that longer duration of therapy may eventually lead to further recovery in these parameters. Additionally, increased connexin43 expression in spontaneously hypertensive rats fed with red palm oil has been suggested to provide anti-arrhythmic effects [239]. Our study included reversal of renally induced hypertension with calcium channel blocker and beta-blocker where connexin43 expression was equally restored to normal levels at the same systolic blood pressure levels in both groups. Our results suggest that reverse structural remodeling involves connexin43 disorganization during hypertension and a possible re-facilitation of electrical coupling with anti-hypertensive treatment.

Furthermore, our study also shows more evidence for the contribution of CTGF and TGF-ß$_1$ in fibrotic substrate formation which eventually is responsible for structural remodeling. Further, our results also demonstrate that these altered protein expressions could be reversed and thus resulting in reverse atrial structural remodeling.

2.4.3 Reverse remodeling and class of anti-hypertensive agents

Specific to the hypertensive substrate for AF, the jury is still out on the best anti-hypertensive agent for secondary prevention. Conflicting data exists regarding the efficacy of different class of anti-hypertensive agents [190, 240-243]. Several secondary prevention trials have reported that inhibitors of the renin angiotensin system may not reduce the risk of arrhythmia recurrence in AF patients [240, 241]. Yamashita *et al* showed that candersartan did not have any advantage over amlodipine in reduction the frequency of paroxysmal AF during treatment of hypertension [190] whereas telmisartan was shown to be more effective than amlodipine in preventing AF recurrences in hypertensive patients with paroxysmal AF [243]. Further, beta blockers have been suggested to reduce remodeling in congestive heart failure and possess anti-arrhythmic effects through reduction of myocyte hypertrophy and apoptosis [244]. Reverse remodeling by beta blockers is brought about by reducing LV volume and improving systolic function [245]. Our results are in keeping with previous observations that beta blockers and calcium channel blockers cause significant structural reverse remodeling. These beneficial

effects were comparable at similar blood pressure level suggesting ‘no class effect’ with different anti-hypertensive agents.

2.4.4 Clinical implications

Our results demonstrate that structural remodeling is progressive and with treatment, could be reversible. The results also suggest that hypertension should be treated aggressively and at an early stage to reduce the atrial insults seen with progressive atrial structural remodeling in hypertension [4]. Appropriate management of blood pressure with anti-hypertensive drugs could help to manage and reduce AF incidence in patients with high blood pressure.

2.4.5 Limitations

1K1C renovascular hypertension may not represent essential hypertension which is multi-factorial and develops over a long period of time in humans. Further, since this is a renally challenged model, ACE inhibitors which have been shown to have potent anti-fibrotic effects could not be studied. The observed improvements in CTGF and TGF-$ß_1$ may have contributed to reduction in fibrosis although other candidate markers may also be contributors that are yet to be fully studied. In addition, since these studies are performed in animal models, careful extrapolation of these results in the clinical area are warranted. Further research is warranted to clarify the understanding of the complex mechanism of fibrosis.

2.5 Conclusions

Our study demonstrates reverse structural remodeling with anti-hypertensive agents. These beneficial effects were similar with different therapy at similar blood pressure level suggesting ‘no class effect’ seen.

2.6 Figures

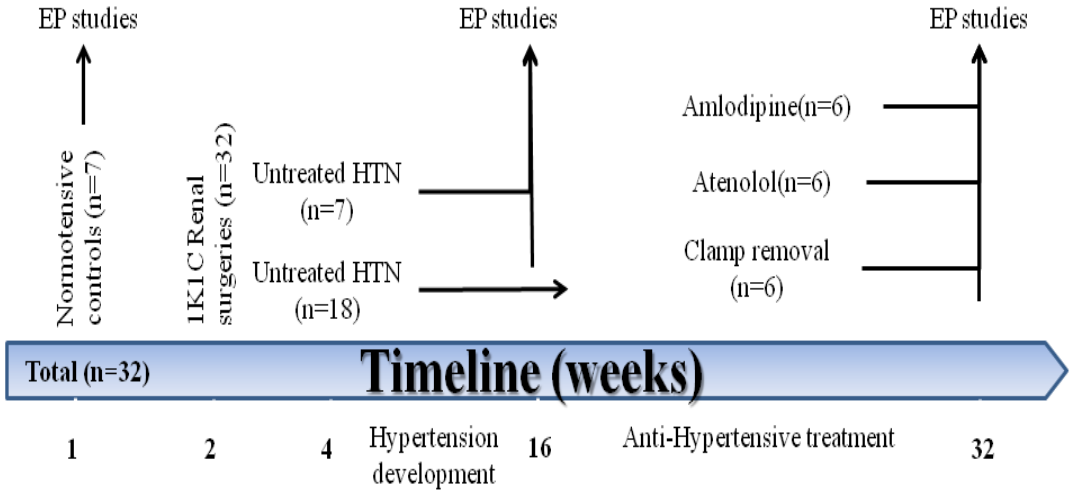

Figure 1: Study timeline

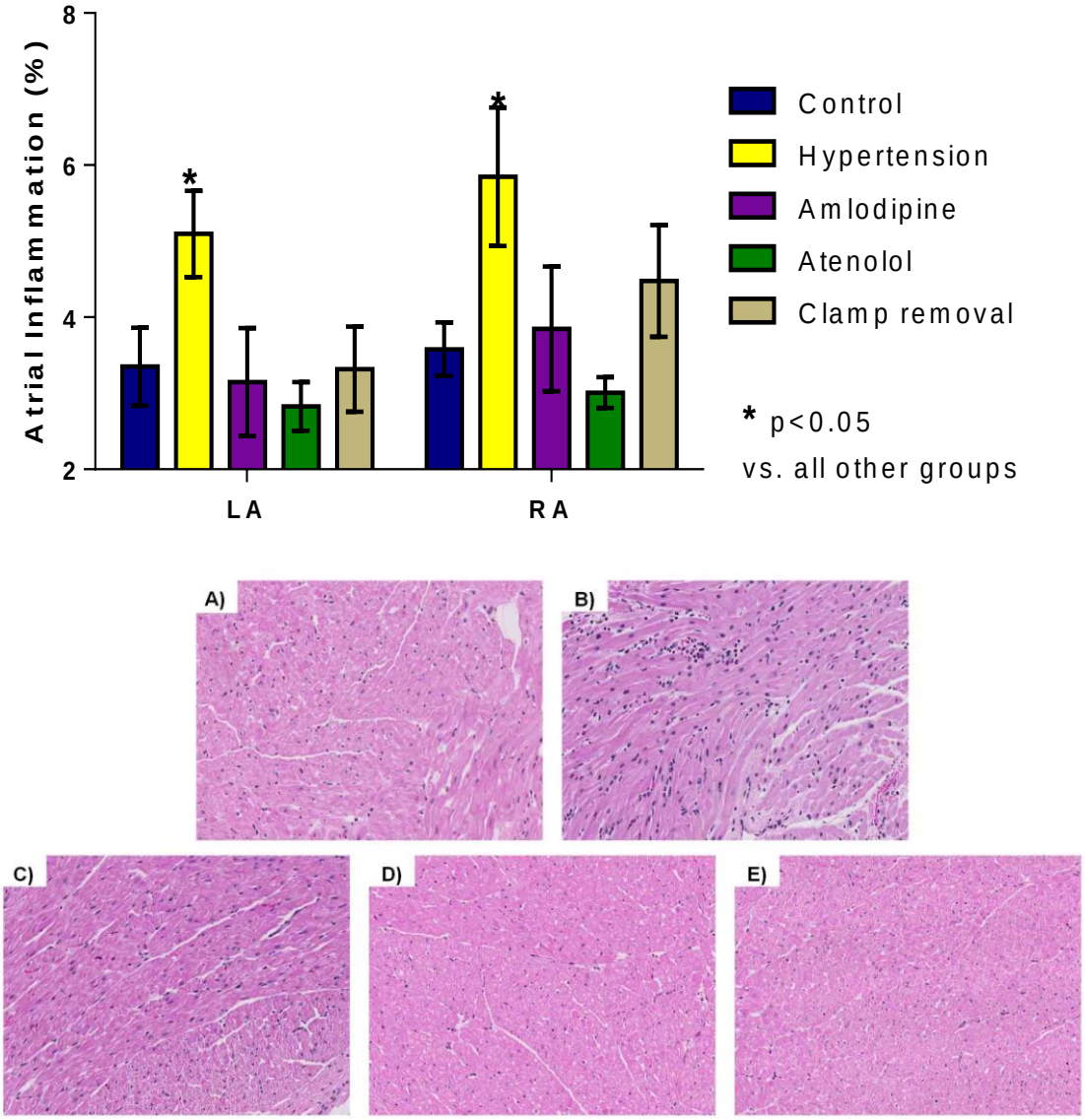

Figure 2: Inflammatory infiltration; A) Control; B) Hypertension; C) Amlodipine; D) Atenolol; E) Clamp removal

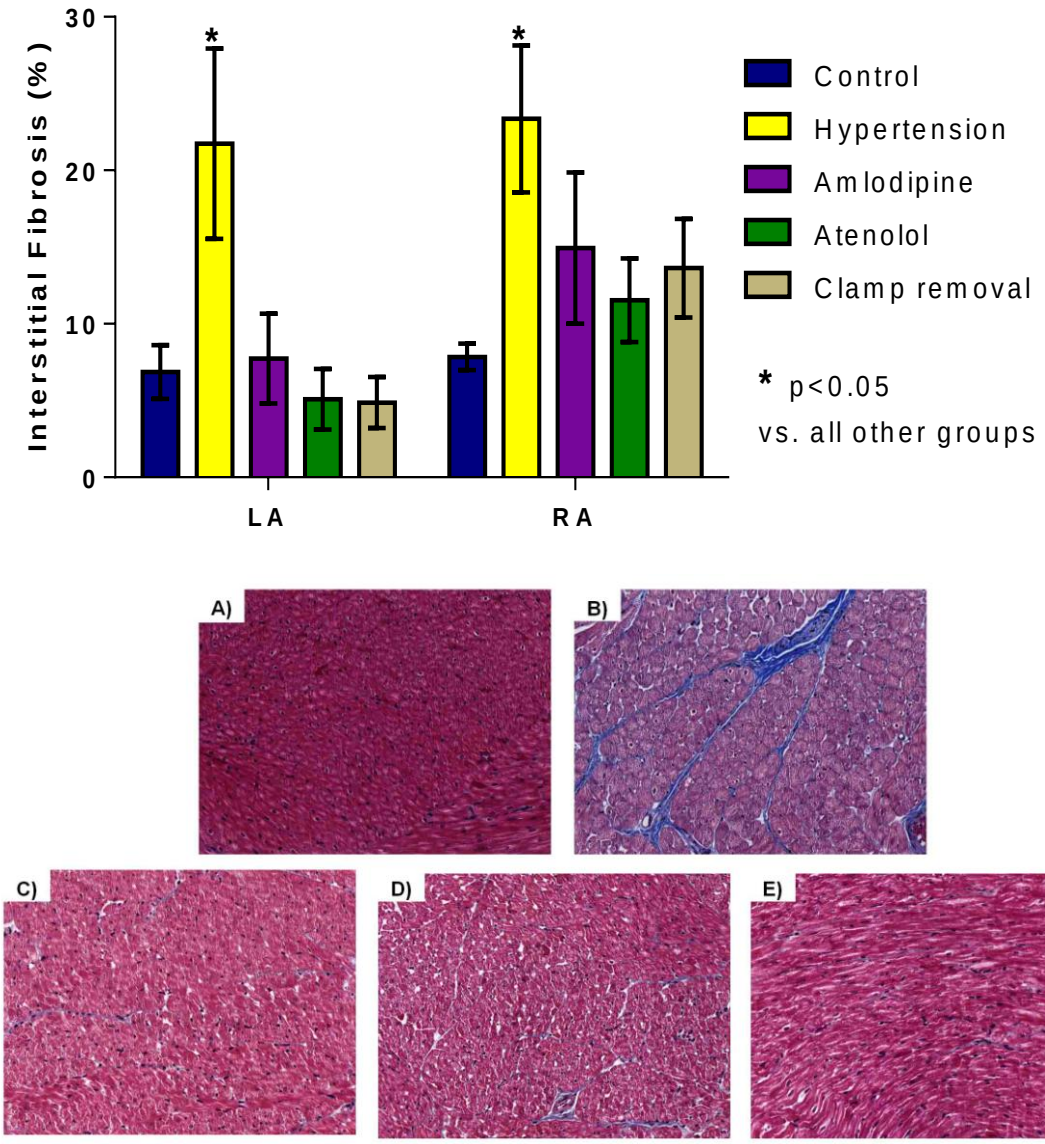

Figure 3: Fibrosis; A) Control; B) Hypertension; C) Amlodipine; D) Atenolol; E) Clamp removal

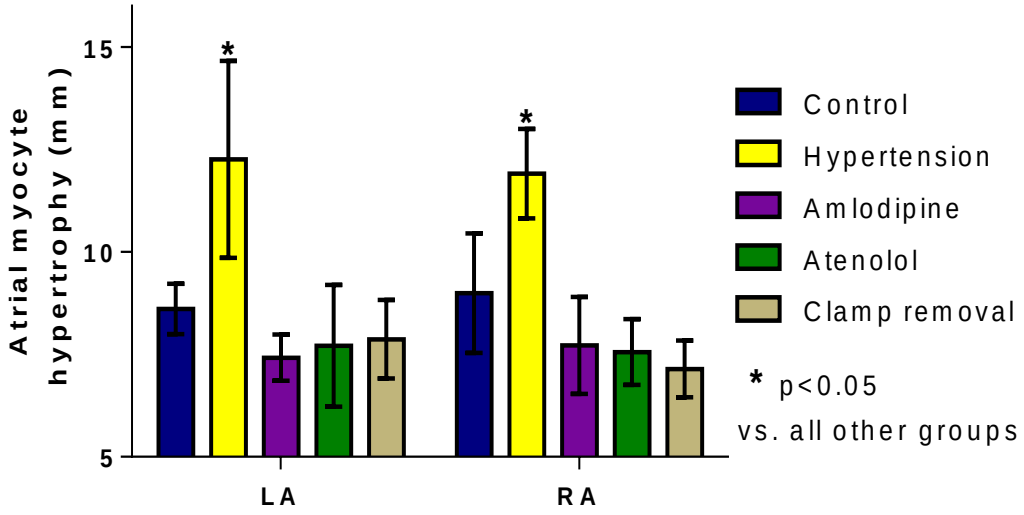

Figure 4: Hypertrophy

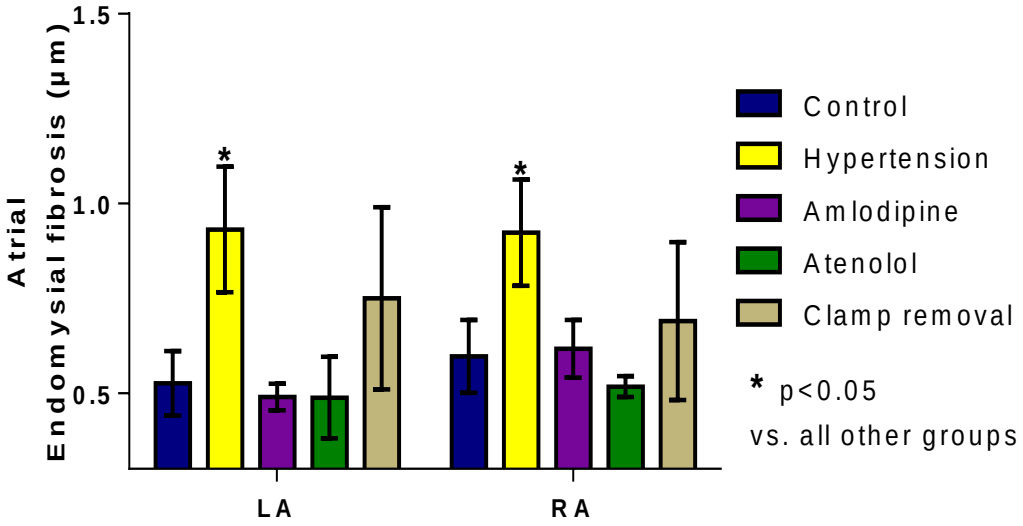

Figure 5: Endomysial fibrosis

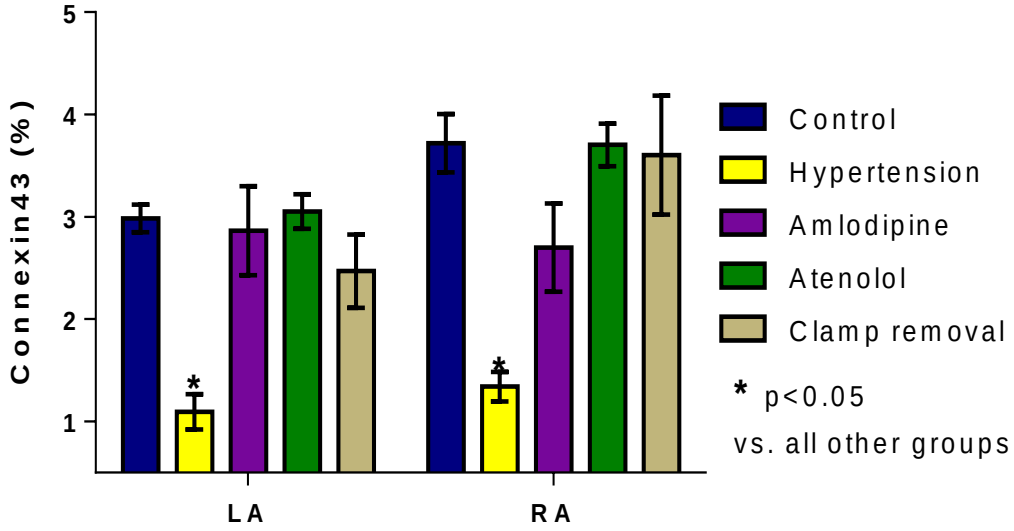

Figure 6: Connexin43 expression

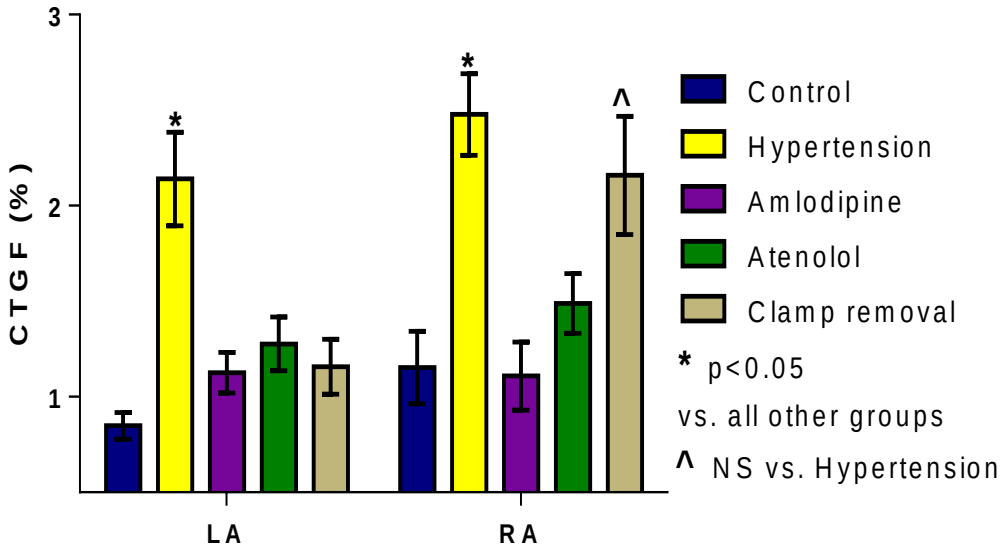

Figure 7: CTGF expression

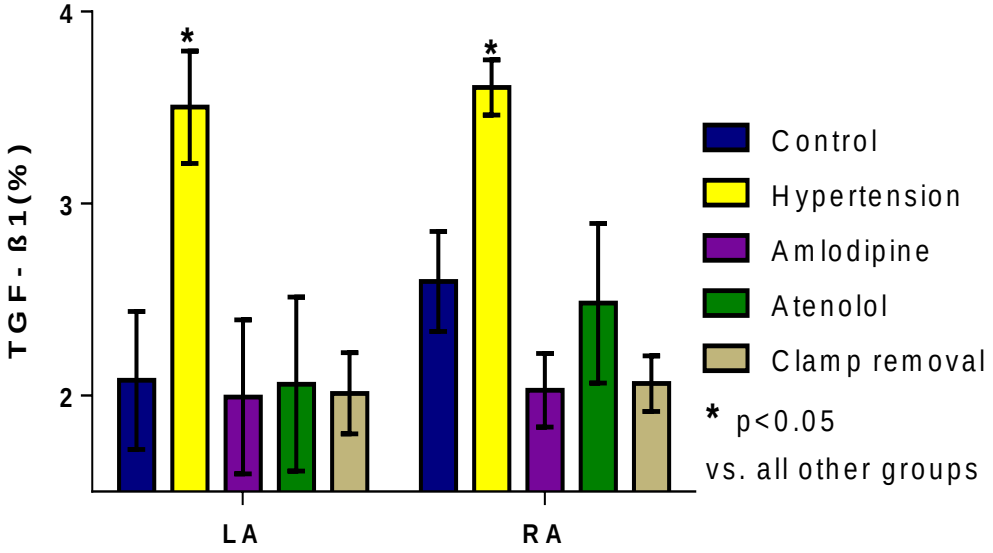

Figure 8: TGF- ß1 expression

2.7 Tables

	Control	**Hypertension**	**Amlodipine**	**Atenolol**	**Clamp removal**
Total (n)	7	7	6	6	6
Weight (kg)	60±3	57±3	65±2	60±5	63±7
Systolic blood pressure (mmHg)	115±7*	156±5	157±7	160±7	151±7
	After 16 weeks treatment		133±3*	131±11*	125±7*
LAEDV (mL)	24±2*	48±8	54±13	41±8	33±4
LAEF (%)	32±3*	13±5	27±16	30±9	25±11
LVEDV (mL)	92±7	103±14	102±15	114±13	113±23
LVEF (%)	45±4	42±5	43±12	40±11	37±8
Pathological examination					
RV mass (g)	47±5	59±8	43±3	55±13	56±15
LV mass(g)	106±9*	129±6	98±9*	106±5*	111±19
IVS mass (g)	44±7*	62±5	42±3*	44±6*	54±14
IVS thickness (mm)	11±1*	18±1	11±1*	14±1*	11±2*
* $p<0.05$ vs. Hypertension					

Table 1: Animal Characteristics and MRI Data

	Control	Hypertension	Amlodipine	Atenolol	Clamp removal
Left atrium					
Myocyte size Epicardial Endocardial	 8.6±0.54* 7±0.35*	 13.6±2.8 10.8±3.2	 8.0±1.0* 8.1±0.9	 8.1±1.2* 8.6±3.1	 8.3±1.17* 7.96±1.65*
Intermyocyte distance Epicardial Endocardial	 0.42±0.1* 0.40±0.05*	 0.93±0.34 0.91±0.45	 0.56±0.20* 0.52±0.15*	 0.54±0.28* 0.51±0.23*	 0.58±0.40 0.49±0.18*
Right atrium					
Myocyte size Epicadial Endocardial	 8.99±1.30* 7.00±0.63*	 12.44±1.55 10.32±2.68	 7.67±1.03* 7.79±1.54*	 7.34±0.78* 7.28±0.67*	 7.79±1.14* 7.48±1.08*
Intermyocyte distance Epicardial Endocardial	 0.46±0.08* 0.44±0.08*	 0.91±0.45 0.92±0.43	 0.55±0.18* 0.54±0.18*	 0.50±0.07* 0.49±0.1*	 0.61±0.36 0.47±0.09*
* p<0.05 vs. Hypertension					

Table 2: Hypertrophy and endomysial fibrosis in LA and RA

3 CHARACTERISATION OF ELECTRICAL 'REVERSE' REMODELING OF HYPERTENSIVE ATRIA WITH PHARMACOLOGICAL INTERVENTION

3.1 Introduction

Hypertension accounts for most atrial fibrillation (AF) than any other risk factors due to its high prevalence. It affects nearly 28.6% of the US population and 972 million people in the world [26, 98]. In addition to its 14% responsibility of AF incidence, it further increases the risk of AF by 1.5 and 1.4 fold in women and men respectively [26]. Despite the high AF incidence in hypertensive subjects, very few studies have characterized the atrial electrical remodeling of hypertensive atria [101, 102, 246].

The electrical changes with hypertension are thought to include changes in ERP, increased conduction slowing/ heterogeneity and increased AF inducibility. Electrical remodeling has been shown in different substrates for AF including heart failure, mitral valve disease, obesity and sleep apnea [7, 112, 115-117, 247, 248]. Previously, Wijffels *et al* demonstrated the 'AF begets AF' phenomenon during the maintenance of electrical remodeling process in AF [54]. A number of studies have shown the reversible nature of the atrial electrical properties in different substrate

models and various ablation procedures with significant improvement in atrial volume, function and minimizing AF recurrence. [61, 187, 193, 249-256].

Whether electrical remodeling in hypertension is reversible is not known. Therefore, in this study we intend to develop a renovascular hypertensive ovine model as described by Goldblatt *et al* [257]. Further, we studied the reverse remodeling process by lowering the blood pressures pharmacologically with different anti-hypertensive drugs and physiologically by deflating the clamp and assessed the electrophysiological characteristics.

3.2 Methods

3.2.1 Study approval and guidelines

This study was approved by the *'University of Adelaide Animal Ethics Committee'* and '*SA Pathology Animal Ethics Committee'*. Guidelines from the "Australian code of practice for the care and use of animals for scientific purposes" 7th edition, 2004 adopted by the 'National health and medical research council' were followed for all the experimental procedures.

3.2.2 Animal Housing & Preparation

Male merino cross sheep were used for this study. All animals were held in group in open paddocks. Animals were placed in a 22°C temperature controlled room 24 hours pre-operative and until full recovery of 2-3 weeks post operatively for survival procedures. Food and water were provided *ad libidium.*

Before each surgical procedure, animals were given water intake only and taken off from food 24 hours prior to general anaesthesia procedure and followed by intravenous sodium thiopentone (10-15 mg/kg) for induction to facilitate endo-tracheal intubation. Isoflurane 2-4% in 100% oxygen at 4L/min was exercised for maintenance throughout the procedure. Lignocaine 2mg/kg was used as local anaesthetic during surgery. Non-invasive blood pressure, heart rate, pulse oximetry, end-tidal CO_2 and temperature were continuously monitored during the whole surgical procedure. Amoxycilin (1 ml/20kg) and Buprenorphine (0.005-0.01 ml/kg) were administered intramuscularly for three days following renal surgeries. General anaesthesia was performed prior to renal surgery, cardiac MR scans and terminal electrophysiology study.

3.2.3 Study timeline:

Seven sheep were used as normotensive controls. All remaining sheep underwent renal surgeries to develop high blood pressure for 12 weeks. At the end of 12th

week, 7 hypertensive animals underwent terminal electrophysiological studies. All remaining animals were grouped sequentially into three different blood pressure lowering groups, namely, Amlodipine (10mg daily), Atenolol (100mg daily) and Clamp removal groups. Treatment was designated for 16 weeks after which all animals were subjected to terminal electrophysiological studies (Figure 9).

3.2.4 'One Kidney One Clip' renovascular hypertension Model

Conventional 'one kidney one clip' model as previously described was used [101]. The animal was placed on left lateral recumbent position under general anaesthesia. Nephrectomy was performed on the right kidney. Two finger breadths were allowed from lateral extent of the paraspinal muscles for making an incision from just beneath the rib cage for about six inches vertically. The perinephric fat and Gerota's fascia were carefully separated from the surface of the kidney. The ureter and renal vessels were separately ligatured and right kidney was removed following which the wound was closed in layers.

In this study, we performed both nephrectomy and renal artery occlusion on the same day. A new vascular occluder clamp was used for the study (heavy duty 8mm, DOCXS Biomedical Products, Ukiah, CA, USA) in order to facilitate blood pressure titration during hypertension development (maintained at 150-160 mmHg approximately and reversal). Following nephrectomy, the sheep was placed onto the right lateral recumbent position. Blunt dissection was performed via similar incision

as the right side to expose the renal artery without interrupting the perinephric fat and Gerota's fascia on the left kidney. Vascular occluder clamp was placed around the renal artery with the actuating tube connected to an external port. The port was placed subcutaneously and sutured to maintain in a stable position. During the surgical procedure, approximately 50% occlusion of renal artery was verified with flow transducer (Transonic Flowmeter TS-401 with precision flow probe, Transonic Systems Inc., NY, USA) and Doppler velocity (Acuson XP-128, 7 MHz probe, Siemens Medical Systems, PA, USA) under direct vision to provide guidance for subsequent vascular occluder inflation.

Heparin (5000 I.U) was given for two days post-operatively to prevent any thrombosis due to renal artery clamping. After surgical procedures, sheep were held in individual pen houses and monitored twice daily during recovery. After complete recovery, usually 2-3 weeks, sheep were sent back to paddocks. Induction of hypertension was initiated after 2-3 weeks of complete recovery from the surgery.

Following renal surgeries, animals were subjected to non invasive blood pressure (BP) procedure to ensure they are acclimatized to the technique. This technique was performed during the animal's recovery from the renal procedure. Measurements were taken twice weekly at the same time of the day by the same handlers in a metabolic crate. All blood pressure measurements on the animals were done 3-5 times with the animals in a completely relaxed state. BP readings were averaged from all repeated measurements. Non invasive blood pressure levels were measured

by placing the blood pressure cuff over the brachial artery of the forelimb in conscious animals (Datascope Passport 2, Datascope Corp., NJ, USA). The measurements were reproducible during repetition.

3.2.5 Electrophysiological study

After attaining the specific timeline, all animals underwent terminal open chest electrophysiological studies under deep sedation. Midline thoracotomy surgery was performed to expose the pericardial region of the heart. Physiological gases and body temperature were maintained with automatic ventilation throughout the electrophysiological assessment study. The pericardium over the atria was divided to afford access to sliding the custom made 80-electrode epicardial plaque for mapping (Figure 10). The plaque with 4mm inter-electrode spacing was placed on the right (RA) and left (LA) atrium separately with the tail connected to a computerized recording system (LabSystem Pro, Bard Electrophysiology, MA, USA). Continuous recording of surface-ECG and overlapping bipolar electrograms were stored for offline analysis. Electrograms were notch filtered from 30-500Hz, and measured with sweep speed of 200mm/s for analysis.

Electrophysiological parameters analyzed in this study represent the electrical and structural remodeling which is conventionally accepted in this field of research. The measured parameters are detailed previously in chapter 2.

3.2.5.1 Atrial effective refractory period

Atrial effective refractory period (ERP) was measured at double the diastolic threshold at varying cycle lengths (S1) of 500, 400, 300 & 200 ms from 8 different sites (RAA, Right atrial free wall, LAA, left atrial free wall, right and left atrial medial and lateral regions). Eight basic stimuli, defined as S1, were followed by a premature beat (S2). This was repeated with a 10ms decrement until the loss of wave propagation. ERP was defined as the shortest S1-S2 coupling interval resulting in a propagated wave response. Measurements were repeated thrice to obtain an average ERP at different CLs in each site. ERP heterogeneity was determined with coefficient of ERP variation calculated as Standard deviation of ERP/Mean * 100%.

3.2.5.2 Atrial conduction

Conduction was assessed at S1 and S2 wave propagations by making conduction activation maps with customized semi-automated software. Vectors within each triangle of electrodes were used to calculate local conduction velocity and a total averaged conduction velocity was determined at different CLs at each site [258, 259]. Local conduction was measured on S1 and S2 beats at different cycle lengths of 500, 400, 300 and 200 ms in all specified sites.

Conduction heterogeneity was calculated using phase mapping method at both S1 and S2 propagated wave responses [260]. The longest activation time difference at

each electrode site was used to plot the phase map and histogram (Figure 19). Absolute conduction phase delay was determined by the difference between 5th and 95th percentile of phase distribution (P5-95). The conduction heterogeneity index was derived from dividing the absolute phase delay by its median (P50).

3.2.5.3 AF Inducibility

Degree of AF inducibility was measured as a ratio of number of AF episodes to the total number of S1-S2 pacing trains and represented in percentage. AF was defined as irregularity in atrial electrograms lasting for ≥2 seconds.

3.2.5.4 Electrogram characteristics during AF

AF episodes of each animal group were analyzed offline using customized software. Only episodes >8 seconds were used.

The Ensite NavX algorithm (St. Jude medical, MN, USA) measures the complex fractionated electrogram-mean (CFE-m) using the mean of time intervals between marked deflections [261] according to the following parameters: Refractory period of 40ms; Minimum electrogram width of 10ms; and peak to peak sensitivity of 0.05-0.1mV .

Dominant Frequency: Electrograms were rectified and filtered using Butterworth filters (1-20Hz) and edge-tapered with a Hanning window before Fast Fourier Transform. DF was defined as the frequency containing maximum power within the frequency domain between 3–15 Hz. Organization index less than 0.2 were excluded. DF max was defined as the highest 20% of the frequencies on the plane of the atria in the given arrhythmia episode.

3.2.6 Statistics

All data were expressed in mean ± standard deviation. Analyses of differential effects of blood pressure lowering therapies on electrical and structural parameters were performed using analysis of variance (ANOVA). Sidak post-hoc tests were used to delineate the differences between specific groups. Statistical significance was taken as $P<0.05$.

3.3 Results

One-kidney, one-clip hypertension model was developed in thirty six age matched male merino cross sheep (61±6 kg). Four out of thirty six sheep had a blocked or inadvertent over-inflation of the vascular occluder leading to renal failure and pulmonary oedema during the period of hypertension development and were excluded from the study. Remaining animals developed renovascular hypertension in

a timely fashion for a mean duration of 12±2 weeks. There was no cardiac or renal failure in all the hypertensive animals during the course of the study.

3.3.1 Blood pressure measurements

From baseline, all animals developed high systolic blood pressure of 156±7 mmHg in 12 week period.

Sixteen weeks of Amlodipine, Atenolol and clamp removal treatment reduced sBP to 133±3 mmHg ($p<0.001$), 131±11 mmHg ($p=0.007$) and 125±7 mmHg ($p<0.001$) respectively showing significant reversal compared to hypertension group (Figure 11).

3.3.2 Atrial electrophysiological reverse remodeling

3.3.2.1 Effective refractory period

Mean atrial refractoriness at S1 300ms cycle lengths during hypertension was unchanged compared to control group in both LA (110±19 vs. 113±13; $p=0.974$) and RA (157±39 vs. 154±27; $p=1.00$). After treatment, amlodipine showed a significant increase in atrial ERP as compared to hypertension group in both LA (110±19 vs. 161±39 ms; $p<0.001$) and RA (157±39 vs. 197±54; $p<0.001$) whereas with atenolol treatment ERP was increased only in LA (110±19 vs. 152±32 ms; $p<0.001$) but not

in RA (157±39 vs.163±19; p= 0.802). Clamp removal did not have any effect on atrial refractoriness in both LA (110±19 vs. 117±17 ms; p=0.456) and RA (157±39 vs. 162±40; p=0.876). ERP changes were similar in all measured pacing cycle lengths (Figure 12 & Figure 13).

Mean ERP heterogeneity showed a positive trend in hypertensive group compared to control group in LA (14.71±1.11 vs. 10.04±1.22; p=0.073) though not significant. In RA, ERP heterogeneity was significantly reduced (18.63±1.19 vs. 12.96±1.33; p=0.024) Amlodipine did not show any effect on both LA (14.71±1.11 vs. 17.23±1.16; p=0.992) and RA (18.63±1.19 vs. 18.67±1.19; p=1.000) whilst in atenolol group, ERP heterogeneity worsened in LA (14.71±1.11 vs. 20.50±1.30; p=0.012) and significantly reversed in RA (18.63±1.19 vs. 10.21±1.22; p<0.0001. No significant reversal was seen in clamp removal group in both LA (14.71±1.11 vs. 11.58±1.08; p=0.499) and RA (18.63±1.19 vs. 16.41±1.16; p=0.952).

3.3.2.2 Atrial conduction

Mean atrial conduction velocity at S1 300 ms cycle lengths was significantly reduced in hypertension compared to control group in both LA (0.88±0.14 vs. 1.06±0.10; p<0.001) and RA (0.89±0.05 vs. 1.04±0.09; p<0.001). This conduction slowing was significantly reversed in amlodipine [LA – 0.88±0.14 vs. 1.09±0.25 m/s; p<0.001; RA – 0.89±0.05 vs. 1.00±0.12 m/s; p<0.001], atenolol [LA – 0.88±0.14 vs. 1.10±0.15 m/s; p<0.001; RA – 0.89±0.05 vs. 1.05±0.13 m/s; p<0.001] and clamp

removal [LA – 0.88±0.14 vs. 1.02±0.14 m/s; p<0.001; RA – 0.89±0.01 vs.1.02±0.14 m/s; p<0.001] treatment (Figure 14). Conduction slowing changes were similar in all measured pacing cycle lengths.

Atrial conduction heterogeneity as calculated with phase mapping at 300 ms cycle length was increased in hypertension compared to control group in both LA (1.67±0.70 vs. 1.37±0.32; p=0.005) and RA (2.16±1.49 vs. 1.31±0.31; p<0.001). Conduction heterogeneity was significantly reversed after treatment with amlodipine [LA – 1.67±0.70 vs. 1.37±0.28; p=0.002; RA – 2.16±1.49 vs. 1.54±0.58; p<0.001], atenolol [LA – 1.67±0.70 vs. 1.34±0.30; p=0.001; RA – 2.16±1.49 vs. 1.32±0.25; p<0.001] and clamp removal [LA – 1.67±0.70 vs. 1.40±0.62; p=0.006; RA – 2.16±1.49 vs. 1.61±0.50; p<0.001] treatment (Figure 15 & Figure 19).

3.3.2.3 AF Inducibility & Duration

During EP study, hypertensive group (165 episodes, 7.9%) showed an increased AF vulnerability whereas treatment with amlodipine (48 episodes, 2.3%), atenolol (53 episodes, 2.7%) and clamp removal (84 episodes, 5.0%) groups showed significant reduction in AF vulnerability.

However, mean AF duration during hypertension (24±98 s) did not change after treatment with amlodipine (39±76; p=1.0), atenolol (34±111; p=1.0) and clamp removal (54±122; p=1.0) (Figure 16). Sustained AF, as defined by the continuance

of AF for more than 15 minutes was significantly higher in hypertensive group (2 out of 7) compared to control group (0 out of 7). The propensity of sustained AF was reversed with amlodipine (0 out of 6) and atenolol (0 out of 6) although not with clamp removal (2 out of 6).

3.3.2.4 AF electrocardiogram characteristics during AF

Compared to hypertensive animals, CFE-m as measured using NavX CFAE algorithm was significantly increased in amlodipine group (99±20 vs. 117±10 ms; p = 0.032), unchanged in atenolol group (96±20 ms; p = NS) and decreased in clamp removal group (75±11 ms; p<0.001) (Figure 17).

Compared to hypertensive group, mean dominant frequency was significantly reduced with amlodipine treatment (7.4±1.1 vs. 6.4±0.23; p=0.002) while having no changes with atenolol (7.3±0.9; p=0.946) and clamp removal (8.6±0.8; p=0.192) treatment groups (Figure 18). Similarly, DF max was significantly reduced after amlodipine treatment compared to hypertensive group (8.8±0.02 vs. 7.4±0.08; p<0.001) but increased significantly with atenolol (10.2±0.1; p<0.001) and clamp removal (10.0±0.04; p<0.001) treatment groups.

3.4 Discussion

This is the first study to characterize the reverse electrical remodeling process in hypertensive substrate of large animal model. Treatment with anti-hypertensive drugs resulted in significant reversal in these electrophysiological parameters.

- Hypertension caused electrical remodeling through conduction slowing/heterogeneity and increased vulnerability to AF.
- Anti-hypertensive treatment resulted in similarly lowered blood pressure levels.
- All treatment groups increased conduction velocity, decreased conduction heterogeneity and reduced vulnerability to AF.
- Only amlodipine increased ERP in both atria while atenolol increased ERP in LA only.
- Amlodipine treatment resulted in increased CFE-mean and reduced DF, while both parameters were unchanged in atenolol.
- CFE-m reduced significantly while DF was unchanged in clamp removal treatment group.

Atrial remodeling due to hypertension was found to be progressive with early electrical remodeling from 5 weeks of hypertension followed by more permanent structural changes with increased fibrosis and resultant conduction abnormalities from 10 weeks onwards [262]. In difference hypertension models, variable ERP,

increased conduction slowing and heterogeneity and increased vulnerability to AF has been reported [102, 104, 231, 263]. Kistler *et al* showed evidence of electrical and structural effects of atrial substrate in a chronic hypertensive ovine model of 4-5 years which was exposed to pre-natal corticosteroids [102]. They demonstrated a significant increase in conduction slowing, conduction heterogeneity and increased induced AF durations although atrial refractoriness was unchanged in this novel model. Lau *et al* showed that the substrate could develop in as early as 7 weeks from onset of hypertension and demonstrated the progression of electrical and structural remodeling with time [101, 246]. They showed a significant increase in refractoriness, conduction slowing, conduction heterogeneity and increased AF propensity and durations during inducibility tests within 5 weeks from onset of hypertension.

3.4.1 Reverse remodeling of abnormal atrial substrate

Reverse remodeling in a canine model of congestive heart failure was demonstrated using angiotensin converting enzyme inhibition [189]. Goette *et al* suggested that shorter duration of arrhythmia was sufficient to cause electrical remodeling which was reversed after maintaining sinus rhythm [57]. Everett *et al* reported on reverse electrical remodeling in a canine model of chronic AF with mitral regurgitation within 7 to 14 days although the vulnerability to AF persisted due to the underlying structural abnormalities caused by the atrial substrate [193]. Mangrum *et al*, in a chronic AF canine model showed that atrial defibrillation threshold was reduced

with reverse electrical remodeling attained by cardioversion and this reduction corresponded to increased atrial fibrillation cycle length, increased atrial refractoriness, and decreased refractory period dispersion [250]. The progressive nature of atrial remodeling with increased exposure to hypertension highlights an opportunity to arrest or reverse the atrial structural and electrical changes. This study confirms the beneficial atrial effects of blood pressure lowering therapies whereby reduced atrial insults from lower systolic blood pressure levels allowed for reversal of atrial remodeling.

In humans, John *et al* demonstrated the reversal of abnormal electrophysiological and electro-anatomical characteristics seen in chronic stretch [187]. A retrospective longitudinal cohort study showed that ACE inhibition was associated with reduced incidence of AF risk in hypertensive patients [237]. Further, a systematic review demonstrated that both ACE inhibitors and ARBs could significantly prevent AF in hypertensive patients, especially those with systolic left ventricular dysfunction or hypertrophy [238]. Yu *et al* suggested atrial reverse remodeling after cardioversion of long-standing atrial fibrillation in humans [61]. Mitral regurgitation patients undergoing MV repair at an early stage showed a significant LA reverse remodeling [264]. This reverse electrical remodeling was also observed after cardioversion [249].

Our data is the first large animal study providing evidence using high density mapping about comparative anti-hypertensive treatment in AF subset patients. Given

the reversible nature of electrical remodeling in a short period, our study had a relatively longer treatment period which elucidates the reversal of electrical remodeling as shown with improved conduction properties after treatment with anti-hypertensive drugs. Reversal of conduction slowing and heterogeneity in clamp removal group could possibly be due to reduced stretch and dilatation of the atria that occurred initially due to high blood pressure

3.4.2 Electrogram characteristics during reverse remodeling

Complex fractionated electrograms and high dominant frequency are being used as anatomical target sites for catheter ablation [261, 265-268]. A recent study by Yoshida *et al* demonstrated that electrogram organization could predict the left atrial reverse remodeling after restoration of sinus rhythm by catheter ablation in patients with persistent atrial fibrillation [251]. We determined the electrogram organization measured in terms of CFAE algorithm. After treatment with amlodipine, electrogram complexity lessened suggesting an electrical reverse remodeling which although was not found with atenolol treatment. Clamp removal treatment worsened the complexity of electrograms further suggesting that blood pressure lowering may not be sufficient to improve electrocardiogram characteristics suggesting a pharmacological benefit.

Dominant frequency is being discussed frequently during remodeling process of atrial fibrillation. Our results show that dominant frequency and DF max was

reduced with amlodipine treatment but not atenolol. This lets us to speculate that dominant frequency and DF max sites could possibly correlate with intracellular calcium overload which is more diminished with calcium channel blocker than beta blocker, thus the frequencies reversing with amlodipine but not atenolol treatment. Goette *et al* suggested that electrical remodeling could be mediated by rate induced intracellular calcium overload [57]. Recently, Martins *et al* demonstrated that in a sheep model, rate of change of DF could predict the transition from paroxysmal to persistent AF with changes reflected in density levels of sodium, L-type calcium and inward rectifier currents [269]. Since anti-hypertensive drugs have a mechanistic action on the atria, electrical reverse remodeling was observed with pharmacological intervention but not clamp removal which was more physiological. In addition, the above suggested interaction of DF and calcium channel could be the rationale for higher beneficial effects seen in calcium channel blocker.

3.4.3 Clinical implications

Our results demonstrate that electrical remodeling is progressive and with treatment, could be reversible. The results also suggest that hypertension should be treated aggressively and at an early stage to reduce the atrial insults seen with progressive atrial remodeling in hypertension. Appropriate management of blood pressure with anti-hypertensive drugs could help to manage and reduce AF incidence in patients with high blood pressure.

3.4.4 Limitations

Artificial 1K1C renovascular hypertension may not represent essential hypertension which is multi-factorial and develops over a long period of time in humans. Though, with relative to previous studies, our results could possibly be the nearer representation of hypertension as developed in animal model. Further, since this is a renally challenged model, we could not employ ACE inhibitors which have been shown to have potent anti-fibrotic effects and would have been interesting to observe its outcome on hypertensive atria with respect to atrial fibrillation. In addition, since these studies are performed in animal models, careful extrapolation of these results in the clinical area are warranted.

3.5 Conclusions

Our results suggest that anti-hypertensive drugs could significantly influence the electrical reverse remodeling process by reversing the conduction abnormalities of the atria. Given the underlying abnormal remodeling in the atria, electrical remodeling could be reversed more effectively with pharmacological intervention rather than blood pressure lowering *per se*.

3.6 Figures

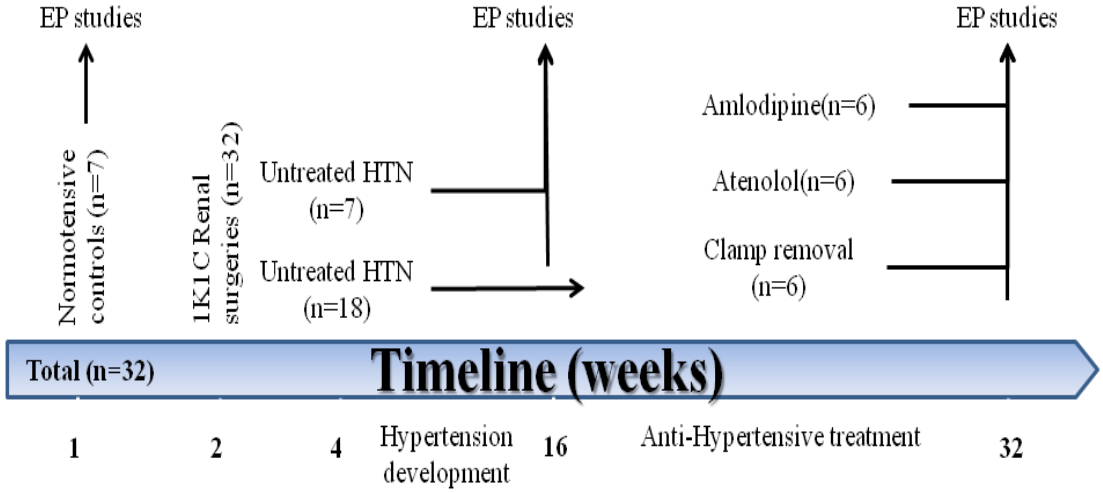

Figure 9: Study timeline

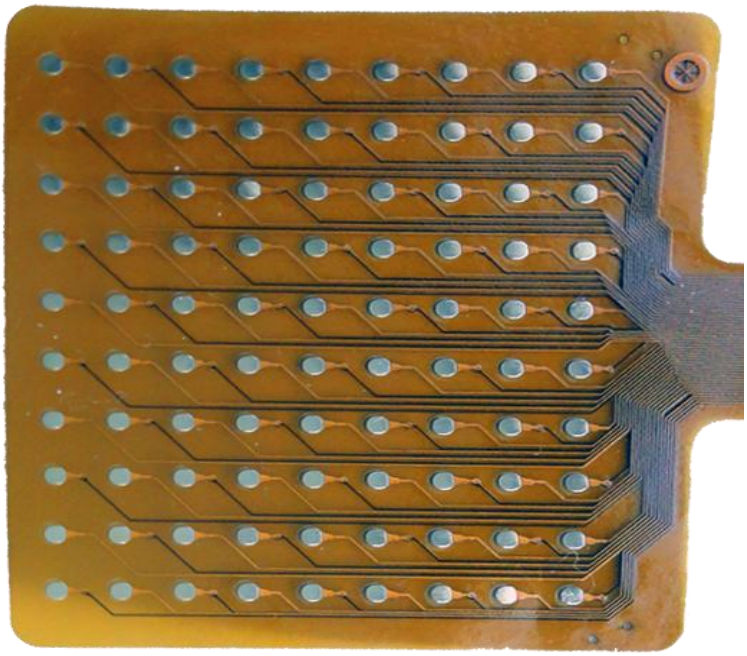

Figure 10: Epicardial plaque with 90 electrodes used for EP study

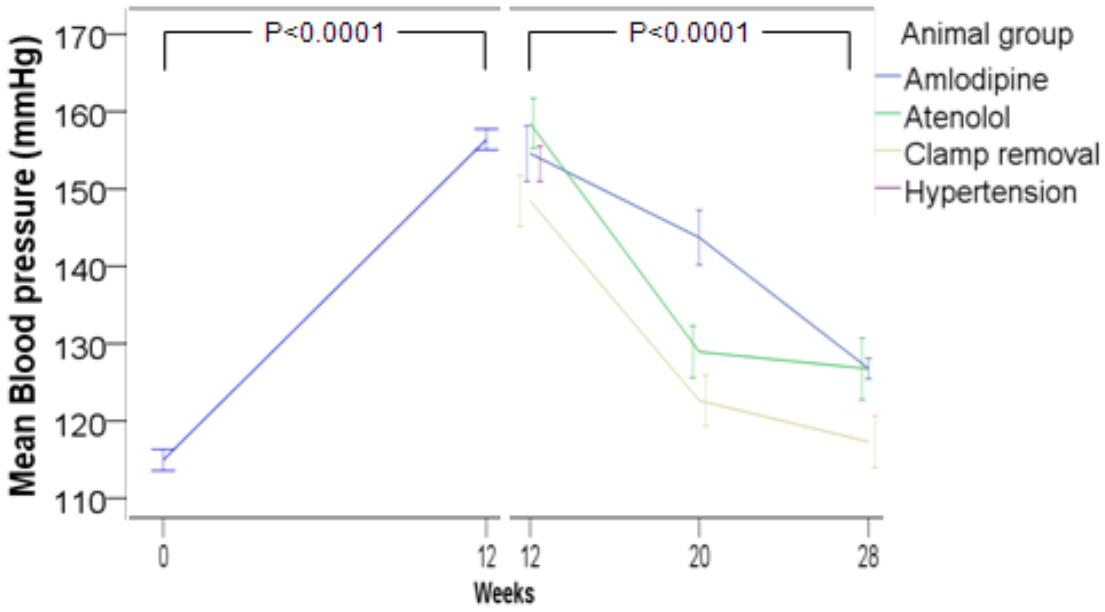

Figure 11: Blood pressure profile before and after treatment

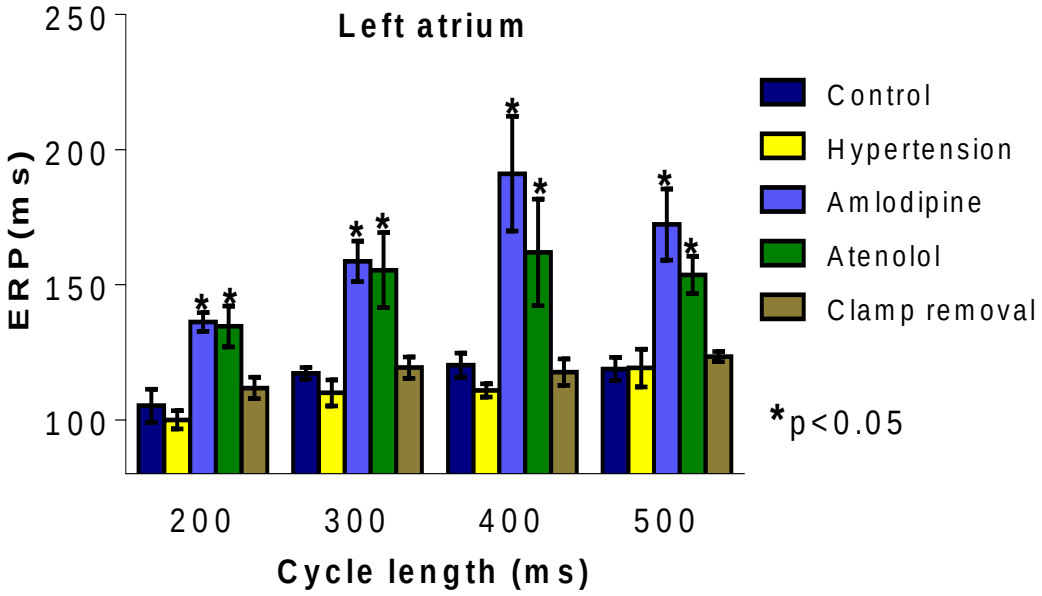

Figure 12: ERP at different cycle lengths in LA

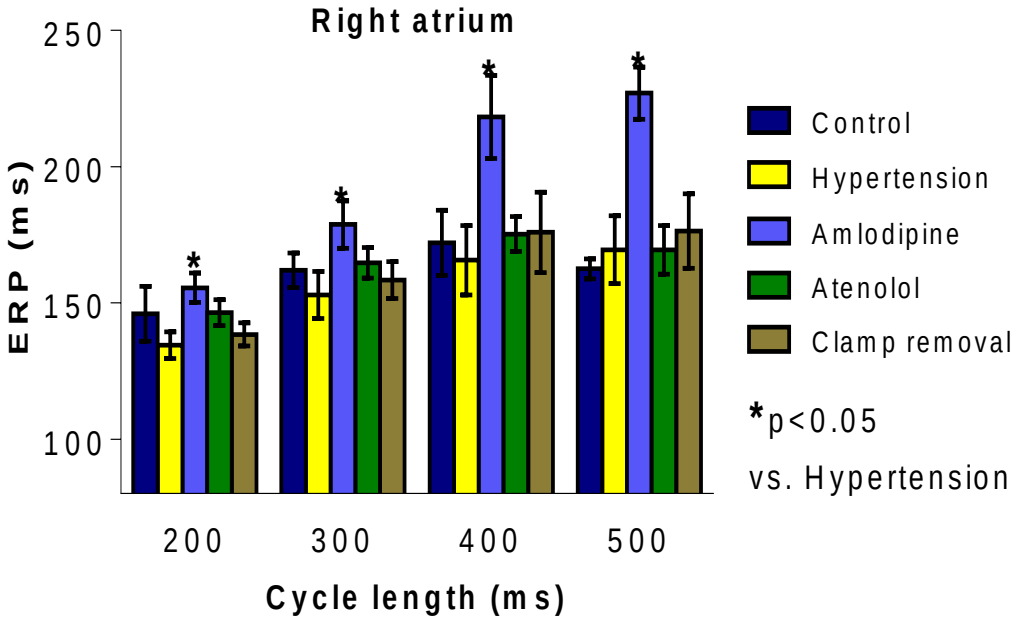

Figure 13: ERP at different cycle lengths in RA

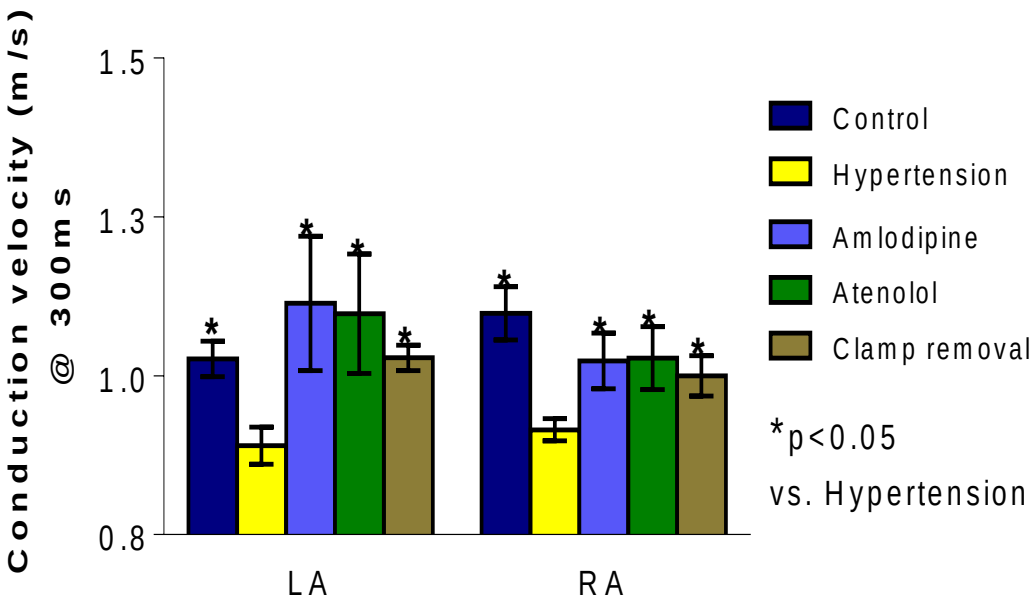

Figure 14: Conduction velocity at 300ms cycle length in LA & RA

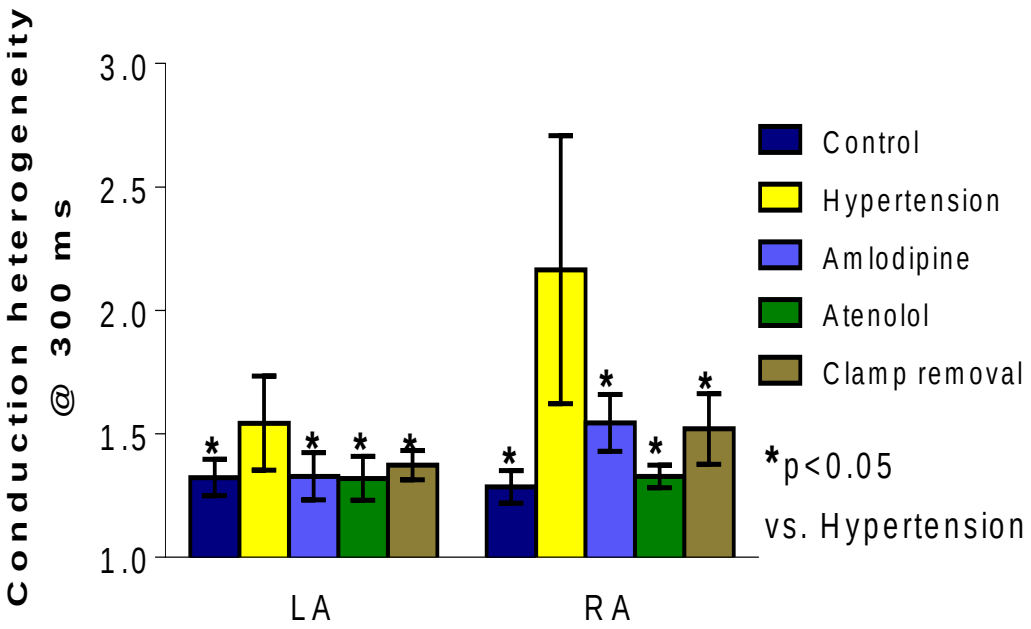

Figure 15: Conduction heterogeneity at different cycle lengths in LA & RA

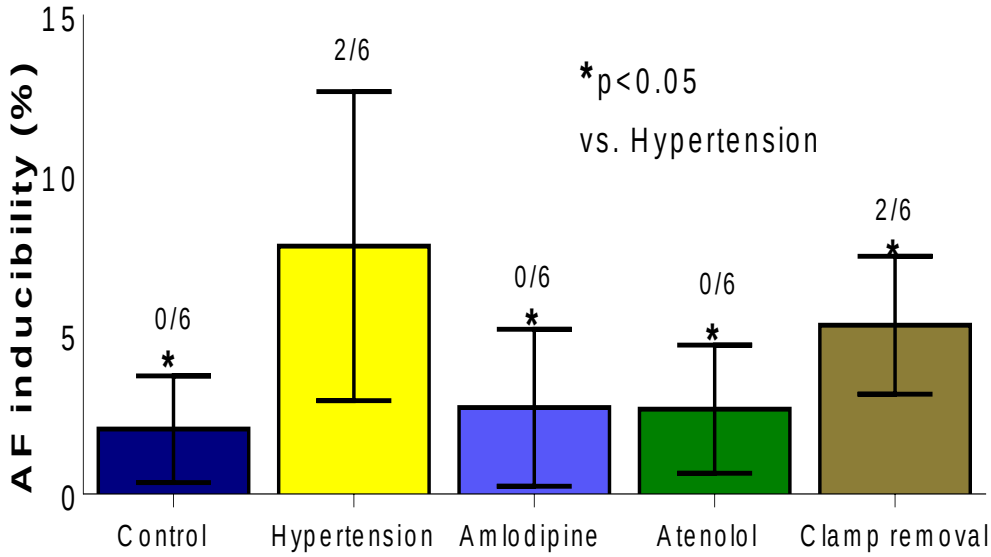

Figure 16: Mean number of AF Episodes with Anti-Hypertensive drugs

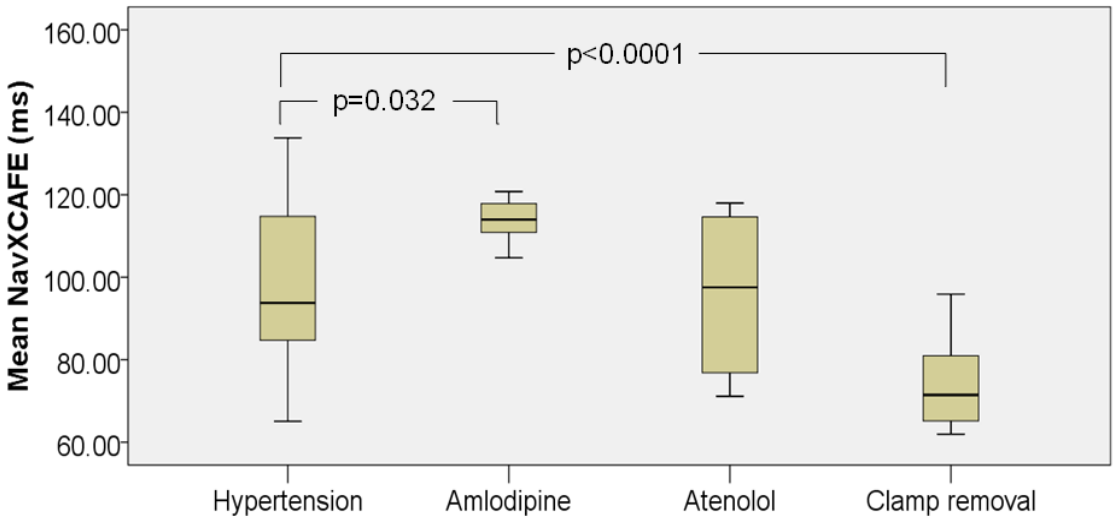

Figure 17: CFAE changes after treatment with anti-hypertensive drugs

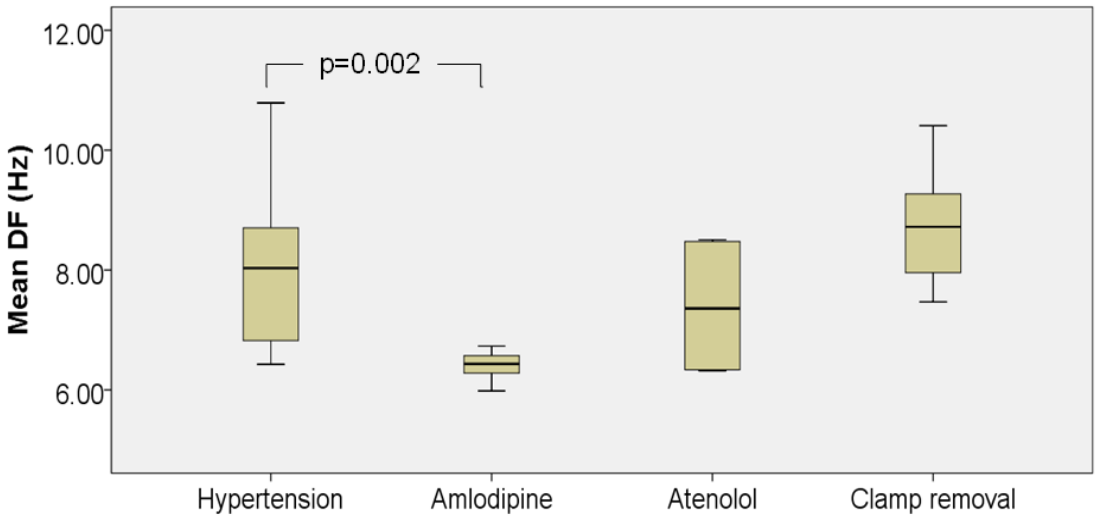

Figure 18: DF changes after treatment with anti-hypertensive drugs

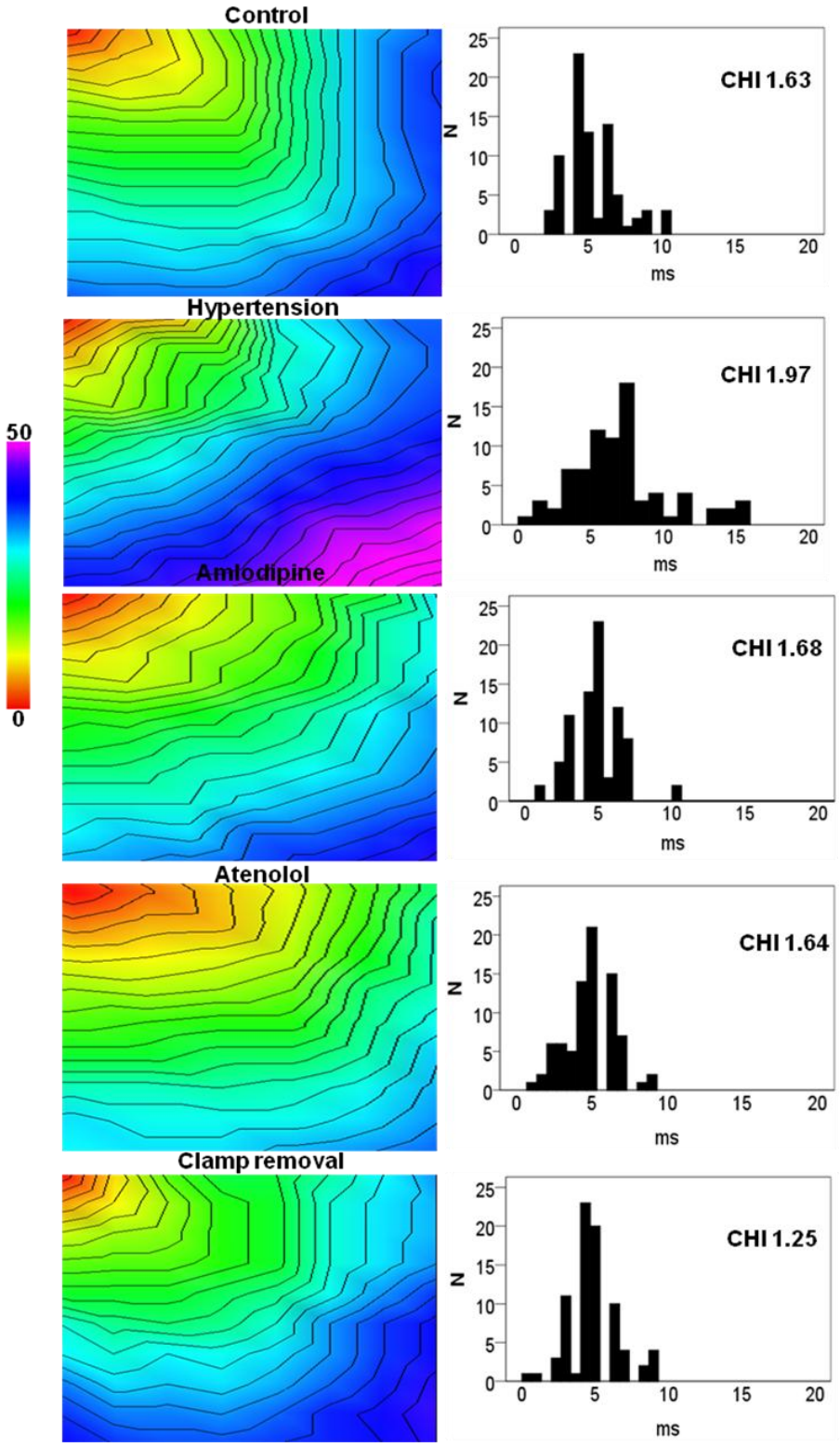

Figure 19: Representative activation maps and corresponding phase histograms of LA at 300 ms cycle length.

4 PREVENTION OF STRUCTURAL REMODELING OF HYPERTENSIVE ATRIA WITH PHARMACOLOGICAL INTERVENTION: EFFECT OF NOVEL ANTI-FIBROTIC DRUG

4.1 Introduction:

Most animal and human studies support the notion of 'fibrotic' substrate as an underlying reason for persistence of atrial fibrillation (AF) [270]. Fibrosis has been reported in various substrate models of heart failure [2], mitral valve disease [271], diabetes [272], obesity [7], obstructive sleep apnea [248] and hypertension [101, 102, 231]. Anti-fibrotic drugs could potentially reduce the prospects of AF development by preventing fibrous tissue formation in the atria [209].

Tranilast, N-(3,4-dimethoxycinnamoyl) anthranilic acid is an anti-fibrotic drug used in topical form for the treatment of hypertrophic scars, scleroderma and various skin disorders related to increased fibrous tissue formation [273, 274]. In addition, tranilast has been shown to prevent ventricular fibrosis and atrial remodeling in canine AF model [215, 216]. Further, effects of tranilast on the release of TGF-$ß_1$[275], MMP2 and Rac1 proteins inhibition [211, 276] in different models demonstrate its potential for inhibition of fibrotic substrate which could prevent likely AF susceptibility. Given the increased inflammatory response and fibrosis in

hypertensive atria, we examined the preventive effects of tranilast on atrial structural remodeling in an ovine 'one-kidney, one-clip' hypertensive model.

4.2 Methods

4.2.1 Study approval and guidelines

This study was approved by the *'University of Adelaide Animal Ethics Committee'* and '*SA Pathology Animal Ethics Committee'*. Guidelines from the "Australian code of practice for the care and use of animals for scientific purposes" 7th edition, 2004 adopted by the 'National health and medical research council' were followed for all the experimental procedures.

4.2.2 Animal housing & preparation

Male merino cross sheep were used for this study. All animals were held in group in open paddocks. Animals were placed in a 22°C temperature controlled room 24 hours pre-operative and until full recovery of 2-3 weeks post operatively for survival procedures. Food and water were provided *ad libidium*.

Before each surgical procedure, animals were given water intake only and fasted 24 hours prior to surgery. Intravenous sodium thiopentone (10-15 mg/kg) was used to facilitate endo-tracheal intubation. Isoflurane 2-4% in 100% oxygen at 4L/min was

administered for maintenance of general anesthesia throughout the procedure. Lignocaine 2mg/kg was used as local anaesthetic during surgery. Non-invasive blood pressure, heart rate, pulse oximetry, end-tidal CO_2 and temperature were continuously monitored. Amoxycilin (1 ml/20kg) and Buprenorphine (0.005-0.01 ml/kg) were administered intramuscularly for three days following renal surgeries. General anaesthesia was performed prior to renal surgery, cardiac MR scans and terminal electrophysiology study.

4.2.3 'One-kidney, one-clip' Renovascular Hypertension model

The conventional 'one-kidney, one-clip' model of ovine hypertension was used as previously described [101]. In brief, the right kidney was removed and the left kidney artery was restricted via a variable pressure cuff. To perform the nephrectomy, the animal was placed on left lateral recumbent position under general anaesthesia. Two finger breadths were measured from lateral extent of the paraspinal muscles before making an incision from just beneath the rib cage for about six inches vertically. The perinephric fat and Gerota's fascia were carefully separated from the surface of the kidney. The ureter and renal vessels were separately ligatured and right kidney was removed following which the wound was closed in layers.

In this study, we performed both nephrectomy and renal artery occlusion on the same day. A new vascular occluder clamp was used for the study (heavy duty 8mm, DOCXS Biomedical Products, Ukiah, CA, USA) in order to facilitate blood pressure

titration during hypertension development (maintained at 150-160 mmHg approximately) and reversal. Following nephrectomy, the sheep was placed onto the right lateral recumbent position. Blunt dissection was performed via a similar incision on the right side to expose the renal artery without interrupting the perinephric fat and Gerota's fascia on the left kidney. The vascular occluder clamp was placed around the renal artery with the actuating tube connected to an external port. The port was placed subcutaneously and sutured to maintain a stable position. During the surgical procedure, approximately 50% occlusion of renal artery was verified with a flow transducer (Transonic Flowmeter TS-401 with precision flow probe, Transonic Systems Inc., NY, USA) and Doppler velocity (Acuson XP-128, 7 MHz probe, Siemens Medical Systems, PA, USA) under direct vision to provide guidance for subsequent vascular occluder inflation.

Heparin (5000 I.U) was given for two days post-operatively to prevent thrombosis due to renal artery clamping. After surgical procedures, sheep were held in individual pen houses and monitored twice daily during recovery. After complete recovery, usually 2-3 weeks, sheep were sent back to paddocks. Induction of hypertension was initiated after 2-3 weeks of complete recovery from the surgery.

Following renal surgeries, animals were subjected to non invasive blood pressure (BP) measurement to ensure their acclimatization to this technique. Non invasive blood pressure levels were measured by placing the blood pressure cuff over the brachial artery of the forelimb in conscious animals (Datascope Passport 2,

Datascope Corp., NJ, USA).After acclimatization, measurements were taken twice weekly at the same time of the day by same handlers and metabolic crate. All blood pressure measurements on the animals were performed 3-5 times with the animals in a completely relaxed state. BP readings were averaged from all repeated measurements.

4.2.4 Cardiac MR Imaging

To conduct a cardiac MRI, all animals were placed under general anaesthesia (as described above) and were securely placed in a dorsal position. While the animals were under automated mechanical ventilation, breath holding was performed to acquire ECG gated images. With no inter slice gap, a slice thickness of 6mm and 10mm through the atria and ventricles respectively were used. CMR (Siemens Sonata 1.5 Tesla MR imaging system, Siemens Medical Solutions, Erlangen, Germany) was used to assess the anatomic and functional characteristics of the animals prior to terminal studies. All analyses were performed offline using Argus software (Leonardo workstation, Siemens Medical Solutions, Erlangen, Germany). The left atrial (LA) and ventricular (LV) volumes, LA and LV ejection fraction (LAEF & LVEF) and inter-ventricular thickness (IVS) were assessed.

4.2.5 Study timeline:

A total of 21 male merino cross sheep were used for this study. Seven sheep were used as normotensive controls. Fourteen sheep underwent renal surgeries to develop high blood pressure for 12 weeks as described earlier. Seven animals were treated with tranilast (600mg twice daily) in parallel with hypertension development. At the end of 12th week, 7 tranilast treated sheep and 7 untreated hypertensive sheep underwent terminal studies wherein an EP study was conducted and the heart was extracted and stored for further analyses.

4.2.6 Anatomical/ Structural Analysis

Animals were humanely killed (Sodium thiopentone 100g/sheep, 2-4% Isoflurane in 100% O_2) after terminal electrophysiological mapping studies. Right and left atrial appendages were isolated, dissected and stored appropriately for specific experimentation. Tissues were triplicated and stored; Fixed in 10% formalin solution and OCT cassettes (Slow freezing with Isopentane under liquid nitrogen) for histology and immunohistochemistry analyses respectively. In addition, left (LV), right (RV) ventricles and Inter-ventricular septum (IVS) were weighed.

4.2.6.1 Histology

All tissues were fixed in formalin for one week and were then subjected to serially diluted alcohol washing and were embedded in paraffin. The embedded tissue was

mounted on the microtome and cut into 5µm thick slices. Slices were placed on the slides and stained with haematoxylin & eosin and Masson's trichrome. The stained slides were digitized using an automated nanozoomer. Digitized images of the slides were used to analyze myocyte hypertrophy, inter-myocyte distance, interstitial fibrosis and inflammatory infiltration. Myocyte hypertrophy and inter-myocyte distance (endomysial fibrosis) were measured in both epicardial and endocardial regions. Regions from borderline up to 300µm depth were considered for analyses of both layers. The assessor was blinded to the groups and types of myocardial layers prior to analyses of all histological parameters.

Mean cell diameters of approximately 30-35 transversely cut myocytes from 5 different fields were measured to determine hypertrophy [229]. Inter-myocyte distance was measured as the closest distance between myocytes at a mean of 40 cell-cell distances for 5 different fields. Fibrosis was quantified at 5 random fields in each slide using color differentiation as described previously [230]. ImageJ 1.47v (National Institute of Health, USA) was used for analysis. All quantified results were expressed in percentage relative to the whole tissue area.

4.2.6.2 Immunostaining

The frozen tissues were used to perform immunohistochemistry and determine the expression levels of Connexin43, connective tissue growth factor (CTGF) and Transforming growth factor ß1 (TGF-ß1). Rabbit polyclonal primary antibodies were

purchased from Abcam laboratories, Cambridge, MA, USA. A primary antibody dilution of 1: 100 was used. Immuno-stained images were scanned at 20 x magnifications for blinded quantification using ImagePro Premium v9.1 (Media cybernetics, Rockville, MD, USA). All quantified results were expressed as percentage relative to the whole tissue area.

4.2.7 Statistical Analysis

All data were expressed in mean ± standard deviation. Analyses of differential effects of blood pressure lowering therapies on structural parameters were performed using analysis of variance (ANOVA). Sidak adjusted post-hoc tests were used to delineate the differences between specific groups. Statistical significance was set as $P<0.05$.

4.3 Results:

One Kidney One Clip hypertension model were developed in fourteen Merino cross sheep (59±5 kg). All animals developed renovascular hypertension in a timely fashion for a mean duration of 12±2 weeks.

4.3.1 Blood pressure measurements

Mean systolic blood pressure levels in 1K1C animals were significantly higher after 12 weeks of hypertension as compared to normotensive controls (156±5 vs. 115±8 mmHg; $p<0.001$). At the conclusion of study period, blood pressure levels were similar in hypertension group compared to Tranilast group (156±5 vs. 162±5 mmHg; $p=1.0$). Further, tranilast treated group showed a significantly higher blood pressure levels compared to normotensive controls (162±5 vs. 115±8 mmHg; $p<0.001$).

4.3.2 Cardiac MRI assessment

As compared to normotensive controls, the hypertensive group had left atrial dilatation (LAEDV: 24±2 vs. 48±8 mL; $p=0.001$) and lower left atrial ejection fraction (LAEF: 32±3 vs. 13±5 %; $p=0.03$). Tranilast treatment did not prevent left atrial dilatation and dysfunction (LAEDV: 48±8 vs. 40±5; p = NS: LAEF - 13±5 vs. 21±2; p = NS). Left ventricular volumes and ejection fraction did not differ in any of the groups indicating that development of hypertension did not lead to heart failure in any animals (Table 1).

4.3.3 Histological examination

4.3.3.1 Inflammatory infiltration

Inflammation was significantly increased during hypertension as compared to the control group [LA – 5.10±0.56% vs. 3.35±0.51%; p=0.001; RA – 5.85±0.91 vs. 3.58±0.35%; p=0.001]. Increased inflammation associated with the hypertensive animals was prevented with tranilast treatment in both atria (both p<0.001) (Figure 20) and was comparable to the normotensive control group (p=0.9).

4.3.3.2 Interstitial fibrosis

Fibrous content was significantly increased in hypertensive animals compared to control group [LA – 21.73±6.20 vs. 4.77±3.71 %; p<0.001; RA – 23.35±4.78 vs. 7.84±0.85 %; p<0.001]. Tranilast treatment prevented hypertensive fibrosis deposition in both atria (p<0,001) for the treated group such that Tranilast group fibrosis levels were similar to normotensive controls (Figure 21).

4.3.3.3 Myocyte size and distance

Epicardial myocyte size (Myocyte hypertrophy) was significantly increased during hypertension compared to normotensive control group in both atria (p<0.001). Tranilast treatment during the development of hypertension inhibited the increased myocyte size in the epicardial region (p<0.001). Epicardial inter-myocyte distance

(Endomysial fibrosis) was significantly increased during hypertension compared to controls ((LA: p=0.010; RA: p=0.03) and was significantly inhibited in the tranilast group (LA: p=0.03; RA: p=0.01) (Figure 22 & Figure 23). Similar findings were observed in endocardial region without any significant differences between epicardial and endocardial myocyte hypertrophy and endomysial fibrosis (Table 2).

4.3.4 Immunostaining

4.3.4.1 Connexin43:

Hypertension was associated with significantly reduced connexin43 expression compared to normotensive controls [LA – 1.09±0.45 vs. 2.98±0.35; p<0.001; RA – 1.34±0.35 vs. 3.71±0.75; p<0.001]. Decreased connexin43 expression as seen with hypertension was inhibited in the tranilast treated group [LA – 1.09±0.45 vs. 2.83±1.32; p=0.008; RA – 1.34±0.35 vs. 3.48±1.02; p=0.004] (Figure 24). No significant differences between normotensive controls and tranilast were seen.

4.3.4.2 CTGF:

Hypertensive animals had significantly increased CTGF expression compared to normotensive controls [LA – 2.13±0.69 vs. 0.70±0.37; p<0.001; RA – 2.47±0.56 vs. 1.15±0.50; p<0.001]. Hypertensive mediated increased CTGF expression was significantly prevented in tranilast treated group [LA – 2.13±0.69 vs. 1.39±0.42;

p=0.04; RA – 2.47±0.56 vs. 1.58±0.14; p=0.03] (Figure 25) to a level where there were no significant differences between normotensive controls and tranilast group.

4.3.4.3 TGF-ß1:

Hypertensive animals had significantly increased TGF-ß1 expression compared to normotensive controls [LA – 3.50±0.77 vs. 2.07±0.88; p<0.001; RA – 3.60±0.38 vs. 2.59±0.58; p<0.001]. Increase in TGF-ß1 expression was significantly prevented in tranilast treated group [LA – 3.50±0.77 vs. 2.10±0.27; p=0.021; RA – 3.60±0.38 vs. 2.06±0.18; p<0.001] (Figure 26). No differences were seen between normotensive controls and tranilast treated group.

4.4 Discussion

Fibrosis has been the hallmark of remodeling process noticed in most atrial fibrillation patients. This study provides us with the following data;

- Hypertension caused structural remodeling through increased myocyte hypertrophy, endomysial and interstitial fibrosis and inflammation along with increased septal thickness, left atrial dilatation and dysfunction.
- Structural remodeling during hypertension was contributed to by increased CTGF and TGF-$ß_1$ and reduced connexin43 expressions.

- Tranilast treatments resulted in significant prevention of structural remodeling through prevention of myocyte hypertrophy, endomysial and interstitial fibrosis and inflammation. Septal thickness was preserved despite high blood pressure levels although left atrial dilatation and dysfunction were not prevented by tranilast.
- Prevention of structural remodeling by tranilast was aided by its preventive effects on altered expression of CTGF, TGF-ß1 and connexin43.

4.4.1 Structural remodeling in various models

Atrial structural remodeling has been widely demonstrated in various models of heart failure, myocardial infarction, obesity and hypertension [3, 7, 102, 116]. In particular, Lau *et al* showed that the substrate could develop within 5 weeks from onset of hypertension and demonstrated the progression of structural remodeling with time [101, 231]. They showed a significant increase in atrial and ventricular hypertrophy, increased lymphocytic infiltration, inflammation and fibrosis in a short term hypertension and it was progressive with long term development of hypertension [4, 231]. Our study is in keeping with the previous findings in hypertensive atria. However, we also demonstrated the prevention of pro-fibrotic and inflammatory cytokines with an anti-fibrotic drug for the first time in large animal model of hypertension. Previously, Verheule *et al* demonstrated in an atrial tachypacing model that the loss of continuity of the epicardial layer is due to increase in endomysial fibrosis leading to complexity of fibrillatory conduction [230]. In our study, we showed the contribution of myocyte hypertrophy and endomysial fibrosis

in hypertensive atria and also the prospects of preventing it with tranilast despite high blood pressure levels. Eckstein *et al* also showed the time dependent dissociation between epicardial and endocardial regions during AF [277]. However, epicardial and endocardial dissociation were not seen in our hypertensive substrate at 12 weeks. Therefore, this electrophysiological phenomenon in AF could be substrate specific.

4.4.2 Prevention of structural remodeling in various models

Pirfenidone, an antifibrotic drug has been shown to prevent fibrosis and TGF-ß1 in addition to reduction of AF vulnerability in a canine heart failure model of atrial fibrillation [209]. Furthermore, pirfenidone has been shown to be anti-fibrotic and reno-protective by inhibiting TGFβ-Smad2/3 signaling, improvement of MMP9/TIMP1 balance, and suppression of fibroblast proliferation in addition to significant attenuation of blood pressure levels in Dahl salt-sensitive hypertensive rats [205]. Additionally, in a mice model, pirfenidone has been shown to be functional in prevention of hypertension induced myocardial fibrosis by inhibiting NLRP3-induced inflammation and fibrosis [206] and hypertension induced cardiac hypertrophy by inhibiting angiotensin II [207] and therefore has been suggested to prevent cardiac remodeling [208]. In addition, Parikh *et al* demonstrated that relaxin, an anti-fibrotic drug prevents conduction slowing along with fibrosis in spontaneously hypertensive rats thereby suppressing AF susceptibility [218]. They also showed that the anti-fibrotic effects of relaxin are attributed, at least in part, to

cardiac Na+ ionic currents. Given the positive effects of pirfenidone and relaxin, anti-fibrotic drugs could be potential adjunctive agents for prevention of AF.

Tranilast is an anti-fibrotic drug shown to inhibit various pro-fibrotic proteins such as TGF-β isoforms and collagen in injured arteries and scar tissues from fibroblasts *per se* [275, 278]. Furthermore, tranilast has been shown to prevent TGF-β1, MMP1 and Rac1 proteins in a canine heart failure model of atrial fibrillation [216]. Despite no attenuation of blood pressure, a comparison with losartan showed that tranilast is equally effective in prevention of TGF-$ß_1$ mRNA, collagen accumulation and hypertrophy in the ventricular myocytes [279]. Further, Kagitani *et al* showed the prevention of cardiac structural remodeling by tranilast through curtailing fibrosis and inflammation in hypertensive rat model [215]. However, in our study, we demonstrated that tranilast is atrial protective independent of blood pressure levels in a large animal model and we provided evidence for its effects on pro-fibrotic and inflammatory cytokines: TGF-$ß_1$ and CTGF.

Parikh *et al* demonstrated a reduction in connexin43 phosphorylation in spontaneously hypertensive rats as a key contributor leading to AF susceptibility [218]. They further showed that relaxin prevented the reduction in connexin43 phosphorylation thereby suppressing AF susceptibility. Similarly, our study in hypertensive large animal model showed that tranilast could prevent reduction in connexin43 expression due to hypertension.

4.5 Limitations

Experimental 1K1C renovascular hypertension may not represent essential hypertension which is multi-factorial and develops over a longer period of time in humans. Though, with relative to hypertension models from previous studies, our results could possibly be the nearer representation of hypertension as developed in animal model. We did not perform any studies on the combinational therapies of tranilast with anti-hypertensive agents to determine potential additive benefits. Despite the encouraging outcomes at cellular level and changes in pro-fibrotic proteins, extrapolation of the benefits in hypertensive patients is cautioned.

4.6 Conclusions

In this study, we demonstrated that tranilast could prevent atrial structural remodeling due to hypertension by acting on pro-fibrotic and inflammatory cytokines and improving connexin43 expression. Interestingly, these beneficial effects were seen despite persistently high blood pressure levels. Due to its non-toxic side-effect profile, tranilast could be an attractive agent for prevention of adverse atrial remodeling in hypertension.

4.7 Figures

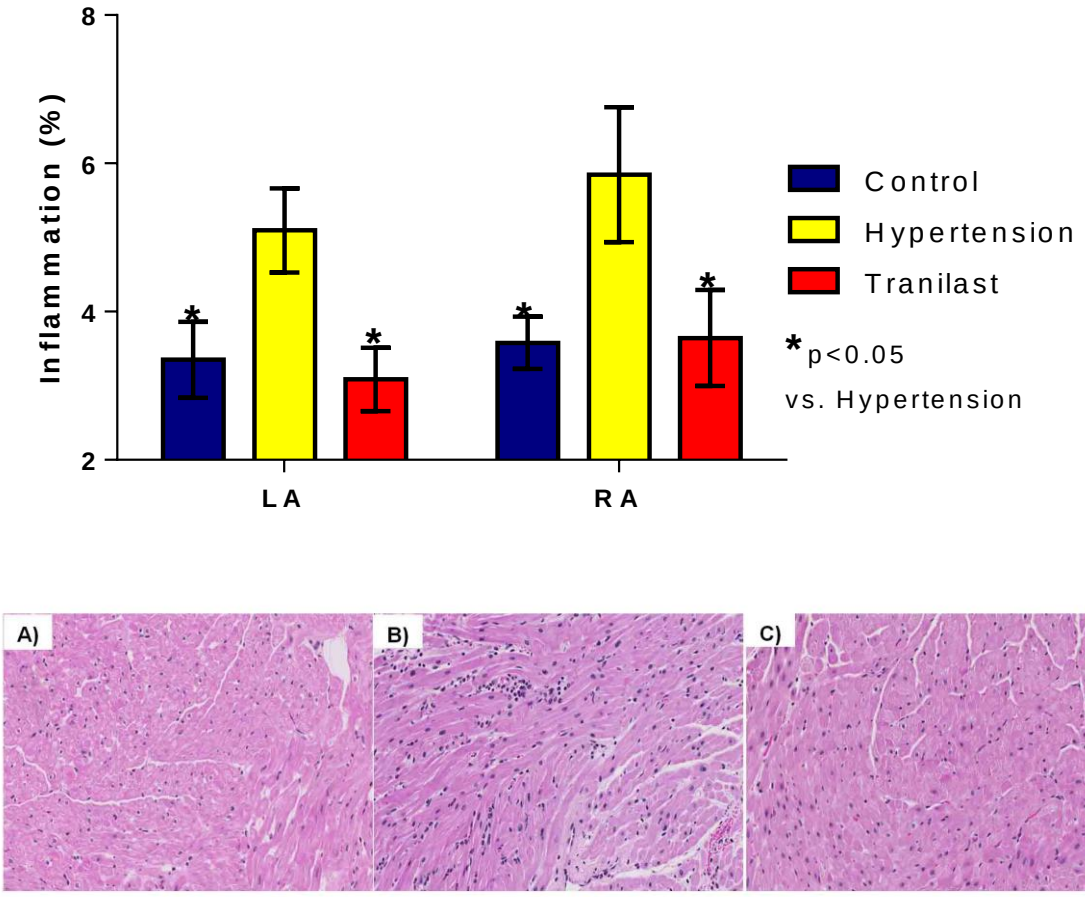

Figure 20: Atrial inflammation; A) Control; B) Hypertension; C) Tranilast

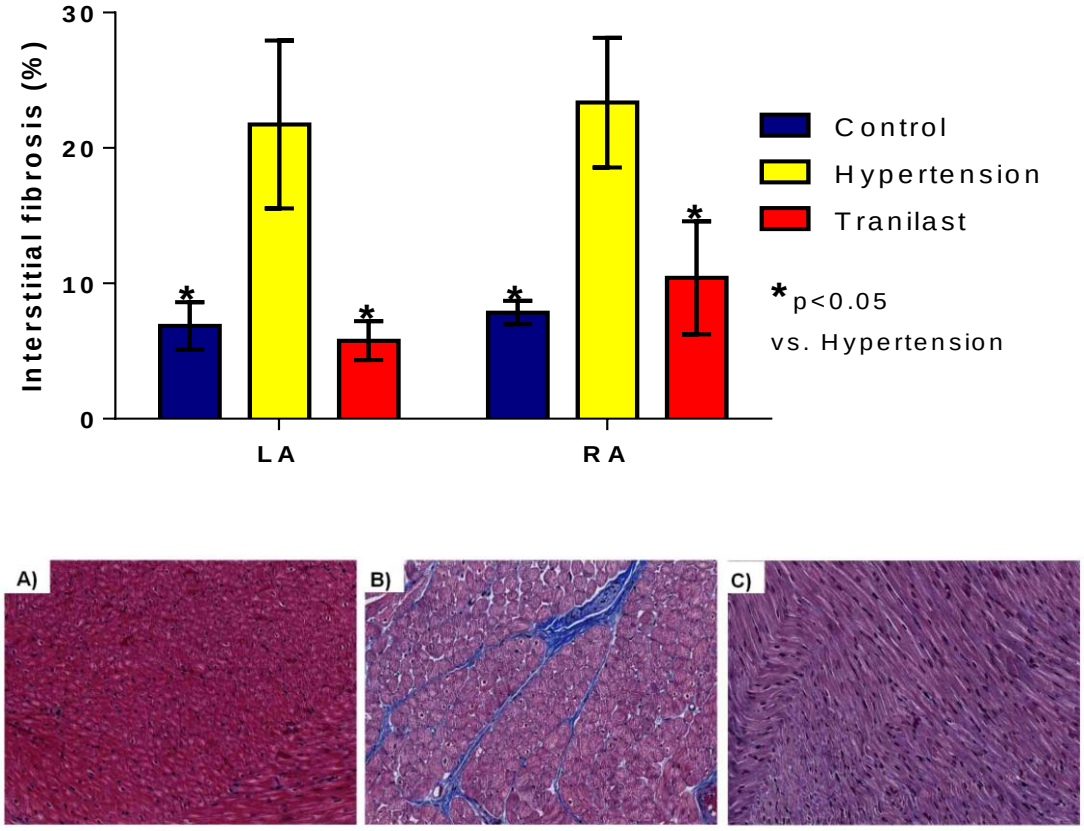

Figure 21: Interstitial fibrosis

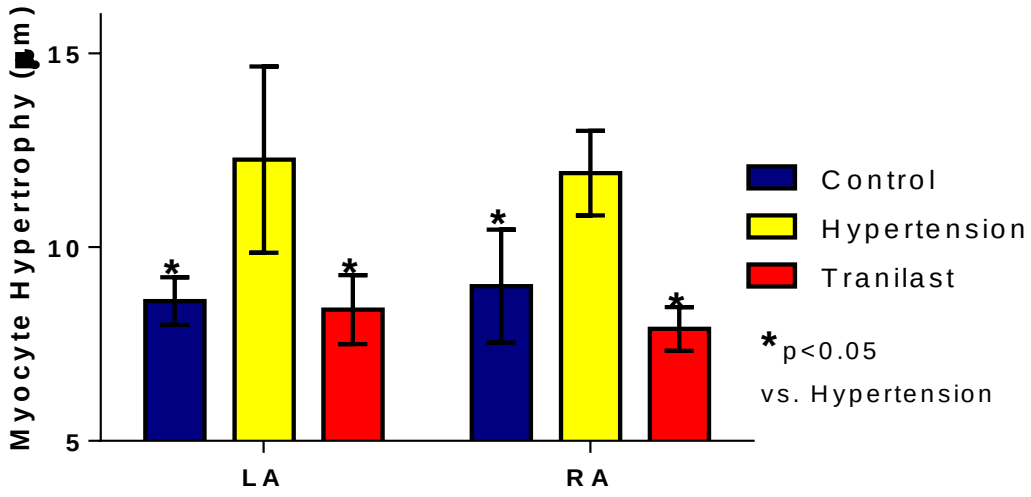

Figure 22: Atrial Hypertrophy

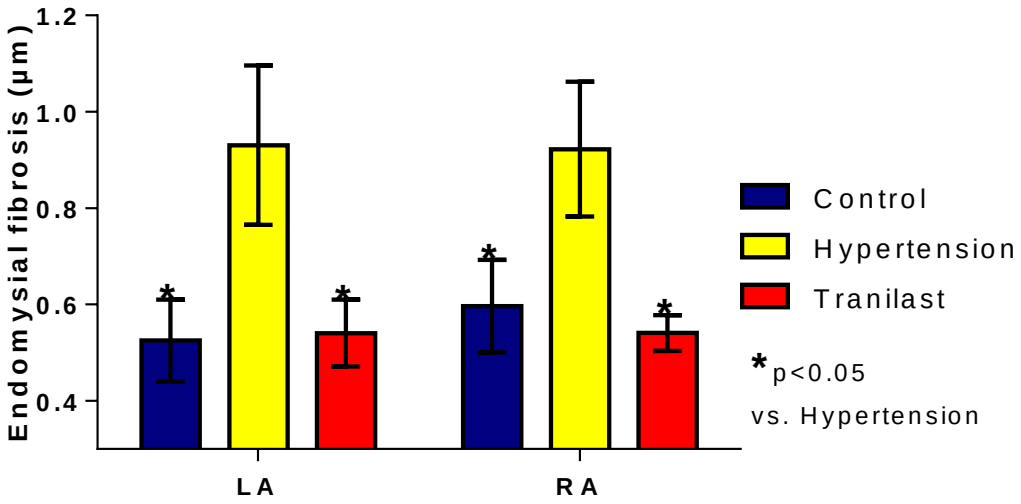

Figure 23: Atrial endomysial fibrosis

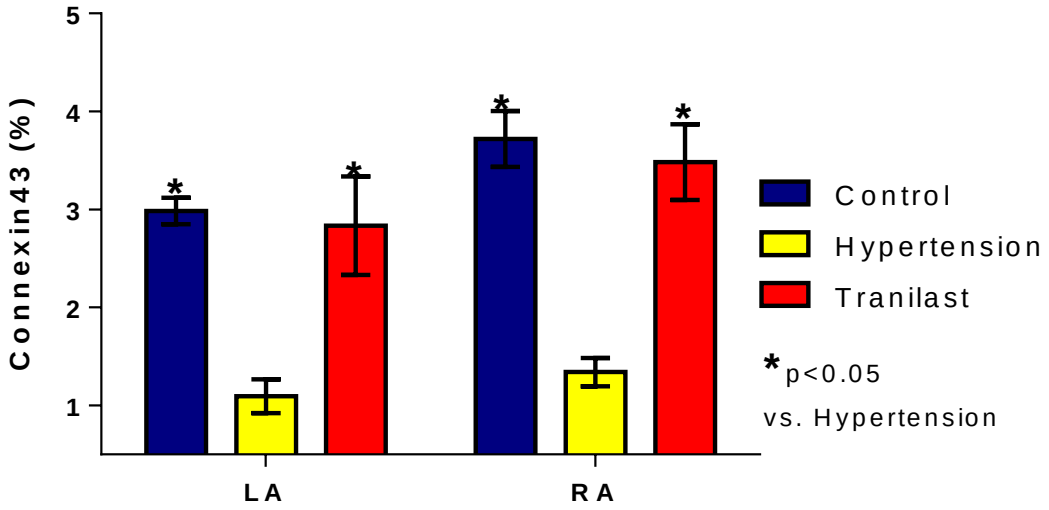

Figure 24: Connexin43 expression

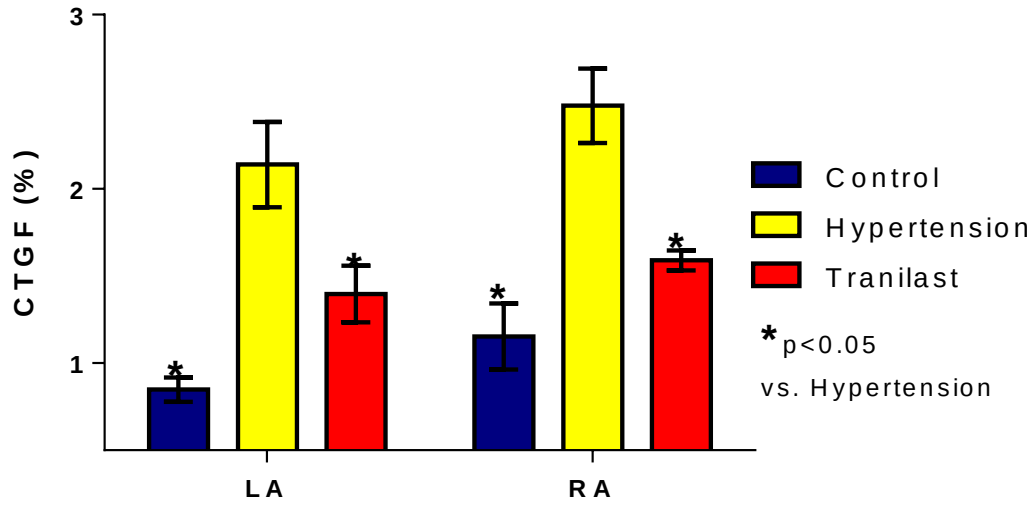

Figure 25: CTGF expression

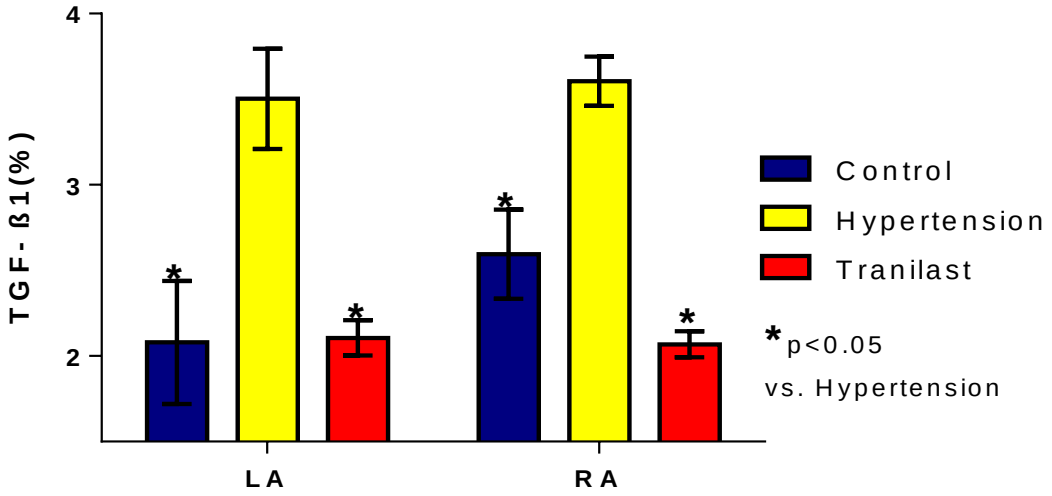

Figure 26: TGF-ß1 expression

4.8 Tables

	Control	**Hypertension**	**Tranilast**
Total (n)	7	7	7
Weight (kg)	60±3	57±3	61±3
Systolic blood pressure (mmHg)	115±7*	156±5	162±5
MRI			
LAEDV (mL)	24±2*	48±8	40±5
LAEF (%)	32±3*	13±5	21±2
LVEDV (mL)	92±7	103±14	100±22
LVEF (%)	45±4	42±5	35±6
PATHOLOGY			
RV (g)	47±5	59±8	53±3
LV (g)	106±9*	129±6	117±12
IVS (g)	44±7*	62±5	42±7*
IVS (mm)	11±1*	18±1	14±1*
*$p<0.05$ compared hypertension group			

Table 1: Animal characteristics and MRI data

	Control (n=7)	Hypertension (n=7)	Tranilast (n=7)
Left atrium			
Myocyte size			
Epicardium	8.6±0.54*	13.6±2.8	9.1±1.2*
Endocardium	7±0.35*	10.8±3.2	8.4±1.0
Intermyocyte distance			
Epicardium	0.42±0.1*	0.93±0.34	0.56±0.18*
Endocardial	0.40±0.05*	0.91±0.45	0.56±0.17*
Right atrium			
Myocyte size			
Epicardium	8.99±1.30*	12.44±1.55	8.14±1.08*
Endocardium	7.00±0.63*	10.32±2.68	7.89±1.76*
Intermyocyte distance			
Epicardium	0.46±0.08*	0.91±0.45	0.52±0.17*
Endocardium	0.44±0.08*	0.92±0.43	0.54±0.18*
*p<0.05 compared to hypertension group			

Table 2: Hypertrophy and endomysial fibrosis in LA and RA

5 PREVENTION OF ELECTRICAL REMODELING OF HYPERTENSIVE ATRIA WITH TRANILAST, A NOVEL ANTI-FIBROTIC DRUG

5.1 Introduction:

The concept of 'AF begets AF' elegantly highlighted the contribution of electrical remodeling to the persistence of atrial fibrillation (AF) [54]. AF induced abbreviations of atrial refractoriness are suggested to be due to high rate of electrical activations [153]. In addition, electrical remodeling due to conduction abnormalities has been demonstrated in both large and small animal hypertension models [4, 102-104]. Conduction slowing and heterogeneity has indeed been implicated in different AF substrates as a vital contributor to the electrical substrate of AF.

The anti-fibrotic potency of tranilast has been demonstrated topically in various skin disorders [273, 274]. Recently, tranilast has been shown to prevent inflammation and atrial interstitial fibrosis in hypertensive rat model and canine model of atrial tachycardia [215, 216]. Given the increased inflammatory response and fibrosis in hypertensive atria, we sought to examine the preventive effects of tranilast on atrial electrical remodeling in a 'one-kidney, one-clip' hypertensive model.

5.2 Methods

5.2.1 Study approval and guidelines

This study was approved by the *'University of Adelaide Animal Ethics Committee'* and '*SA Pathology Animal Ethics Committee'*. Guidelines from the "Australian code of practice for the care and use of animals for scientific purposes" 7th edition, 2004 adopted by the 'National health and medical research council' were followed for all the experimental procedures.

5.2.2 Animal housing & Preparation

Male merino cross sheep were used for this study. All animals were held in group in open paddocks. Animals were placed in a 22°C temperature controlled room 24 hours pre-operative and until full recovery of 2-3 weeks post operatively for survival procedures. Food and water were provided *ad libidium*.

Before each surgical procedure, animals were given water intake only and taken off from food 24 hours prior to general anaesthesia procedure and followed by intravenous sodium thiopentone (10-15 mg/kg) for induction to facilitate endo-tracheal intubation. Isoflurane 2-4% in 100% oxygen at 4L/min was exercised for maintenance throughout the procedure. Lignocaine 2mg/kg was used as local anaesthetic during surgery. Non-invasive blood pressure, heart rate, pulse oximetry,

end-tidal CO_2 and temperature were continuously monitored during the whole surgical procedure. Amoxycilin (1 ml/20kg) and Buprenorphine (0.005-0.01 ml/kg) were administered intramuscularly for three days following renal surgeries. General anaesthesia was performed prior to renal surgery, cardiac MR scans and terminal electrophysiology study.

5.2.3 Study timeline:

A total of 21 male merino cross sheep were used for this study. Seven sheep were used as normotensive controls. Fourteen sheep underwent renal surgeries to develop high blood pressure for 12 weeks as described earlier. Seven animals were treated with tranilast (600mg twice daily) in parallel with hypertension development. At the end of 12th week, 7 tranilast treated sheep and 7 untreated hypertensive sheep underwent terminal electrophysiological studies (Figure 27).

5.2.4 'One-kidney, one-clip' renovascular hypertension model

Conventional 'one-kidney, one-clip' model as previously described was used [101]. The animal was placed on left lateral recumbent position under general anaesthesia. Nephrectomy was performed on the right kidney. Two finger breadths were allowed from lateral extent of the paraspinal muscles for making an incision from just beneath the rib cage for about six inches vertically. The perinephric fat and Gerota's fascia were carefully separated from the surface of the kidney. The ureter and renal

vessels were separately ligatured and right kidney was removed following which the wound was closed in layers.

In this study, we performed both nephrectomy and renal artery occlusion on the same day. A new vascular occluder clamp was used for the study (heavy duty 8mm, DOCXS Biomedical Products, Ukiah, CA, USA) in order to facilitate blood pressure titration during hypertension development (maintained at 150-160 mmHg approximately) and reversal. Following nephrectomy, the sheep was placed onto the right lateral recumbent position. Blunt dissection was performed via similar incision as the right side to expose the renal artery without interrupting the perinephric fat and Gerota's fascia on the left kidney. Vascular occluder clamp was placed around the renal artery with the actuating tube connected to an external port. The port was placed subcutaneously and sutured to maintain in a stable position. During the surgical procedure, approximately 50% occlusion of renal artery was verified with flow transducer (Transonic Flowmeter TS-401 with precision flow probe, Transonic Systems Inc., NY, USA) and Doppler velocity (Acuson XP-128, 7 MHz probe, Siemens Medical Systems, PA, USA) under direct vision to provide guidance for subsequent vascular occluder inflation.

Heparin (5000 I.U) was given for two days post-operatively to prevent renal artery thrombosis due to vascular occlusion. After surgical procedures, sheep were held in individual pen houses and monitored twice daily during recovery. After complete

recovery, usually 2-3 weeks, sheep were sent back to paddocks. Induction of hypertension was initiated after 2-3 weeks of complete recovery from the surgery.

Following renal surgeries, animals were subjected to non invasive blood pressure (BP) procedure to ensure they are acclimatized to the technique. This technique was performed during the animal's recovery from the renal procedure. Measurements were taken twice weekly at the same time of the day by same handlers and metabolic crate. All blood pressure measurements on the animals were done 3-5 times with the animals in a completely relaxed state. BP readings were averaged from all repeated measurements. Non invasive blood pressure levels were measured by placing the blood pressure cuff over the brachial artery of the forelimb in conscious animals (Datascope Passport 2, Datascope Corp., NJ, USA).

5.2.5 Electrophysiological study

All hypertensive (n=7), tranilast treated hypertensive (n=7) and normotensive (n=7) control animals underwent terminal open chest electrophysiological studies under deep sedation. Physiological gases and body temperature were maintained with automatic ventilation throughout the electrophysiological assessment study.

A midline thoracotomy was performed to expose the pericardial region of the heart. The pericardium was divided to slide a custom made 80-electrode epicardial plaque for mapping. The plaque had 4mm inter-electrode spacing with 10 rows and 9

columns of electrodes. The plaque was placed on the right (RA) and left (LA) atrium separately with the tail connected to a computerized recording system (LabSystem Pro, Bard Electrophysiology, MA, USA). Continuous recording of surface-ECG and overlapping bipolar electrograms were stored for offline analysis. Electrograms were notch filtered from 30-500Hz, and measured with sweep speed of 200mm/s for analysis. The electrophysiological parameters analyzed in this study included:

5.2.5.1 Atrial effective refractory period

Atrial effective refractory period (ERP) was measured at double the diastolic threshold at varying cycle lengths (S1) of 500, 400, 300 & 200 ms from 8 different sites (RAA, Right atrial free wall, LAA, left atrial free wall, right and left atrial medial and lateral regions). Eight basic stimuli, defined as S1, were followed by a premature beat (S2). This was repeated with a 10ms decrement until the loss of wave propagation. ERP was defined as the shortest S1-S2 coupling interval resulting in a propagated wave response. Measurements were repeated thrice to obtain an average ERP at different cycle lengths (CL) at each site. ERP heterogeneity was determined with coefficient of ERP variation calculated as the regional standard deviation of ERP/Mean * 100.

5.2.5.2 Atrial conduction

Conduction was assessed at S1 and S2 wave propagations by making conduction activation maps with customized semi-automated software. Vectors within each triangle of electrodes were used to calculate local conduction velocity and a total averaged conduction velocity was determined at different cycle lengths at each site [258, 259]. Local conduction was measured on S1 and S2 beats at different cycle lengths of 500, 400, 300 and 200 ms at all specified sites.

Conduction heterogeneity was calculated using phase mapping method for both S1 and S2 propagated wave responses [260]. The longest activation time difference at each electrode site was used to plot the phase map and histogram. Absolute conduction phase delay was determined by the difference between 5th and 95th percentile of phase distribution (P5-95). The conduction heterogeneity index was derived from dividing the absolute phase delay by its median (P50).

5.2.5.3 AF Inducibility

Degree of AF inducibility was measured as a ratio of number of AF episodes to the total number of S1-S2 pacing trains. AF was defined as irregularity in atrial electrograms lasting for ≥ 2 seconds.

5.2.5.4 Electrogram characteristics during AF

AF episodes of each animal group were analyzed offline using customized software. Only sustained episodes >8 seconds were used.

The Ensite NavX algorithm (St. Jude medical, MN, USA) measures the complex fractionated electrogram-mean (CFE-m) using the mean of time intervals between marked deflections [261] according to the following parameters: Refractory period of 40ms; Minimum electrogram width of 10ms; and peak to peak sensitivity of 0.05-0.1mV.

5.2.6 Statistics

All data were expressed in mean±SD. Mixed model analyses were performed to examine the differences in electrophysiological parameters between groups due to multiple measures within each animal. Animal group was used as a fixed effect and animal ID was modelled as a random effect. In datasets that did not have a nested data structure, one-way ANOVA with post hoc testing were performed to analyze the difference between groups. $P<0.05$ was considered to indicate statistical significance

5.3 Results

One-kidney, one-clip hypertension model was developed in fourteen age-matched male merino cross sheep (59±5 kg). All animals developed renovascular hypertension in a timely fashion for a mean duration of 12±2 weeks. There was no cardiac or renal failure in any hypertensive animal during the course of the study.

5.3.1 Blood pressure measurements

Mean systolic blood pressure levels in 1K1C animals were significantly higher after 12 weeks of hypertension as compared to normotensive controls (156±5 vs. 115±8 mmHg; $p<0.001$). At the conclusion of study period, blood pressure levels were similar in hypertension group compared to Tranilast group (156±5 vs. 162±5 mmHg; $p=1.0$) (Figure 28). Further, tranilast treated group showed a significantly higher blood pressure levels compared to normotensive controls (162±5 vs. 115±8 mmHg; $p<0.001$).

5.3.2 Atrial electrophysiological reverse remodeling

5.3.2.1 Effective refractory period

Mean atrial refractoriness at S1 300 ms pacing cycle length during hypertension was unchanged compared to control group in both LA (110±19 vs. 113±13 ms; $p=0.974$)

and RA (157±39 vs. 154±27 ms; p=1.00). Effective refractory period (ERP) did not change in LA (110±19 vs. 114±20 ms; p=0.48) and RA (157±40 vs. 146±23; p=0.47) with tranilast treatment (Figure 29 & Figure 30). In hypertensive group, changes in ERP were similar for all pacing cycle lengths whilst in tranilast treated group, ERP reduced at 500 cycle length in RA and unchanged at all other cycle lengths.

ERP heterogeneity showed an increasing trend in hypertensive group compared to control group in LA (14.71±1.11 vs. 10.04±1.22 %; p=0.073) though this did not reach statistical significance. In RA, ERP heterogeneity was significantly increased (18.63±1.19 vs. 12.96±1.33 %; p=0.024) during hypertension. Tranilast treatment did not have any effect on ERP heterogeneity in LA (14.71±1.11 vs. 13.87±1.04%; p=1.000) although highly significant reduction was seen in RA (18.63±1.19 vs. 12.01±1.14 %; p=0.001).

5.3.2.2 Atrial conduction

Mean atrial conduction velocity at S1 300 ms pacing cycle length was significantly reduced in hypertension compared to control group in both LA (0.88±0.14 vs. 1.06±0.11 m/s; p<0.001) and RA (0.89±0.05 vs. 1.06±0.11 m/s; p<0.001). This conduction slowing was significantly inhibited with tranilast treatment in both the LA and RA (both p<0.001) (Figure 31). Prevention of conduction slowing was similar for all cycle lengths examined.

Atrial conduction heterogeneity as calculated with phase mapping, was increased in hypertension compared to control group in both the LA (1.67±0.70 vs. 1.38±0.31; p=0.005) and RA (2.16±1.49 vs.1.30±0.30; p<0.001). The tranilast treated hypertensive sheep demonstrated conduction heterogeneity similar to normotensive control levels in both the LA (p=0.55) and RA (p=0.99) (Figure 32). The isochrones in the activation maps were drawn at 2 ms interval with red color indicating areas of fast conduction through to purple indicating slower conduction of propagating wavefront (Figure 33). Representative local activation maps and their corresponding histograms clearly demonstrate the conduction heterogeneity differences between hypertension and tranilast treated group.

5.3.2.3 AF Inducibility & Duration

During EP study, the hypertensive group showed an increased AF vulnerability (7.9%) as compared to control group (2.0%; p=0.008). Tranilast treatment suppressed AF to control levels (1.8%; p=0.006) (Figure 34). Sustained AF, as defined by the continuance of AF for more than 15 minutes was more prevalent in the hypertensive group (2/7) compared to normotensive controls (0/7) although this was unaltered after tranilast treatment (3/7). Consequently, mean AF duration in the hypertensive sheep (24±98 s) was not different to the tranilast treated group. (105±222; p=0.74).

5.3.2.4 Electrogram characteristics during AF

No AF episodes lasted more than 8 seconds in the control group. CFE-m measured with NaVX algorithm was significantly reduced after treatment with tranilast compared to hypertensive animals (84±15 vs 99±20 ms; p = 0.04) indicating a higher fibrillatory signal complexity (Figure 35).

5.4 Discussion

This study provides insights regarding the effect of anti-fibrotic drug on prevention of electrical remodeling in the hypertensive substrate.

Major findings of this study are as follows:

- Hypertension increased conduction slowing, conduction heterogeneity, ERP heterogeneity and AF vulnerability. In contrast, no significant changes in mean ERP were observed.
- Tranilast treatment resulted in largely unchanged ERP with some reduction in ERP heterogeneity. In contrast, Tranilast inhibited the conduction slowing and heterogeneity in the hypertensive substrate almost down to normotensive control levels. In concordance, there was reduced AF susceptibility, although fibrillatory electrogram complexity was higher once AF was initiated.

5.4.1 Prevention of atrial electrical remodeling

Li *et al* demonstrated the significance of atrial fibrotic substrate and conduction heterogeneity in a canine model of heart failure [2]. They also demonstrated in the same model that ACE inhibition interferes with the signal transduction leading to AF substrate by preventing conduction heterogeneity and thereby reducing AF vulnerability [189]. Lau *et al* demonstrated the atrial protective effects of omega-3 fatty acids in a chronic ovine heart failure model [217]. Further, Nakatani *et al* demonstrated in a canine model of atrial tachycardia that tranilast prevents atrial remodeling and reduced AF susceptibility which was largely linked to an inhibition of underlying fibrosis substrate [216]. Previous studies in a hypertensive ovine model demonstrated atrial electrical remodeling through increased conduction slowing and heterogeneity along with fibrosis resulting in increased AF susceptibility in short term [231], progressive [4] and longer periods of hypertension [102]. Previously, in small animal models of hypertension, atrial remodeling associated with increased fibrosis leading to AF vulnerability was established [103, 104]. Our study in the hypertensive ovine model is consistent with the previous findings of increased conduction slowing and heterogeneity leading to increased AF vulnerability.

5.4.2 Role of anti-fibrotic drugs in preventing atrial electrical remodeling

We demonstrated that tranilast prevented conduction slowing and heterogeneity in both atria highlighting its role in prevention of atrial remodeling of hypertensive atria. Interestingly, these beneficial effects were seen despite persistent hypertension and increased complex electrograms in tranilast treated animals.

Limited studies are available on the effects of anti-fibrotic drug on atrial remodeling. Pirfenidone, an antifibrotic drug has been shown to prevent conduction heterogeneity index attributing to reduced vulnerability to arrhythmias in a canine heart failure model of AF [209]. Further, Parikh *et al* demonstrated that relaxin prevents conduction velocity slowing and flattened its restitution kinetics along with reduction of action potential duration at 90% recovery to baseline range in spontaneously hypertensive rats thereby suppressing AF susceptibility [218]. They also showed that the anti-fibrotic effects of relaxin are further attributed, at least in part, to cardiac Na+ ionic currents. Our study is in keeping with previous observations of anti-fibrotic agents in various AF substrates; however, we provide new evidence in relation to prevention of atrial electrical remodeling in a large animal hypertensive AF substrate.

5.4.3 Clinical implications

Tranilast appears to be effective in preventing electrical remodeling in hypertensive atria. Given the high prevalence of hypertension and its consequent high population attributable risk for AF, novel therapeutic strategy with tranilast may have significant impact in reducing the burden of AF. Further research is required for assessment of its efficacy in other substrates of AF including obesity, obstructive sleep apnea, myocardial infarction and heart failure. Tranilast has minimal side-effect profile rendering it an attractive adjunctive treatment in hypertensive patients

5.4.4 Limitations

Artificial 1K1C renovascular hypertension may not represent essential hypertension which is multi-factorial and develops over a long period of time. We did not study tranilast in combination with anti-hypertensive agents to determine whether additive benefits may be present. In addition, since these studies are performed in animal models, careful extrapolation of these results to humans is warranted.

5.5 Conclusions

Our results demonstrated that tranilast can successfully inhibit conduction slowing and heterogeneity associated with the hypertensive substrate that predisposes to AF. The reduction in AF vulnerability with tranilast was seen despite high blood pressure

levels. Presumably, these outcomes are largely attributable to the anti-fibrotic effects of tranilast on the atrial substrate (chapter 4).

5.6 FIGURES

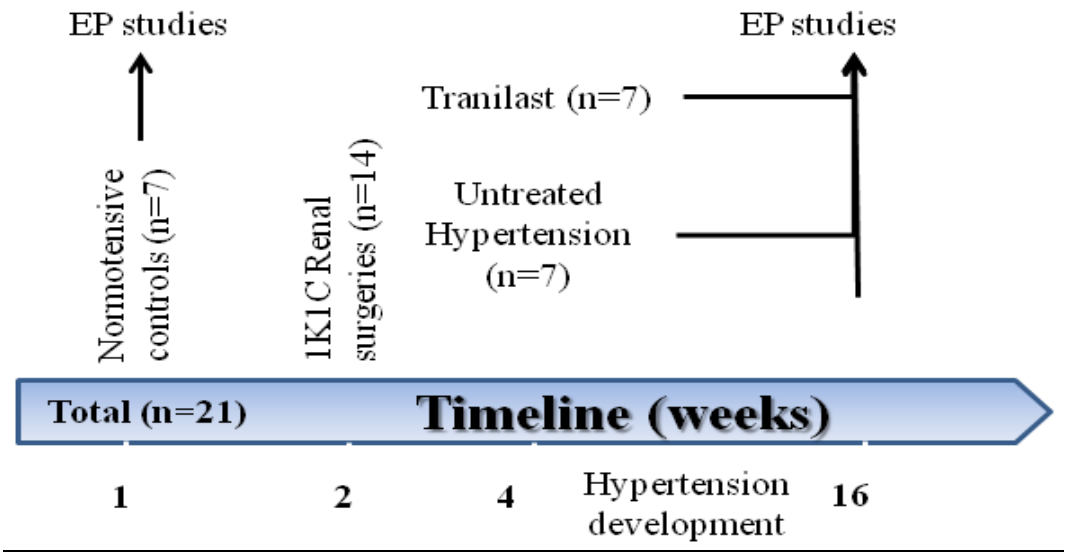

Figure 27: Study timeline

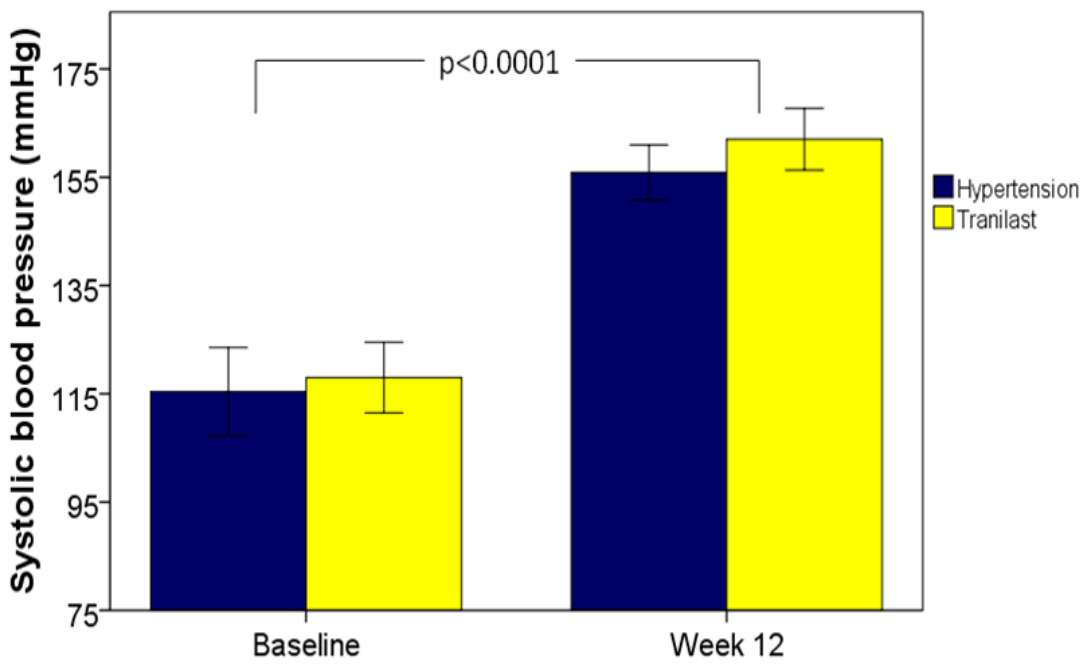

Figure 28: Blood pressure development over 12 week period following renal surgery

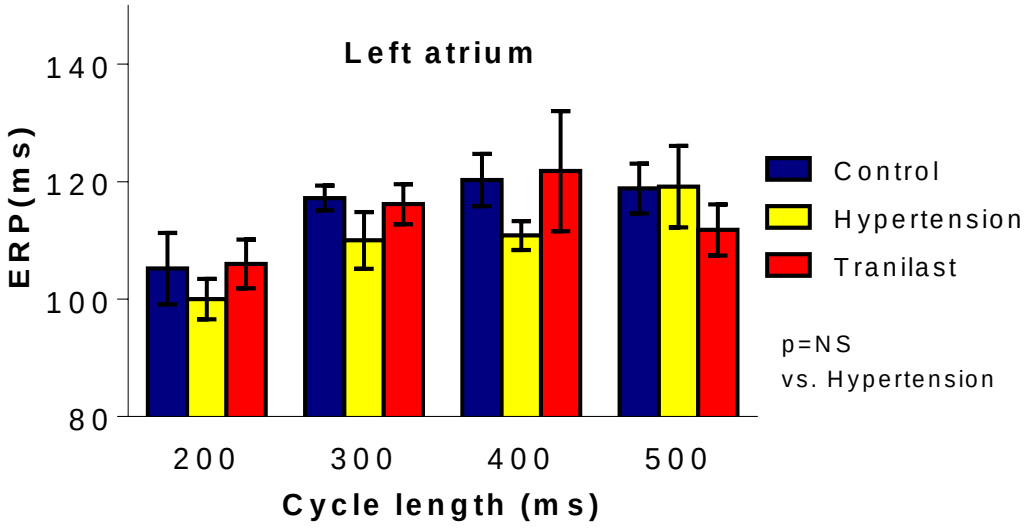

Figure 29: Atrial effective refractory period changes in LA

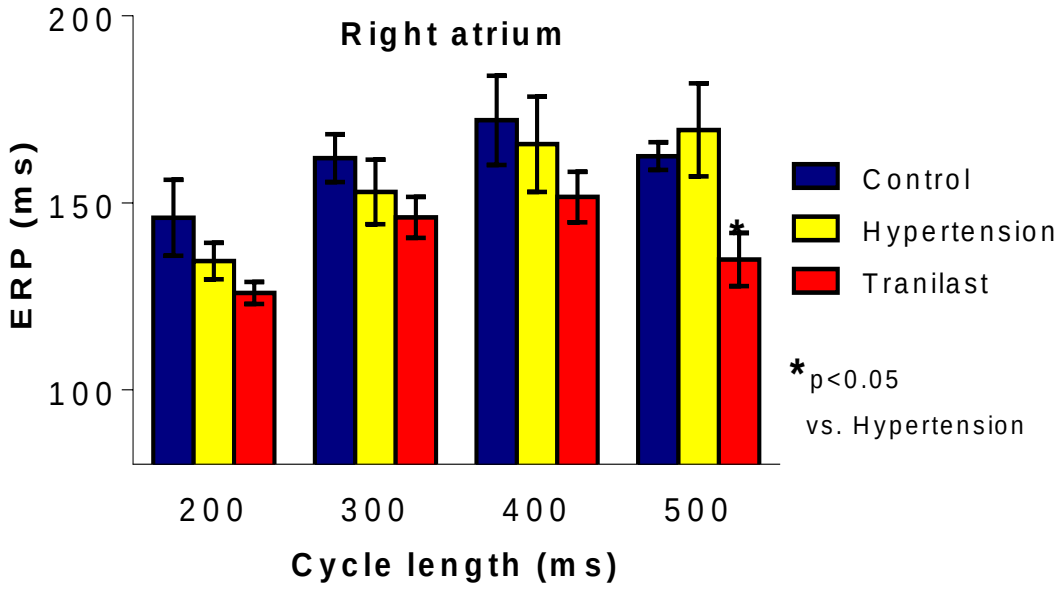

Figure 30: Atrial effective refractory period changes in RA

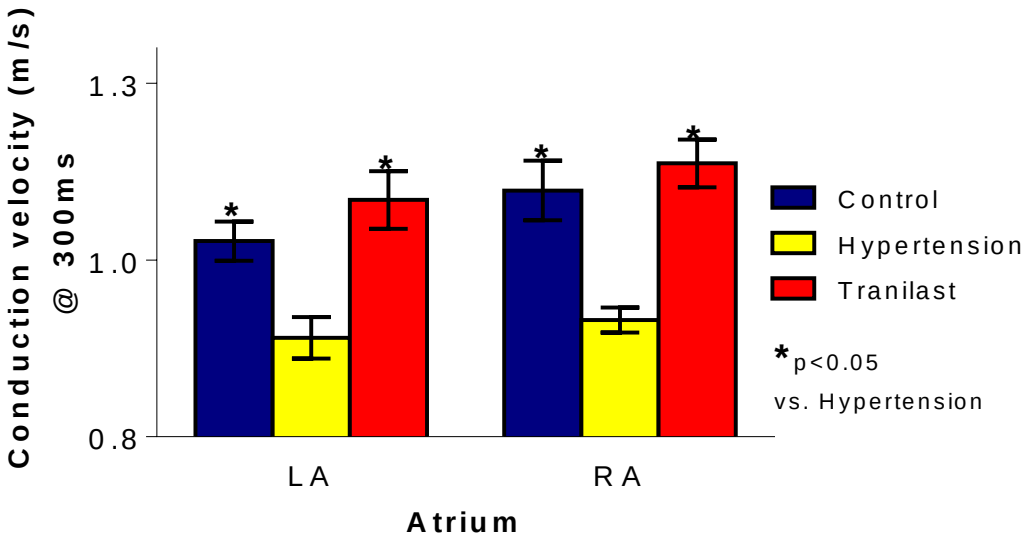

Figure 31: Prevention of conduction velocity slowing after tranilast treatment

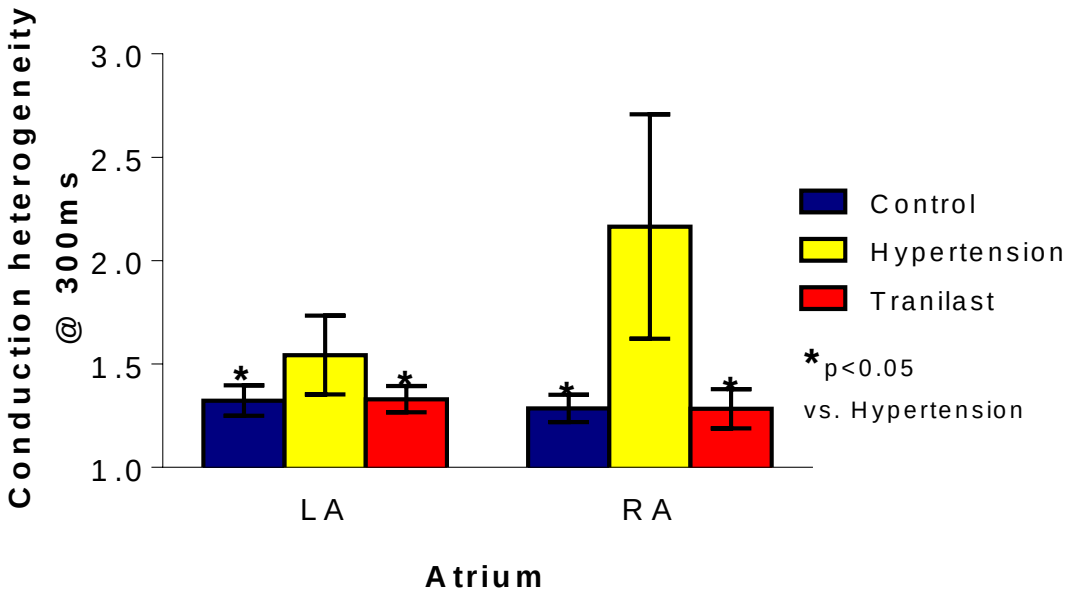

Figure 32: Prevention of conduction heterogeneity after tranilast treatment

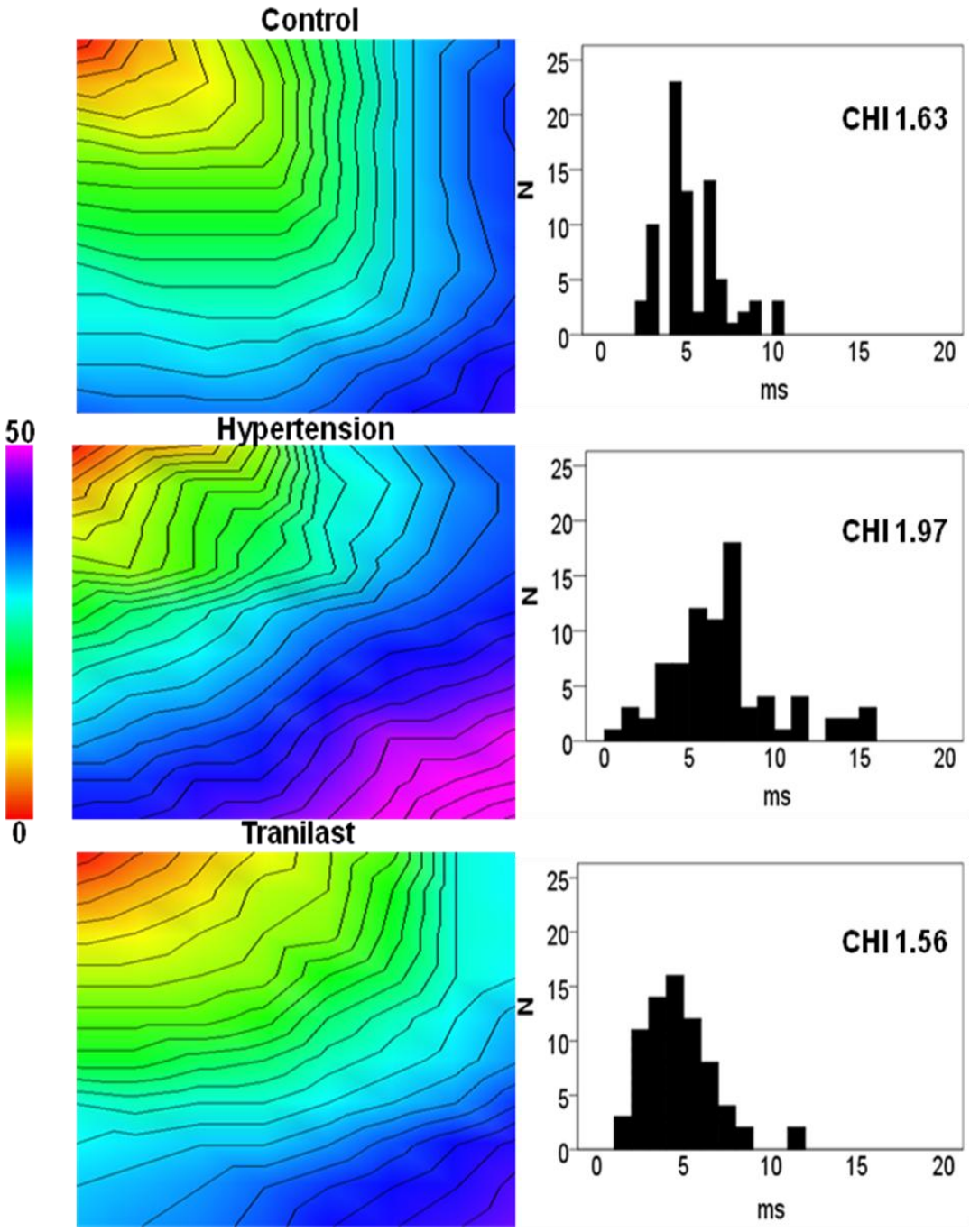

Figure 33: Representative activation maps and corresponding phase histograms in LA at 300 ms cycle length; A) Hypertension; B) Tranilast

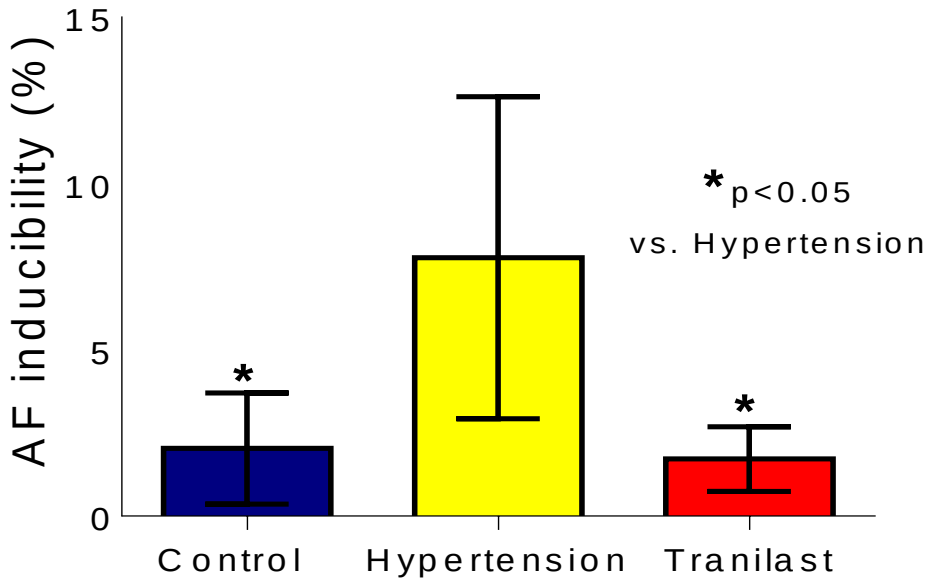

Figure 34: AF susceptibility reduction after tranilast treatment

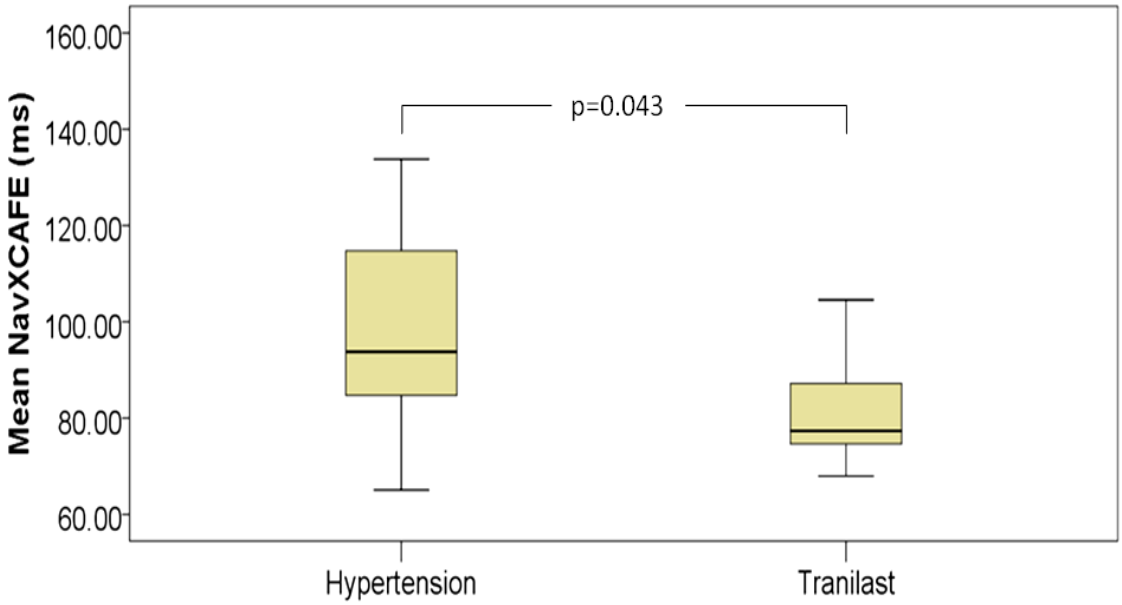

Figure 35: CFAE changes after treatment with anti-fibrotic drug, tranilast

6 SPATIO-TEMPORAL CHARACTERISTICS OF ATRIAL FIBRILLATION ELECTROGRAMS IN SELF-TERMINATING VERSUS SUSTAINED AF EPISODES

6.1 Introduction:

Atrial fibrillation (AF) is a progressive disease where the initial diagnosis of paroxysmal AF often develop into a more persistent or chronic condition over years and/or decades [53]. Substantial research interest has focused on characterizing the substrate underlying AF with common pathways of atrial enlargement, fibrosis, inflammation and conduction abnormalities associated with an increased risk of sustained AF [228, 270]. However, AF episode duration has been shown to vary significantly from minutes, hours, days and months within the same patient and over a similar time frame [280]. It is poorly understood how the 'same' atrial substrate could perpetuate both sustained and spontaneously terminating AF episodes.

Both complex fractionated atrial electrograms (CFAE) and dominant frequency (DF) are thought to represent substrate regions contributing to the perpetuation and sustenance of AF [261, 265, 268]. The conventional methodology of mapping AF in the human electrophysiology laboratory is limited by point-by-point and temporally disconnected electrogram sampling of continuous AF. This sequential mapping technique cannot adequately map the chaotic and complex spatio-temporal

activations during AF using currently available high-density mapping catheters. Indeed, the variable outcomes associated with ablation of CFAE [281-285] and/or high DF [261, 268, 286, 287] sites may be due to the limitation of this mapping capability. Although most data suggest that CFAE is spatially and temporally stable [265, 283, 288-297], these findings are often based on stability of "means" over discrete epochs of time rather than continuous monitoring of AF dynamics. In contrast, contemporary studies with more eloquent methods of assessing signal stability have challenged whether CFAE is spatio-temporal stable [266, 284, 298].

To date, no studies have assessed whether the degree of CFAE or DF spatio-temporal stability maybe a marker of arrhythmia stability, especially during the different phases of an AF episode from its initiation to maintenance and termination. Furthermore, how the relative spatio-temporal stability of fibrillatory signal characteristics differs in self-terminating and sustained episodes remains unknown. Here, we utilized a novel statistical methodology for quantifying spatio-temporal stability of AF electrograms obtained from direct contact multi-electrode mapping of both self-terminating and sustained AF episodes in sheep with induced hypertension. We hypothesized that the spatio-temporal stability of CFAE or DF are more robust markers for predicting AF sustenance or termination than comparing their sequential mean values.

6.2 Methods:

We analyzed AF episodes from epicardial contact mapping in 'one-kidney, one-clip' (1K1C) hypertensive sheep model. The 1K1C model has been described previously [246]. In brief, nephrectomy was performed on the right kidney followed by placement of a vascular occluder over the left renal artery. This could be inflated from a subcutaneous port subsequently to maintain high blood pressure.

This study was approved by the *'University of Adelaide Animal Ethics Committee'* and '*SA Pathology Animal Ethics Committee'*. Guidelines from the "Australian code of practice for the care and use of animals for scientific purposes" 7th edition, 2004 adopted by the 'National health and medical research council' were followed for all the experimental procedures.

6.2.1 Direct contact mapping

Animals were under general anaesthesia with sodium thiopentone (10-15 mg/kg) used for induction to facilitate endo-tracheal intubation and Isoflurane 2-4% in 100% oxygen at 4L/min for maintenance throughout the procedure. Non-invasive blood pressure, heart rate, pulse oximetry, end-tidal CO_2 and temperature were continuously monitored during the study. Direct contact mapping was performed during open chest study using a custom-made epicardial plaque with 90 electrodes (4mm inter-electrode spacing) on both left (LA) and right (RA) atrium. Midline

sternotomy was used to access the heart for mapping with epicardial plaque over the atria. The plaque was then connected to a computerized recording system (LabSystem Pro, Bard Electrophysiology, MA, USA). Continuous recording of surface-ECG and overlapping bipolar electrograms were stored for offline analysis. Electrograms were notch filtered from 30-500Hz, and measured with sweep speed of 200mm/s.

6.2.2 Atrial fibrillation episodes

AF was defined by a fast irregularly irregular a-a interval lasting for ≥ 2 seconds. We excluded any episode with < 28 seconds to allow for effective spatio-temporal stability comparisons. AF that terminated spontaneously without any intervention was defined as self-terminating episodes (n=42; 19 sheep), and AF that continued for more than 15 minutes was defined as sustained episodes (n=6; 6 sheep). All signals were analyzed offline with custom analysis software to calculate signal characteristics. Each AF episode was broken down into 4-second epochs from the end of the AF episode backwards to ensure complete characterization of the epoch exactly prior to spontaneous termination.

6.2.3 Spatio-temporal stability index

Spatio-temporal stability of CFAE and DF was determined by calculating the intraclass correlation coefficient (ICC). As per standard statistical methodology, ICC

is defined as a ratio of relative variance of data across the plaque (i.e., spatial variation) as compared with variance across time (i.e., temporal variation). ICC therefore provided a level of spatial agreement across time (herewith labeled Spatio-temporal stability index; STSI) with higher values being associated with greater spatio-temporal stability in signal characteristics. Heat maps representing the plaque area with respective electrodes were utilized to further support visualization of changes in signal characteristics at a given time point. Firstly, inverse CFE-m (1/1000*CFE-m) was calculated and plotted on with their respective electrodes for each 4-second epoch of an episode. Figure 36 shows a representative 4-second epoch whereby electrograms with higher fractionation (lower CFE-m) are shown with higher intensity on the heat map. In this example, DF was similar across the entire plaque. Figure 37 shows an example of CFE-m heat maps during AF initiation, maintenance and termination. Note that the intensity of each heat map varies with the degree of electrogram complexity within each 4-second epoch. We used the following equation to calculate ICC agreement in a two way random mixed effects model for each episode, where electrode and epoch were modelled as random effects:

$$STSI = \sigma^2(b) / \sigma^2(a) + \sigma^2(b) + \sigma^2(w)$$

$\sigma^2(a)$ is the variance of the measured parameter (CFE-m or DF) between epochs (time variance), $\sigma^2(b)$ is the variance of between electrodes for each epoch (spatial variance) and $\sigma^2(w)$ is the residual variance in the model. STSI was sensitive to

changes in spatial variance over time, but also mean changes in signal characteristics, even if spatial patterns were essentially the same. For example, if the overall electrogram complexity increases between epochs, but still had the same spatial pattern of complexity, the STSI would still reduce. Furthermore, the ICC is sample size independent, such that episodes that had 7 to 30 epochs could be equally compared without sample size bias.

6.2.4 AF electrogram analysis

Electrogram analysis was performed using custom made software (Electrophysiological plaque analysis software), with settings analogous to the Ensite NavX system (St. Jude medical, MN, USA). The algorithm calculated CFE-m as the average of time intervals between marked deflections on the fibrillatory signal using a refractory period of 40ms; Peak to peak sensitivity of 0.05 mV; Minimum electrogram duration of 10 ms; and downstroke threshold of 0.03 V/s. These settings were optimized for detecting the relevant signal above the baseline threshold of 0.05mV whilst avoiding over-tagging of far field signals or noise. Each episode was exported from the Bard system and CFE-m was calculated for each of the 80 bipolar electrograms (90 electrodes) across 4 second epochs from the beginning to the end of the AF recording or from the first two minutes and last two minutes of the sustained 15 minute episodes. Electrograms were rectified and filtered using Butterworth filters (1-20Hz) and edge-tapered with a Hanning window before Fast Fourier Transform was applied to derive DF. DF values were excluded if the regularity index

was less than 0.2. DF was defined as the frequency containing maximum power within the frequency domain between 3–15 Hz.

6.2.5 Statistics:

Normally distributed data were expressed as mean ± standard deviation. STSI was calculated for all episodes recorded during our experiments as described above. Mean STSI was compared with an independent *t* test to examine the differences in spatio-temporal stability between the initial phase of self-terminating (n=42) and sustained episodes (n=6). All self-terminating episodes had a minimum duration of 28 seconds as per our selection criteria. To account for the different duration of the self-terminating episodes and sustained episodes we chose to compare the first 16 seconds of self-terminating and sustained episodes. In addition DF median and CFE-m for each episode was calculated and compared.

To explore whether spatio-temporal stability evolved over time during continuous 15 minute recording of sustained episodes, we compared the STSI of first two minutes (n=6) and the last two minutes (n=6) with a paired samples *t* test. In addition, the DF median and CFE-m was calculated for each of these time periods and compared using a paired t-test. Finally, we assessed the STSI differences between the complete self terminating episode (n=42) and the same episode with the last epoch removed (n=42) and the same episode with last two epochs (n=42) removed to examine whether spatio-temporal stability changed prior to spontaneous termination of AF.

This approach was taken because STSI could not be calculated on single epoch of time. A significant increase in STSI upon removal of ultimate and penultimate epochs inferred spatio-temporal destabilization of signal characteristics prior to termination of arrhythmia. In contrast, the CFE-m and DF were calculated for the last epoch, and its penultimate epoch and compared via a mixed effects model to the remaining epochs of the episodes to provide effective comparisons of means in the final stages of arrhythmia prior to spontaneous termination. All tests were performed using PASW (Version 20; IBM, New York, USA) with statistical significance set at $p < 0.05$.

6.3 Results:

A total of 19 male merino cross sheep (57±6 kg) with induced 1K1C hypertension (12±2 weeks) were used for this study. A total of 42 self-terminating episodes (mean duration; 60±23 secs; range 28-100 secs; 19 sheep) and 6 longstanding sustained episodes (>15 min; 6 sheep) were recorded. A total of 72,156 four-second epochs were assessed for CFE-m and DF. A total of 67,733 four-second epochs from the 48 episodes of AF were used for analysis. This was after manual verification to ensure consistently annotated electrograms and removal of data points with poor contact during mapping.

6.3.1 Spatio-temporal stability in the initiation phase of self-terminating versus sustained AF episodes

A 16-second window from AF initiation was used to study the complexity pattern of self-terminating against the sustained AF episodes (Figure 38**)**. During AF initiation, self-terminating AF episodes demonstrated higher CFE-m (91±22 vs. 73±7 ms; p=0.06) although this did not reach statistical significance; and significantly lower median DF (8.0±1.5 vs. 10.4±0.9 Hz; p=0.001) as compared to sustained AF episodes. On the other hand, both STSI of CFE-m (0.60±0.19 vs. 0.57±0.21; p=0.73) and DF (0.21±0.28 vs. 0.33±0.20; p=0.32) did not differ during the initial phases of self-terminating and sustained AF episodes.

6.3.2 Spatio-temporal stability with sustained AF

We further sought to examine if the spatio-temporal pattern in sustained episodes stabilizes over time by comparing the first and last 2 minutes of the 15-minute sustained episodes (Figure 39). The results showed that both CFE-m (73±7 vs. 72±7 ms; p=0.5) and median DF (10.8±0.9 vs. 10.3±0.8 Hz; p=0.07) were unchanged over time. Interestingly, STSI of CFE-m increased significantly (0.59±0.19 vs. 0.76±0.09; p =0.025) whereas STSI of DF remained unchanged (0.27±0.14 vs. 0.36±0.17; p=0.48) with more sustained arrhythmia. Figure 40 shows the CFE-m heat maps during the first and last 2-minutes of the 15-minute sustained AF episodes. The color intensity of the heat maps remained quite consistent between these two time-periods

within each episode, consistent with the non-significant changes in mean CFE-m. However, higher spatio-temporal stability with less variability is evident from these heat maps during the 13th to 15th minute as compared to the first 2 minutes in each sustained AF episodes except for episode 6 where STSI was unchanged.

6.3.3 Significant changes prior to termination in self-terminating AF episodes

CFE-m (last epoch vs. penultimate epoch vs. all remaining epochs: 96±20 vs. 92±20 vs. 92±22 ms; p=0.14) was similar but the median DF (7.7±1.0 vs. 8.1±1.2 vs. 8.0±1.3 Hz; p=0.006) was significantly lower prior to AF termination (Figure 41). Comparatively, STSI of CFE-m increased significantly after removal of the penultimate and last 2 epochs (0.49±0.18 vs. 0.54±0.18 vs. 0.56±0.18; p=0.01) indicating increased spatio-temporal variability of CFE-m changed prior to termination. This pattern was not seen with STSI of DF (0.19±0.17 vs. 0.21±0.19 vs. 0.20±0.18; p=0.81) (Figure 42).

6.4 Discussion

In this study, we assessed the spatio-temporal stability of CFE-m and DF during: 1) self-terminating and sustained AF episodes; 2) Initial and maintenance phases of sustained AF; and 3) at the pre-termination phase of arrhythmia. The principal findings are as follows:

- STSI of CFE-m increased with stabilization of AF during sustained AF episodes and decreased just prior to spontaneous AF termination;

- Neither STSI of DF nor the means of CFE-m/DF demonstrate any significant change during the same phases of an AF episode;

- Median DF was significantly higher in the initiation phase of sustained than self-terminating AF episodes;

- In both self-terminating and sustained AF episodes, mean STSI of CFE-m and DF were only marginal indicating poor spatio-temporal stability.

6.4.1 Do CFAE and DF sites represent substrates for AF?

Konings *et al* illustrated changes in fibrillatory pattern and varying degree of CFAE during human AF that correlated with pivoting waves, wave collisions, lines of conduction block and areas of slow conduction [299, 300]. Further, CFAE sites have been observed around fibrous tissue that could sustain complex electrograms due to lines of conduction block or slowing [120, 301, 302]. In human AF, ablation at sites with high DF activity has been shown to prolong the AF cycle length and terminate the arrhythmia [303]. Such high frequency sites are thought to be drivers of AF that have a role in maintaining the arrhythmia [46, 304, 305]. Further, sites with CFAE have been shown to be in close proximity to high DF areas [306, 307]. However, CFAE based ablation has only achieved comparable results to other contemporary

techniques in patients with longstanding persistent AF [308]. Although prospective DF guided catheter ablation in addition to pulmonary vein isolation did not improve AF termination rate or sinus rhythm maintenance [309], adjunctive CFAE ablation to pulmonary vein isolation was beneficial in those with non-paroxysmal AF [310, 311].

Given the lack of clear-cut advantages with data from ablation studies, it is therefore uncertain whether areas with CFAE and high DF always represent substrate sites relevant to AF. Indeed, areas with CFAE during AF do not always represent abnormal underlying atrial substrate since these sites may also demonstrate normal electrophysiological characteristics during sinus rhythm [312]. More recently, activation mapping with monophasic action potential recordings have suggested that a majority of CFAE sites represent non-local activations, with only a minority of CFAE sites attributable to high activation rates in human AF [313]. Adding to these, the limitations of current techniques in real-time mapping of DF/CFAE and the diverse ways by which CFAE are defined may also contribute to the underwhelming ablation results [314, 315]. In the present study, our novel method of assessing CFE-m using STSI resonated well with the change in AF dynamics. We had anticipated that we would observe a difference in STSI at the onset of self-sustained and persistent AF episodes; however, it seems that all episodes begin similarly with the arrhythmia ‘searching’ for a stable environment to anchor or self-terminate in the absence of such. While this phenomenon of increasing STSI with AF stabilization and decreasing STSI just prior to AF termination implies the physiologic aspects of

CFAE, it does not necessary implicate CFAE as substrate sites for AF. In this study, the AF substrate appears to be dynamic as the each sustained AF episode as seen in different sheep was preceded by shorter paroxysmal episodes in the same sheep or 'substrate'. The distinct lack of changes in both DF and its STSI with AF dynamics seem to suggest a lesser importance for the frequency domain component of fibrillatory signals although higher median DF during AF initiation seems to predict more sustained AF episodes.

6.4.2 Poor spatio-temporal stability of AF electrograms

Clinical studies of CFAE have reported that they were stable and reproducible using sequential mapping data [293, 296, 297]. In contrast, Habel *et al* reported variability in spatio-temporal characteristics of CFAE when the analysis was performed with continuously recorded signals over a 5-minute period [298]. Recent systemic review of CFAE stability showed a moderate *r* value of only 0.67 for CFAE correlation between sequential mapping [314]. In the same review, CFAE sites remained fractionated from sequential and continuous recordings between 75 and 81% of the time [314]. Here, our assessment of AF electrogram stability took into account both spatial and temporal aspects by using the STSI. The mean STSI of all self-terminating AF episodes (Figure 42) were low for both CFE-m and DF (0.59±0.18 & 0.25±0.21 respectively). Likewise, mean STSI of CFE-m of the first 2 minutes and between 13^{th} & 15^{th} minute of the sustained AF episodes was 0.69 (Figure 40). Taken together, the poor stability of fibrillatory electrograms in both time- and

frequency- domains is in keeping with the dynamic nature of AF and previous studies showing the sources sustaining AF to be non-repetitive, unrestricted to any atrial sites, disorganized and unstable [316-318].

6.4.3 Clinical Implications

This study provided evidence that both CFAE and DF are dynamic and unstable. Therefore, sequential mapping technique used in the clinical laboratories cannot adequately provide guidance for catheter ablation. Although CFAE appears to be more physiologic than DF with its STSI more reflecting of AF maintenance or de-stabilization, it remains unknown whether they represent better substrate than DF. Better clinical mapping equipment with higher density and area of coverage is crucial to improve our ability to identify and target critical sites that sustain AF.

6.5 Limitations

The ovine data used for this analysis may not reflect human AF. Arbitrary segmentation of AF into 4-second epochs could have been smaller to gain finer temporal information; however, it is well established that you need a reasonable signal sample to estimate CFAE in a reliable fashion.

6.6 Conclusions

AF electrogram characteristics demonstrate poor spatio-temporal stability in keeping with the dynamic nature of the arrhythmia. Spatio-temporal stability index of CFAE and DF did not differ at AF onset. However, spatio-temporal stabilization of CFAE breeds AF sustenance and its de-stabilization heralds spontaneous termination.

6.7 Figures

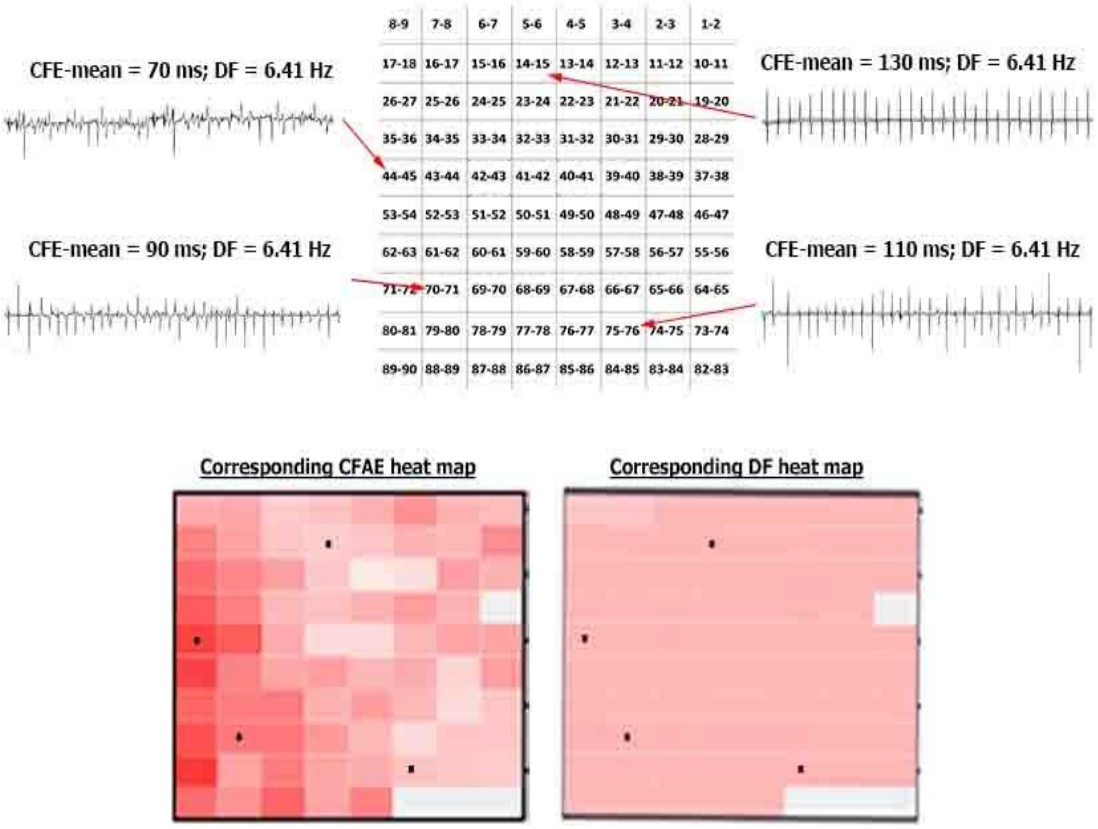

Figure 36: Electrograms at varying CFE-mean and DF representing the plaque region along with their corresponding heat maps.

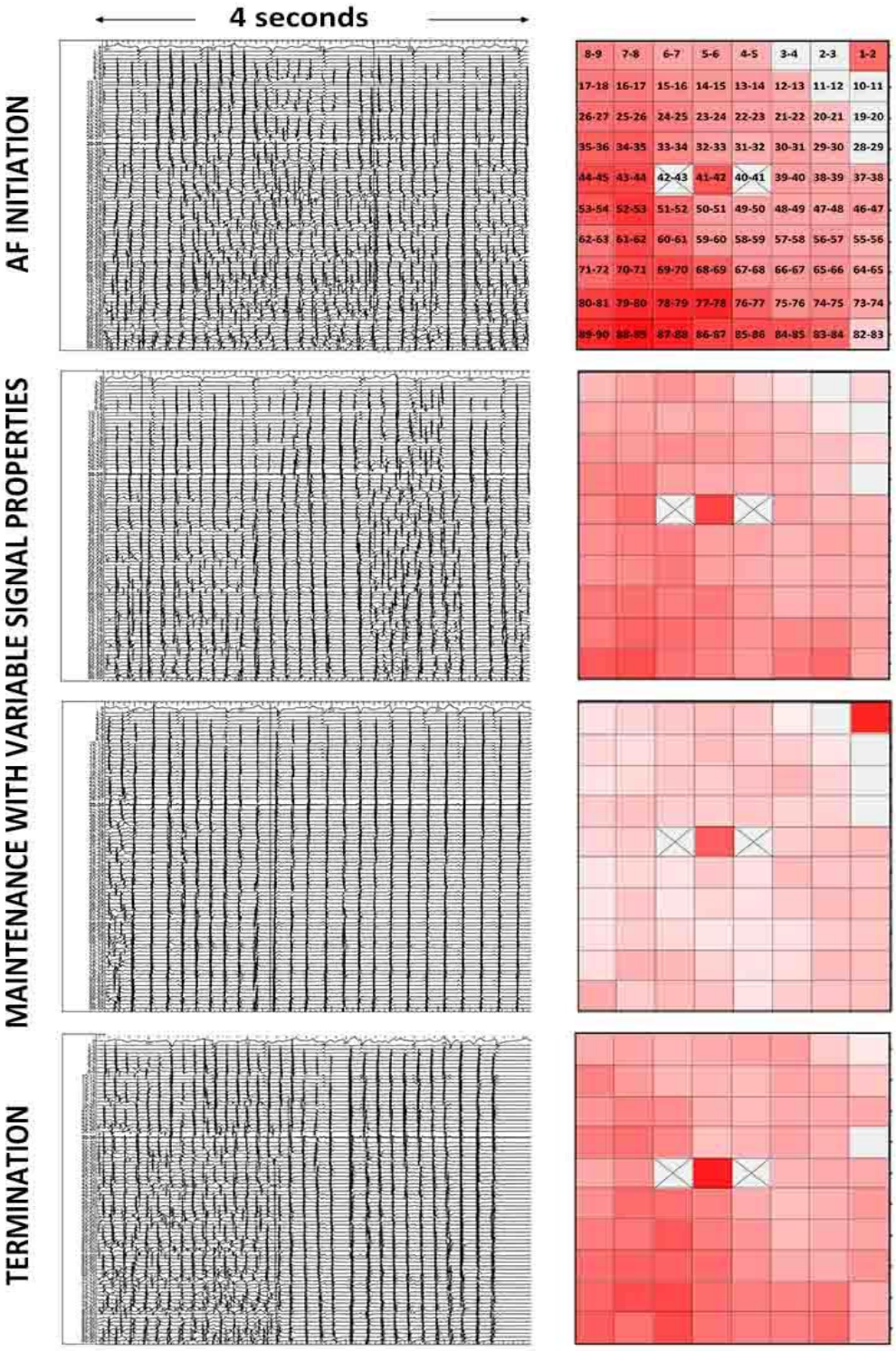

Figure 37: Different stages of AF as expressed with heat maps in relation to its electrograms

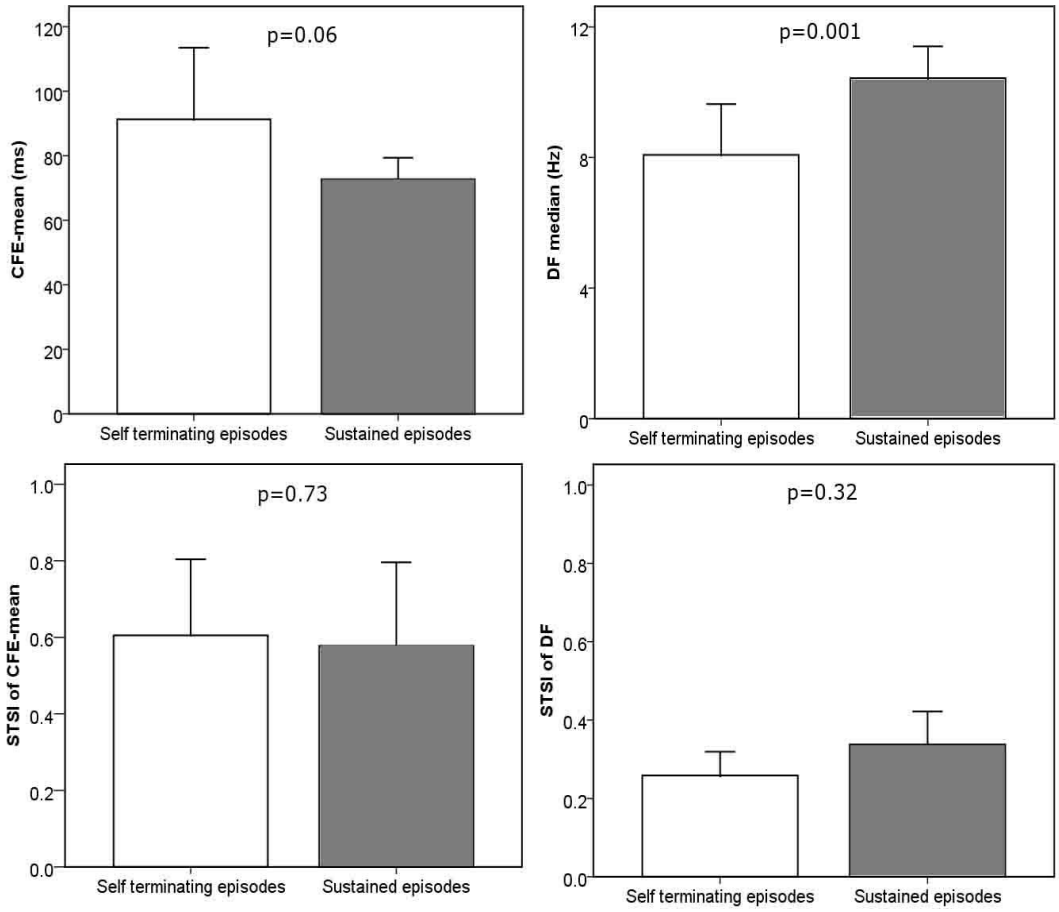

Figure 38: Differences between self terminating and sustained episodes at the initiation phase of AF (First 16 seconds)

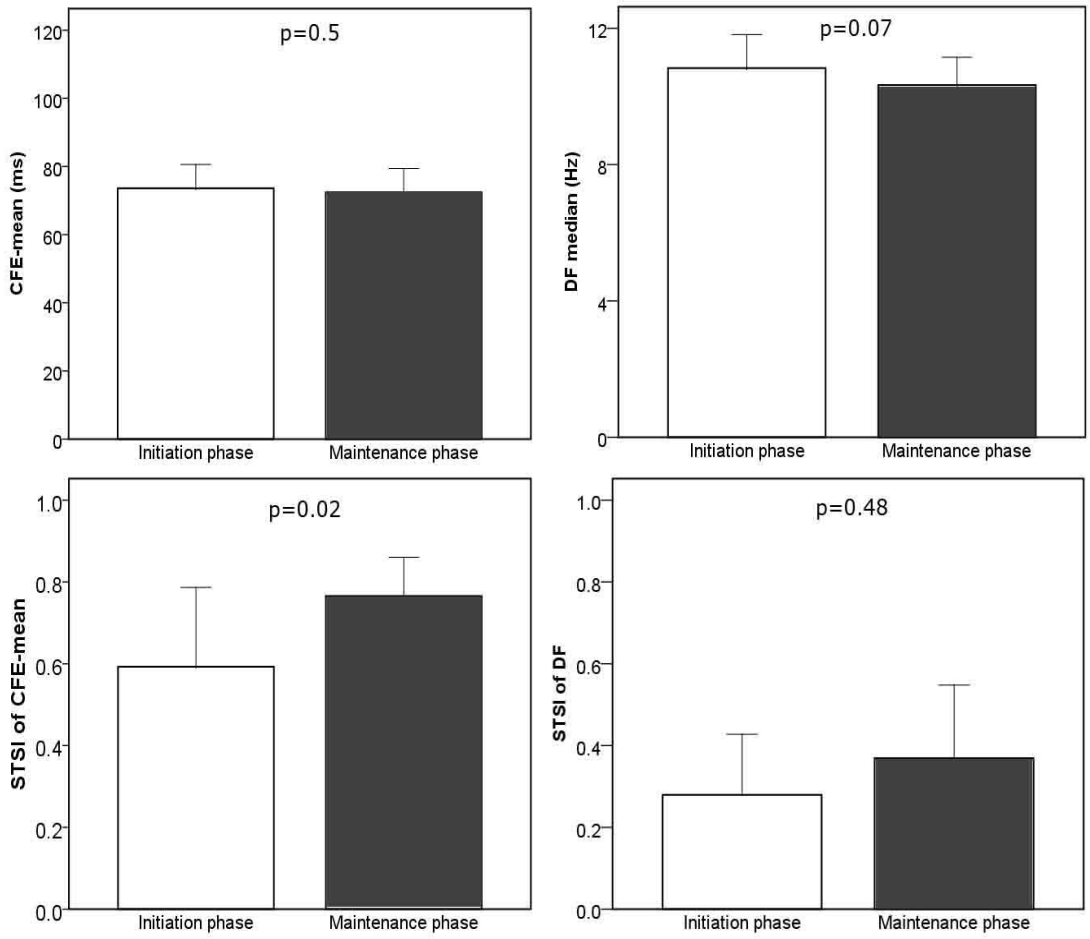

Figure 39: Sustained episodes stabilizes over time from initiation to maintenance phase

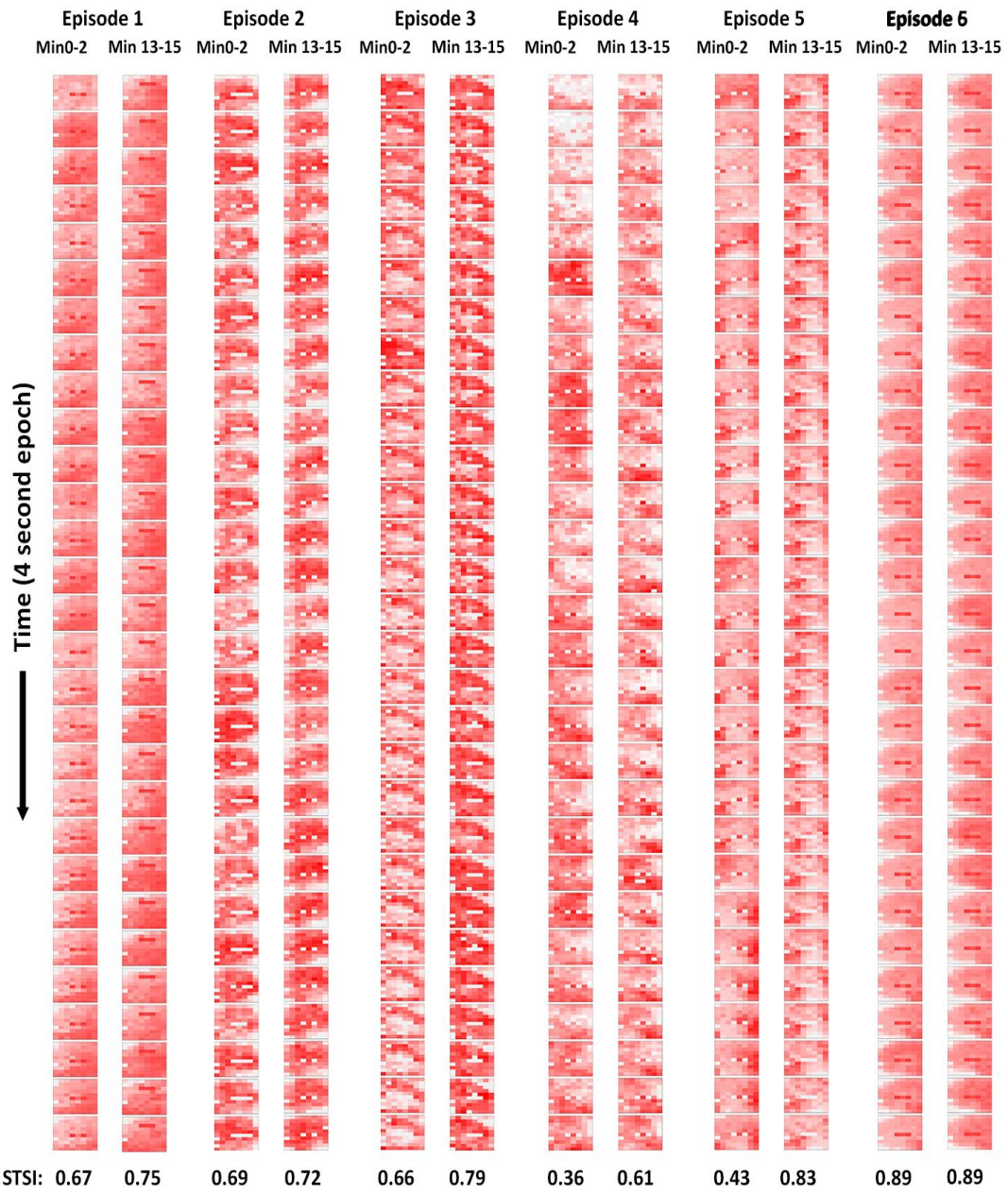

Figure 40: Individual breakdown of sustained episodes expressed in heat maps with their corresponding STSI of CFE-mean

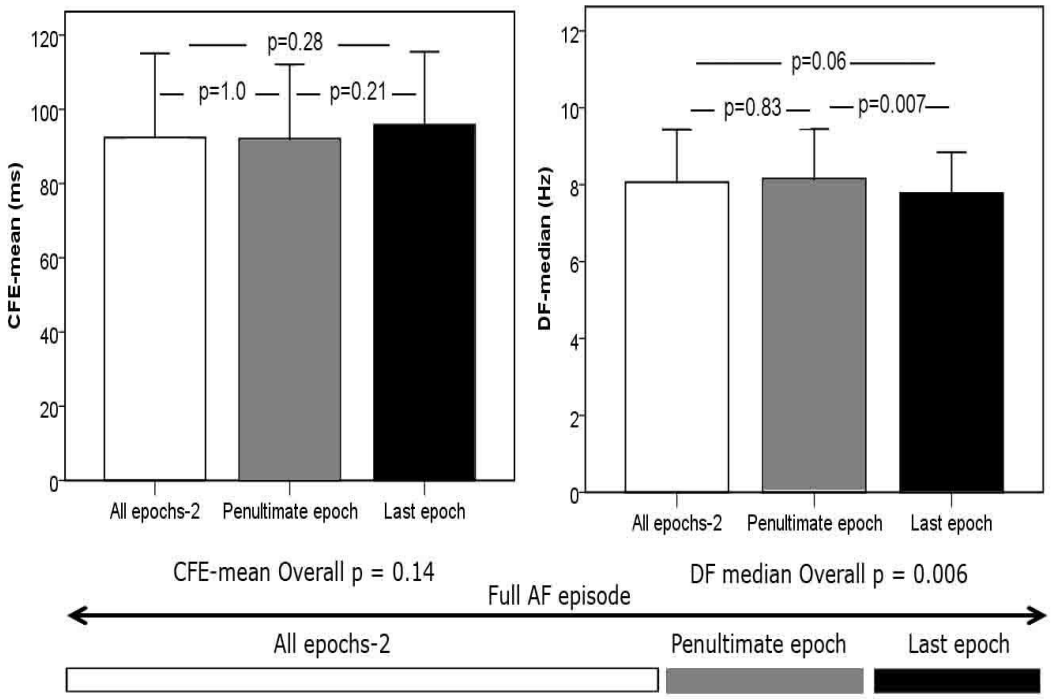

Figure 41: Comparison of overall CFE-mean and DF median with terminal phases

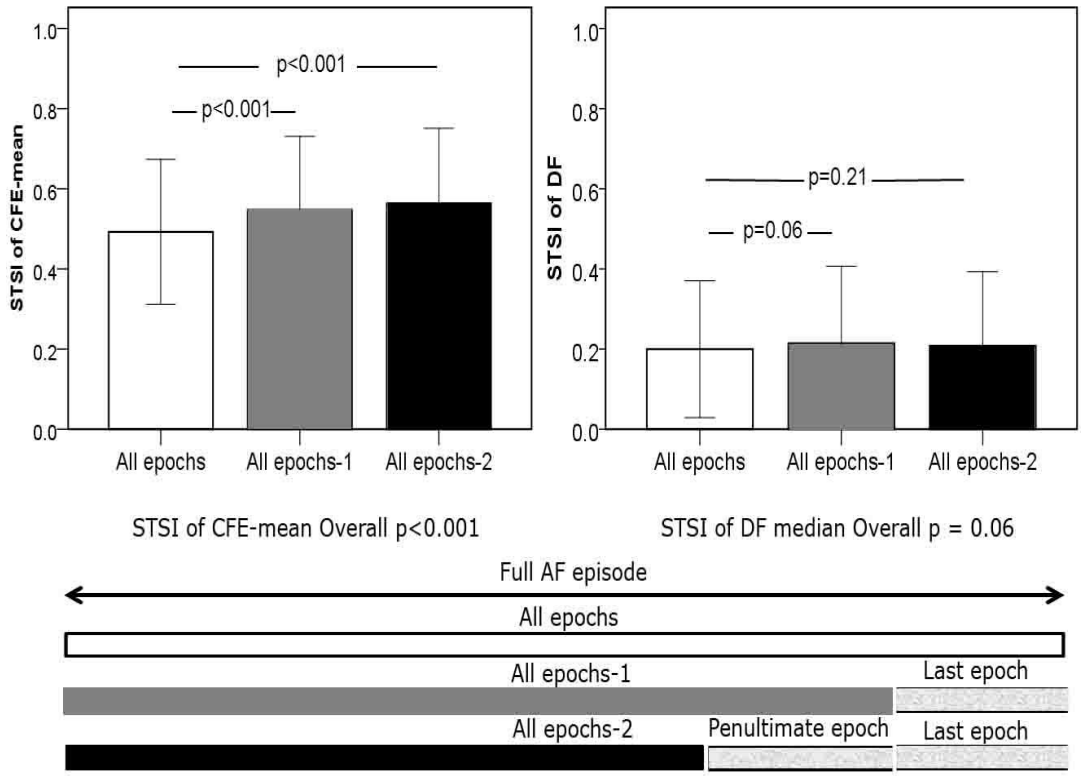

Figure 42: Comparison of STSI changes between whole episode and terminal phases of AF

7 FINAL DISCUSSIONS & FUTURE DIRECTIONS

This thesis discusses in detail the reverse remodeling effects of anti-hypertensive and anti-fibrotic drugs in a hypertensive ovine model. Given the multi-factorial complexity of human hypertensive disease, 'one-kidney one-clip' hypertensive model is the closest physiological condition that could be developed artificially. Hypertension, being an important substrate for atrial fibrillation, targeting this risk factor will have impact on the overall burden of AF with public health implications. Importantly, different studies in diverse substrates have shown that abnormal structural and electrical changes can be prevented and reversed with different therapies.

This works shows that primary prevention and secondary treatment in hypertensive substrate improves electrical and structural changes through beneficial effects on conduction properties, inflammation, fibrosis, myocyte hypertrophy, endomysial fibrosis, reduced expression levels of CTGF and TGF-ß$_1$ along with increased connexin43 expression levels resulting in reduced AF susceptibility in experimental setting. Results of this work provide the basis for future clinical studies. It supports aggressive blood pressure management in patients with AF and hypertension. Specifically, there are no current guidelines to direct therapy to significant blood pressure targets.

Further, electrogram characteristics have been used to guide catheter ablation of AF. Complex fractionated atrial electrogram (CFAE) ablation have shown variable results. Our findings confirm that CFAE is not spatio-temporally stable during AF. A new spatio-temporal stability index (STSI) has been shown in this study to be able to predict AF termination. Further studies with this index would be needed in clinical settings.

8 REFERENCES

1. Go, A.S., et al., *Prevalence of Diagnosed Atrial Fibrillation in Adults.* JAMA: The Journal of the American Medical Association, 2001. **285**(18): p. 2370-2375.

2. Li, D., et al., *Promotion of Atrial Fibrillation by Heart Failure in Dogs : Atrial Remodeling of a Different Sort.* Circulation, 1999. **100**(1): p. 87-95.

3. Alasady, M., et al., *Myocardial Infarction and Atrial Fibrillation: Importance of Atrial Ischemia.* Circulation: Arrhythmia and Electrophysiology, 2013.

4. Lau, D.H., et al., *Hypertension and atrial fibrillation: Evidence of progressive atrial remodeling with electrostructural correlate in a conscious chronically instrumented ovine model.* Heart rhythm : the official journal of the Heart Rhythm Society, 2010. **7**(9): p. 1282-1290.

5. Benjamin, E.J., et al., *Independent risk factors for atrial fibrillation in a population-based cohort. The Framingham Heart Study.* JAMA, 1994. **271**(11): p. 840-4.

6. Verheule, S., et al., *Alterations in Atrial Electrophysiology and Tissue Structure in a Canine Model of Chronic Atrial Dilatation Due to Mitral Regurgitation.* Circulation, 2003. **107**(20): p. 2615-2622.

7. Abed, H.S., et al., *Obesity results in progressive atrial structural and electrical remodeling: Implications for atrial fibrillation.* Heart Rhythm, 2013. **10**(1): p. 90-100.

8. Gami, A.S., et al., *Association of Atrial Fibrillation and Obstructive Sleep Apnea.* Circulation, 2004. **110**(4): p. 364-367.

9. Guidera, S. and J. Steinberg, *The signal-averaged P wave duration: a rapid and noninvasive marker of risk of atrial fibrillation.* J Am Coll Cardiol, 1993. **21**(7): p. 1645-1651.

10. Loaldi, A., et al., *Cardiac rhythm in hypertension assessed through 24 hour ambulatory electrocardiographic monitoring. Effects of load manipulation with atenolol, verapamil, and nifedipine.* Br Heart J, 1983. **50**(2): p. 118-26.

11. Haïssaguerre, M., et al., *Spontaneous Initiation of Atrial Fibrillation by Ectopic Beats Originating in the Pulmonary Veins.* New England Journal of Medicine, 1998. **339**(10): p. 659-666.

12. Wachtell, K., et al., *Cardiovascular morbidity and mortality in hypertensive patients with a history of atrial fibrillation: The Losartan Intervention For End point reduction in hypertension (LIFE) study.* Journal of the American College of Cardiology, 2005. **45**(5): p. 705-711.

13. Ciaroni, S., L. Cuenoud, and A. Bloch, *Clinical study to investigate the predictive parameters for the onset of atrial fibrillation in patients with essential hypertension.* American Heart Journal, 2000. **139**(5): p. 814-819.

14. Lip, G.Y. and D.G. Beevers, *ABC of atrial fibrillation. History, epidemiology, and importance of atrial fibrillation.* BMJ, 1995. **311**(7016): p. 1361-3.

15. Benjamin, E.J., et al., *Impact of Atrial Fibrillation on the Risk of Death: The Framingham Heart Study.* Circulation, 1998. **98**(10): p. 946-952.

16. Ball, J., et al., *Atrial fibrillation: Profile and burden of an evolving epidemic in the 21st century.* International Journal of Cardiology, 2013. **167**(5): p. 1807-1824.

17. Kannel, W.B., *Blood Pressure as a Cardiovascular Risk Factor.* JAMA: The Journal of the American Medical Association, 1996. **275**(20): p. 1571-1576.

18. FERRER, M.I., *The Sick Sinus Syndrome.* Circulation, 1973. **47**(3): p. 635-641.

19. CRAIG, R.J. and A. SELZER, *Natural History and Prognosis of Atrial Septal Defect.* Circulation, 1968. **37**(5): p. 805-815.

20. Korantzopoulos, P., et al., *Atrial Fibrillation in End-Stage Renal Disease.* Pacing and Clinical Electrophysiology, 2007. **30**(11): p. 1391-1397.

21. McMichael, J., *History of atrial fibrillation 1628-1819 Harvey - de Senac - Laennec.* Br Heart J, 1982. **48**(3): p. 193-7.

22. Cushny, A.E., *ON THE INTERPRETATION OF PULSE-TRACINGS.* J Exp Med, 1899. **4**(3-4): p. 327-47.

23. Mackenzie, J., *Observations on the Inception of the Rhythm of the Heart by the Ventricle: As the cause of Continuous Irregularity of the Heart.* Br Med J, 1904. **1**(2253): p. 529-36.

24. Rivera-Ruiz, M., C. Cajavilca, and J. Varon, *Einthoven's string galvanometer: the first electrocardiograph.* Tex Heart Inst J, 2008. **35**(2): p. 174-8.

25. Barold, S.S. and T. Fazekas, *Einthoven's first electrocardiogram 100 years ago.* Pacing Clin Electrophysiol, 2002. **25**(12): p. 1792-3.

26. Kannel WB, W.P., Benjamin EJ, Levy D *Prevalence, incidence, prognosis, and predisposing conditions for atrial fibrillation: population-based estimates* American Journal of Cardiology, 1998. **82**: p. 2N-9N.

27. Wang, T.J., et al., *Obesity and the risk of new-onset atrial fibrillation.* JAMA, 2004. **292**(20): p. 2471-2477.

28. Wyse, D.G., et al., *Lone Atrial FibrillationDoes it Exist?* Journal of the American College of Cardiology, 2014. **63**(17): p. 1715-1723.

29. Vulpian, A., *Note sur les effets de la faradisation directe des ventricules du coeur chez le chien.* Archives de Physiologie Normale et Pathologique, 1874. **6**: p. 975.

30. Nothnagel, H., *Ueber arythmische Herzthatigkeit.* Dtsch Arch Klin Med, 1876. **17**: p. 190-220.

31. Lewis, T., *REPORT CXIX. AURICULAR FIBRILLATION: A COMMON CLINICAL CONDITION.* Br Med J, 1909. **2**(2552): p. 1528.

32. Winterberg, H., *Ueber Herzflimmern und seine Beeinflussung durch Kampher.* Z Exp Pthol Ther, 1906. **3**: p. 182-208.

33. Rothenberger, C. and H. Winterberg, *Ber Vorhofflimmern und Vorhofflattern.* Pflugner's Archiv fur die Gesamte Physiologie des Menschen und der Tiere, 1915. **160**(42-90).

34. Lewis, T., H. Feil, and W. Stroud, *Observations upon flutter and fibrillation. II. The nature of auricular flutter.* Heart, 1920. **7**: p. 191-233.

35. Mines, G.R., *On dynamic equilibrium in the heart.* The Journal of Physiology, 1913. **46**(4-5): p. 349-383.

36. Garrey, W.E., *AURICULAR FIBRILLATION.* Physiological Reviews, 1924. **4**(2): p. 215-250.

37. Moe, G.K. and J.A. Abildskov, *Atrial fibrillation as a self-sustaining arrhythmia independent of focal discharge.* American Heart Journal, 1959. **58**(1): p. 59-70.

38. Allessie, M., et al., *Experimental evaluation of Moe's multiple wavelet hypothesis of atrial fibrillation*, in *Cardiac Electrophysiology and Arrhythmias*, D. Zipes and J. Jalife, Editors. 1985, Grune and Stratton: New york.

39. ALLESSIE, M.A., F.I.M. BONKE, and F.J.G. SCHOPMAN, *Circus Movement in Rabbit Atrial Muscle as a Mechanism of Tachycardia.* Circulation Research, 1973. **33**(1): p. 54-62.

40. Konings, K., et al., *High-density mapping of electrically induced atrial fibrillation in humans.* Circulation, 1994. **89**(4): p. 1665-1680.

41. Cox, J.L., et al., *Operations for atrial fibrillation.* Clin Cardiol, 1991. **14**(10): p. 827-34.

42. Scherf, D., *Studies on auricular tachycardia caused by aconitine administration.* Proc Soc Exp Biol Med, 1947. **64**(2): p. 233-9.

43. Zipes, D.P. and R.F. Knope, *Electrical properties of the thoracic veins.* The American Journal of Cardiology, 1972. **29**(3): p. 372-376.

44. Chen, Y.J., et al., *Electrophysiology of single cardiomyocytes isolated from rabbit pulmonary veins: implication in initiation of focal atrial fibrillation.* Basic Res Cardiol, 2002. **97**(1): p. 26-34.

45. Haissaguerre, M., et al., *Radiofrequency catheter ablation in unusual mechanisms of atrial fibrillation: report of three cases.* J Cardiovasc Electrophysiol, 1994. **5**(9): p. 743-51.

46. Jais, P., et al., *A Focal Source of Atrial Fibrillation Treated by Discrete Radiofrequency Ablation.* Circulation, 1997. **95**(3): p. 572-576.

47. Chen, S.-A., et al., *Initiation of Atrial Fibrillation by Ectopic Beats Originating From the Pulmonary Veins : Electrophysiological Characteristics, Pharmacological Responses, and Effects of Radiofrequency Ablation.* Circulation, 1999. **100**(18): p. 1879-1886.

48. Tsai, C.-F., et al., *Initiation of Atrial Fibrillation by Ectopic Beats Originating From the Superior Vena Cava : Electrophysiological Characteristics and Results of Radiofrequency Ablation.* Circulation, 2000. **102**(1): p. 67-74.

49. Hwang, C., et al., *Vein of Marshall Cannulation for the Analysis of Electrical Activity in Patients With Focal Atrial Fibrillation.* Circulation, 2000. **101**(13): p. 1503-1505.

50. Mainigi, S.K., et al., *Incidence and Predictors of Very Late Recurrence of Atrial Fibrillation After Ablation.* Journal of Cardiovascular Electrophysiology, 2007. **18**(1): p. 69-74.

51. Ortiz, J., et al., *Mapping the conversion of atrial flutter to atrial fibrillation and atrial fibrillation to atrial flutter. Insights into mechanisms.* Circulation Research, 1994. **74**(5): p. 882-894.

52. Narayan, S.M., et al., *Treatment of Atrial Fibrillation by the Ablation of Localized SourcesCONFIRM (Conventional Ablation for Atrial Fibrillation With or Without Focal Impulse and Rotor Modulation) Trial.* Journal of the American College of Cardiology, 2012. **60**(7): p. 628-636.

53. Kerr, C.R., et al., *Progression to chronic atrial fibrillation after the initial diagnosis of paroxysmal atrial fibrillation: Results from the Canadian Registry of Atrial Fibrillation.* American Heart Journal, 2005. **149**(3): p. 489-496.

54. Wijffels, M.C.E.F., et al., *Atrial Fibrillation Begets Atrial Fibrillation : A Study in Awake Chronically Instrumented Goats.* Circulation, 1995. **92**(7): p. 1954-1968.

55. Morillo, C.A., et al., *Chronic Rapid Atrial Pacing : Structural, Functional, and Electrophysiological Characteristics of a New Model of Sustained Atrial Fibrillation.* Circulation, 1995. **91**(5): p. 1588-1595.

56. Elvan, A., K. Wylie, and D.P. Zipes, *Pacing-Induced Chronic Atrial Fibrillation Impairs Sinus Node Function in Dogs: Electrophysiological Remodeling.* Circulation, 1996. **94**(11): p. 2953-2960.

57. Goette, A., C. Honeycutt, and J.J. Langberg, *Electrical Remodeling in Atrial Fibrillation: Time Course and Mechanisms.* Circulation, 1996. **94**(11): p. 2968-2974.

58. Gaspo, R., et al., *Functional Mechanisms Underlying Tachycardia-Induced Sustained Atrial Fibrillation in a Chronic Dog Model.* Circulation, 1997. **96**(11): p. 4027-4035.

59. Fareh, S., C. Villemaire, and S. Nattel, *Importance of Refractoriness Heterogeneity in the Enhanced Vulnerability to Atrial Fibrillation Induction Caused by Tachycardia-Induced Atrial Electrical Remodeling.* Circulation, 1998. **98**(20): p. 2202-2209.

60. Lee, S.-H., et al., *Regional Differences in the Recovery Course of Tachycardia-Induced Changes of Atrial Electrophysiological Properties.* Circulation, 1999. **99**(9): p. 1255-1264.

61. Yu, W.-C., et al., *Reversal of atrial electrical remodeling following cardioversion of long-standing atrial fibrillation in man.* Cardiovascular Research, 1999. **42**(2): p. 470-476.

62. Morton, J.B., et al., *Electrical Remodeling of the Atrium in an Anatomic Model of Atrial Flutter.* Circulation, 2002. **105**(2): p. 258-264.

63. Daoud, E.G., et al., *Effect of Atrial Fibrillation on Atrial Refractoriness in Humans.* Circulation, 1996. **94**(7): p. 1600-1606.

64. Kumagai, K., et al., *Electrophysiological properties in chronic lone atrial fibrillation.* Circulation, 1991. **84**(4): p. 1662-1668.

65. Sparks, P.B., et al., *Electrical Remodeling of the Atria Associated With Paroxysmal and Chronic Atrial Flutter.* Circulation, 2000. **102**(15): p. 1807-1813.

66. Attuel, P., et al., *Failure in the rate adaptation of the atrial refractory period: its relationship to vulnerability.* International Journal of Cardiology, 1982. **2**(2): p. 179-197.

67. Misier, A., et al., *Increased dispersion of "refractoriness" in patients with idiopathic paroxysmal atrial fibrillation.* J Am Coll Cardiol, 1992. **19**(7): p. 1531-1535.

68. Kamalvand, K., et al., *Alterations in atrial electrophysiology associated with chronic atrial fibrillation in man.* European Heart Journal, 1999. **20**(12): p. 888-895.

69. Tse, H.F., C.P. Lau, and G.M. Ayers, *Heterogeneous changes in electrophysiologic properties in the paroxysmal and chronically fibrillating human atrium.* J Cardiovasc Electrophysiol, 1999. **10**(2): p. 125-35.

70. Manios, E.G., et al., *Sinus pacemaker function after cardioversion of chronic atrial fibrillation: is sinus node remodeling related with recurrence?* J Cardiovasc Electrophysiol, 2001. **12**(7): p. 800-6.

71. Daoud, E.G., et al., *Remodeling of sinus node function after catheter ablation of right atrial flutter.* J Cardiovasc Electrophysiol, 2002. **13**(1): p. 20-4.

72. Hadian, D., et al., *Short-term rapid atrial pacing produces electrical remodeling of sinus node function in humans.* J Cardiovasc Electrophysiol, 2002. **13**(6): p. 584-6.

73. Luck, J. and T. Engel, *Dispersion of atrial refractoriness in patients with sinus node dysfunction.* Circulation, 1979. **60**(2): p. 404-412.

74. Sanfilippo, A.J., et al., *Atrial enlargement as a consequence of atrial fibrillation. A prospective echocardiographic study.* Circulation, 1990. **82**(3): p. 792-7.

75. Chen, Y.-J., et al., *Electrophysiologic Characteristics of a Dilated Atrium in Patients with Paroxysmal Atrial Fibrillation and Atrial Flutter.* Journal of Interventional Cardiac Electrophysiology, 1998. **2**(2): p. 181-186.

76. Allessie, M., J. Ausma, and U. Schotten, *Electrical, contractile and structural remodeling during atrial fibrillation.* Cardiovascular Research, 2002. **54**(2): p. 230-246.

77. Kostin, S., et al., *Structural correlate of atrial fibrillation in human patients.* Cardiovascular Research, 2002. **54**(2): p. 361-379.

78. Aime-Sempe, C., et al., *Myocardial cell death in fibrillating and dilated human right atria.* J Am Coll Cardiol, 1999. **34**(5): p. 1577-1586.

79. Ausma, J., et al., *Dedifferentiation of atrial cardiomyocytes as a result of chronic atrial fibrillation.* Am J Pathol, 1997. **151**(4): p. 985-97.

80. Ausma, J., et al., *Structural Changes of Atrial Myocardium due to Sustained Atrial Fibrillation in the Goat.* Circulation, 1997. **96**(9): p. 3157-3163.

81. Inoue, N., et al., *Rapid electrical stimulation of contraction modulates gap junction protein in neonatal rat cultured cardiomyocytes: Involvement of mitogen-activated protein kinases and effects of angiotensin ii-receptor antagonist.* J Am Coll Cardiol, 2004. **44**(4): p. 914-922.

82. Hagendorff, A., et al., *Conduction Disturbances and Increased Atrial Vulnerability in Connexin40-Deficient Mice Analyzed by Transesophageal Stimulation.* Circulation, 1999. **99**(11): p. 1508-1515.

83. van der Velden, H.M., et al., *Altered pattern of connexin40 distribution in persistent atrial fibrillation in the goat.* J Cardiovasc Electrophysiol, 1998. **9**(6): p. 596-607.

84. Ehrlich, J.R., et al., *Atrial-Selective Approaches for the Treatment of Atrial Fibrillation.* J Am Coll Cardiol, 2008. **51**(8): p. 787-792.

85. Bosch, R.F., et al., *Ionic mechanisms of electrical remodeling in human atrial fibrillation.* Cardiovascular Research, 1999. **44**(1): p. 121-131.

86. Workman, A.J., K.A. Kane, and A.C. Rankin, *The contribution of ionic currents to changes in refractoriness of human atrial myocytes associated with chronic atrial fibrillation.* Cardiovascular Research, 2001. **52**(2): p. 226-235.

87. Pau, D., et al., *Electrophysiological and arrhythmogenic effects of 5-hydroxytryptamine on human atrial cells are reduced in atrial fibrillation.* Journal of Molecular and Cellular Cardiology, 2007. **42**(1): p. 54-62.

88. Gaborit, N., et al., *Human Atrial Ion Channel and Transporter Subunit Gene-Expression Remodeling Associated With Valvular Heart Disease and Atrial Fibrillation.* Circulation, 2005. **112**(4): p. 471-481.

89. Van Wagoner, D.R., et al., *Outward K+ Current Densities and Kv1.5 Expression Are Reduced in Chronic Human Atrial Fibrillation.* Circulation Research, 1997. **80**(6): p. 772-781.

90. Brandt, M.C., et al., *The Ultrarapid and the Transient Outward K+Current in Human Atrial Fibrillation. Their Possible Role in Postoperative Atrial Fibrillation.* Journal of Molecular and Cellular Cardiology, 2000. **32**(10): p. 1885-1896.

91. Caballero, R., et al., *In Humans, Chronic Atrial Fibrillation Decreases the Transient Outward Current and Ultrarapid Component of the Delayed Rectifier Current*

Differentially on Each Atria and Increases the Slow Component of the Delayed Rectifier Current in Both. Journal of the American College of Cardiology, 2010. **55**(21): p. 2346-2354.

92. Dobrev, D., et al., *Molecular Basis of Downregulation of G-Protein–Coupled Inward Rectifying K+ Current (IK,ACh) in Chronic Human Atrial Fibrillation.* Circulation, 2001. **104**(21): p. 2551-2557.

93. Dobrev, D., et al., *The G Protein–Gated Potassium Current IK,ACh Is Constitutively Active in Patients With Chronic Atrial Fibrillation.* Circulation, 2005. **112**(24): p. 3697-3706.

94. Passier, R., et al., *CaM kinase signaling induces cardiac hypertrophy and activates the MEF2 transcription factor in vivo.* The Journal of Clinical Investigation, 2000. **105**(10): p. 1395-1406.

95. Molkentin, J.D., et al., *A Calcineurin-Dependent Transcriptional Pathway for Cardiac Hypertrophy.* Cell, 1998. **93**(2): p. 215-228.

96. Chelu, M.G., et al., *Calmodulin kinase II–mediated sarcoplasmic reticulum Ca2+ leak promotes atrial fibrillation in mice.* The Journal of Clinical Investigation, 2009. **119**(7): p. 1940-1951.

97. Bukowska†, A., et al., *Activation of the calcineurin signaling pathway induces atrial hypertrophy during atrial fibrillation.* Cellular and Molecular Life Sciences CMLS, 2006. **63**(3): p. 333-342.

98. Hajjar, I., J.M. Kotchen, and T.A. Kotchen, *HYPERTENSION: Trends in Prevalence, Incidence, and Control.* Annual Review of Public Health, 2006. **27**(1): p. 465-490.

99. Verdecchia, P., et al., *Atrial Fibrillation in Hypertension: Predictors and Outcome.* Hypertension, 2003. **41**(2): p. 218-223.

100. Ozer, N., et al., *P Wave Dispersion in Hypertensive Patients with Paroxysmal Atrial Fibrillation.* Pacing and Clinical Electrophysiology, 2000. **23**(11P2): p. 1859-1862.

101. Lau, D.H., et al., *Characterization of cardiac remodeling in a large animal one-kidney, one-clip hypertensive model.* Blood Pressure, 2010. **19**(2): p. 119-125.

102. Kistler, P.M., et al., *Atrial electrical and structural abnormalities in an ovine model of chronic blood pressure elevation after prenatal corticosteroid exposure: implications for development of atrial fibrillation.* European Heart Journal, 2006. **27**(24): p. 3045-3056.

103. Choisy, S.C.M., et al., *Increased Susceptibility to Atrial Tachyarrhythmia in Spontaneously Hypertensive Rat Hearts.* Hypertension, 2007. **49**(3): p. 498-505.

104. Lau, D.H., et al., *Atrial Arrhythmia in Ageing Spontaneously Hypertensive Rats: Unraveling the Substrate in Hypertension and Ageing.* PLoS ONE, 2013. **8**(8): p. e72416.

105. Tsioufis, C., et al., *Relationships of CRP and P Wave Dispersion With Atrial Fibrillation in Hypertensive Subjects.* American Journal of Hypertension, 2010. **23**(2): p. 202-207.

106. Medi, C., et al., *Atrial Electrical and Structural Changes Associated with Longstanding Hypertension in Humans: Implications for the Substrate for Atrial Fibrillation.* Journal of Cardiovascular Electrophysiology, 2011. **22**(12): p. 1317-1324.

107. Vinogradova, T.M., K.Y. Bogdanov, and E.G. Lakatta, *β-Adrenergic Stimulation Modulates Ryanodine Receptor Ca2+ Release During Diastolic Depolarization to Accelerate Pacemaker Activity in Rabbit Sinoatrial Nodal Cells.* Circulation Research, 2002. **90**(1): p. 73-79.

108. Schotten, U., et al., *Pathophysiological Mechanisms of Atrial Fibrillation: A Translational Appraisal.* Physiological Reviews, 2011. **91**(1): p. 265-325.

109. Baker, E.H., *Ion channels and the control of blood pressure.* British Journal of Clinical Pharmacology, 2000. **49**(3): p. 185-198.

110. Ehrlich, J.R., et al., *Characterization of a hyperpolarization-activated time-dependent potassium current in canine cardiomyocytes from pulmonary vein myocardial sleeves and left atrium.* The Journal of Physiology, 2004. **557**(2): p. 583-597.

111. Ohya, Y., et al., *Single L-Type Calcium Channels in Smooth Muscle Cells From Resistance Arteries of Spontaneously Hypertensive Rats.* Hypertension, 1998. **31**(5): p. 1125-1129.

112. Stevenson, W.G. and L.W. Stevenson, *Atrial Fibrillation in Heart Failure.* New England Journal of Medicine, 1999. **341**(12): p. 910-911.

113. Whipple GH, et al., *Reversible congestive heart failure due to chronic rapid stimulation of the normal heart.* Proc N Engl Cardiovasc Soc, 1962. **20**: p. 39-40.

114. Boyden, P., et al., *Mechanisms for atrial arrhythmias associated with cardiomyopathy: a study of feline hearts with primary myocardial disease.* Circulation, 1984. **69**(5): p. 1036-1047.

115. Power, J.M., et al., *Susceptibility to atrial fibrillation: a study in an ovine model of pacing-induced early heart failure.* J Cardiovasc Electrophysiol, 1998. **9**(4): p. 423-35.

116. Sanders, P., et al., *Electrical Remodeling of the Atria in Congestive Heart Failure.* Circulation, 2003. **108**(12): p. 1461-1468.

117. Steer, A.C., et al., *Systematic review of rheumatic heart disease prevalence in children in developing countries: The role of environmental factors.* Journal of Paediatrics and Child Health, 2002. **38**(3): p. 229-234.

118. John, B., et al., *Electrical remodelling of the left and right atria due to rheumatic mitral stenosis†.* European Heart Journal, 2008. **29**(18): p. 2234-2243.

119. Feinberg, W.M., et al., *Prevalence, age distribution, and gender of patients with atrial fibrillation: Analysis and implications.* Archives of Internal Medicine, 1995. **155**(5): p. 469-473.

120. Spach, M.S. and P.C. Dolber, *Relating extracellular potentials and their derivatives to anisotropic propagation at a microscopic level in human cardiac muscle. Evidence for electrical uncoupling of side-to-side fiber connections with increasing age.* Circulation Research, 1986. **58**(3): p. 356-71.

121. Kistler, P.M., et al., *Electrophysiologic and electroanatomic changes in the human atrium associated with age.* Journal of the American College of Cardiology, 2004. **44**(1): p. 109-116.

122. Roberts-Thomson, K.C., et al., *Fractionated atrial electrograms during sinus rhythm: Relationship to age, voltage, and conduction velocity.* Heart Rhythm. **6**(5): p. 587-591.

123. Krahn, A.D., et al., *The natural history of atrial fibrillation: Incidence, risk factors, and prognosis in the manitoba follow-up study.* The American Journal of Medicine, 1995. **98**(5): p. 476-484.

124. Sinno, H., et al., *Atrial Ischemia Promotes Atrial Fibrillation in Dogs.* Circulation, 2003. **107**(14): p. 1930-1936.

125. Jayachandran, J.V., et al., *Role of the Na+/H+ Exchanger in Short-Term Atrial Electrophysiological Remodeling.* Circulation, 2000. **101**(15): p. 1861-1866.

126. Miyauchi, Y., et al., *Altered Atrial Electrical Restitution and Heterogeneous Sympathetic Hyperinnervation in Hearts With Chronic Left Ventricular Myocardial Infarction: Implications for Atrial Fibrillation.* Circulation, 2003. **108**(3): p. 360-366.

127. Wanahita, N., et al., *Atrial fibrillation and obesity—results of a meta-analysis.* American Heart Journal, 2008. **155**(2): p. 310-315.

128. Munger, T.M., et al., *Electrophysiological and Hemodynamic Characteristics Associated With Obesity in Patients With Atrial Fibrillation.* Journal of the American College of Cardiology, 2012. **60**(9): p. 851-860.

129. Wong, C.X., et al., *Pericardial Fat Is Associated With Atrial Fibrillation Severity and Ablation Outcome.* Journal of the American College of Cardiology, 2011. **57**(17): p. 1745-1751.

130. Venteclef, N., et al., *Human epicardial adipose tissue induces fibrosis of the atrial myocardium through the secretion of adipo-fibrokines.* European Heart Journal, 2013.

131. Hatem, S.N. and P. Sanders, *Epicardial adipose tissue and atrial fibrillation.* Cardiovascular Research, 2014. **102**(2): p. 205-213.

132. Gami, A.S., et al., *Obstructive Sleep Apnea, Obesity, and the Risk of Incident Atrial Fibrillation.* Journal of the American College of Cardiology, 2007. **49**(5): p. 565-571.

133. Stevenson, I.H., et al., *Prevalence of sleep disordered breathing in paroxysmal and persistent atrial fibrillation patients with normal left ventricular function.* European Heart Journal, 2008. **29**(13): p. 1662-1669.

134. Ghias, M., et al., *The Role of Ganglionated Plexi in Apnea-Related Atrial Fibrillation.* Journal of the American College of Cardiology, 2009. **54**(22): p. 2075-2083.

135. Iwasaki, Y.-k., et al., *Determinants of atrial fibrillation in an animal model of obesity and acute obstructive sleep apnea.* Heart Rhythm. **9**(9): p. 1409-1416.e1.

136. Linz, D., et al., *Effect of Renal Denervation on Neurohumoral Activation Triggering Atrial Fibrillation in Obstructive Sleep Apnea.* Hypertension, 2013. **62**(4): p. 767-774.

137. Linz, D., et al., *Renal Sympathetic Denervation Suppresses Postapneic Blood Pressure Rises and Atrial Fibrillation in a Model for Sleep Apnea.* Hypertension, 2012. **60**(1): p. 172-178.

138. Murphy, J.G., et al., *Long-Term Outcome after Surgical Repair of Isolated Atrial Septal Defect.* New England Journal of Medicine, 1990. **323**(24): p. 1645-1650.

139. Gatzoulis, M.A., et al., *Atrial Arrhythmia after Surgical Closure of Atrial Septal Defects in Adults.* New England Journal of Medicine, 1999. **340**(11): p. 839-846.

140. Morton, J.B., et al., *Effect of Chronic Right Atrial Stretch on Atrial Electrical Remodeling in Patients With an Atrial Septal Defect.* Circulation, 2003. **107**(13): p. 1775-1782.

141. Roberts-Thomson, K.C., et al., *Left atrial remodeling in patients with atrial septal defects.* Heart rhythm : the official journal of the Heart Rhythm Society, 2009. **6**(7): p. 1000-1006.

142. Kalman, J.M. and P.B. Sparks, *Electrical remodeling of the atria as a consequence of atrial stretch.* J Cardiovasc Electrophysiol, 2001. **12**(1): p. 51-5.

143. Fraser, H.R. and R.W. Turner, *Auricular fibrillation; with special reference to rheumatic heart disease.* Br Med J, 1955. **2**(4953): p. 1414-8.

144. PROBST, P., N. GOLDSCHLAGER, and A. SELZER, *Left Atrial Size and Atrial Fibrillation in Mitral Stenosis: Factors Influencing Their Relationship.* Circulation, 1973. **48**(6): p. 1282-1287.

145. Vaziri, S., et al., *Echocardiographic predictors of nonrheumatic atrial fibrillation. The Framingham Heart Study.* Circulation, 1994. **89**(2): p. 724-730.

146. Vasan, R.S., et al., *Distribution and Categorization of Echocardiographic Measurements in Relation to Reference Limits : The Framingham Heart Study: Formulation of a Height- and Sex-Specific Classification and Its Prospective Validation.* Circulation, 1997. **96**(6): p. 1863-1873.

147. Psaty, B.M., et al., *Incidence of and Risk Factors for Atrial Fibrillation in Older Adults.* Circulation, 1997. **96**(7): p. 2455-2461.

148. Dittrich, H.C., et al., *Left atrial diameter in nonvalvular atrial fibrillation: An echocardiographic study. Stroke Prevention in Atrial Fibrillation Investigators.* Am Heart J, 1999. **137**(3): p. 494-9.

149. Suarez, G.S., et al., *Changes in left atrial size in patients with lone atrial fibrillation.* Clin Cardiol, 1991. **14**(8): p. 652-6.

150. Rostagno, C., et al., *Left atrial size changes in patients with paroxysmal lone atrial fibrillation. An echocardiographic follow-up.* Angiology, 1996. **47**(8): p. 797-801.

151. Villecco, A.S., et al., *Left atrial size in paroxysmal atrial fibrillation: echocardiographic evaluation and follow-up.* Cardiology, 1992. **80**(2): p. 89-93.

152. SOLTI, F., et al., *The effect of atrial dilatation on the genesis of atrial arrhythmias.* Cardiovascular Research, 1989. **23**(10): p. 882-886.

153. Wijffels, M.C.E.F., et al., *Electrical Remodeling due to Atrial Fibrillation in Chronically Instrumented Conscious Goats : Roles of Neurohumoral Changes, Ischemia, Atrial Stretch, and High Rate of Electrical Activation.* Circulation, 1997. **96**(10): p. 3710-3720.

154. Satoh, T. and D.P. Zipes, *Unequal atrial stretch in dogs increases dispersion of refractoriness conducive to developing atrial fibrillation.* J Cardiovasc Electrophysiol, 1996. **7**(9): p. 833-42.

155. SIDERIS, D.A., et al., *Some observations on the mechanism of pressure related atrial fibrillation.* European Heart Journal, 1994. **15**(11): p. 1585-1589.

156. Ravelli, F. and M. Allessie, *Effects of Atrial Dilatation on Refractory Period and Vulnerability to Atrial Fibrillation in the Isolated Langendorff-Perfused Rabbit Heart.* Circulation, 1997. **96**(5): p. 1686-1695.

157. Zarse, M., et al., *Verapamil prevents stretch-induced shortening of atrial effective refractory period in langendorff-perfused rabbit heart.* J Cardiovasc Electrophysiol, 2001. **12**(1): p. 85-92.

158. Boyden, P. and B. Hoffman, *The effects on atrial electrophysiology and structure of surgically induced right atrial enlargement in dogs.* Circulation Research, 1981. **49**(6): p. 1319-1331.

159. Boyden, P.A., et al., *Effects of left atrial enlargement on atrial transmembrane potentials and structure in dogs with mitral valve fibrosis.* Am J Cardiol, 1982. **49**(8): p. 1896-908.

160. Neuberger, H.-R., et al., *Development of a Substrate of Atrial Fibrillation During Chronic Atrioventricular Block in the Goat.* Circulation, 2005. **111**(1): p. 30-37.

161. Calkins, H., et al., *Effect of the atrioventricular relationship on atrial refractoriness in humans.* Pacing Clin Electrophysiol, 1992. **15**(5): p. 771-8.

162. Calkins, H., et al., *Effects of an acute increase in atrial pressure on atrial refractoriness in humans.* Pacing Clin Electrophysiol, 1992. **15**(11 Pt 1): p. 1674-80.

163. Tse, H.F., et al., *Effects of simultaneous atrioventricular pacing on atrial refractoriness and atrial fibrillation inducibility: role of atrial mechanoelectrical feedback.* J Cardiovasc Electrophysiol, 2001. **12**(1): p. 43-50.

164. Klein, L., W. Miles, and D. Zipes, *Effect of atrioventricular interval during pacing or reciprocating tachycardia on atrial size, pressure, and refractory period. Contraction-excitation feedback in human atrium.* Circulation, 1990. **82**(1): p. 60-68.

165. Chen, Y.J., et al., *Inducibility of atrial fibrillation during atrioventricular pacing with varying intervals: role of atrial electrophysiology and the autonomic nervous system.* J Cardiovasc Electrophysiol, 1999. **10**(12): p. 1578-85.

166. Nazir, S.A. and M.J. Lab, *Mechanoelectric feedback in the atrium of the isolated guinea-pig heart.* Cardiovascular Research, 1996. **32**(1): p. 112-119.

167. Nazir, S.A., *Mechanoelectric feedback and atrial arrhythmias*, University of London.

168. Tavi, P., M. Laine, and M. Weckstrom, *Effect of gadolinium on stretch-induced changes in contraction and intracellularly recorded action- and afterpotentials of rat isolated atrium.* Br J Pharmacol, 1996. **118**(2): p. 407-13.

169. Kelly, D., et al., *GENE EXPRESSION OF STRETCH-ACTIVATED CHANNELS AND MECHANOELECTRIC FEEDBACK IN THE HEART.* Clinical and Experimental Pharmacology and Physiology, 2006. **33**(7): p. 642-648.

170. Kim, D., *A mechanosensitive K+ channel in heart cells. Activation by arachidonic acid.* J Gen Physiol, 1992. **100**(6): p. 1021-40.

171. Kim, D., *Novel cation-selective mechanosensitive ion channel in the atrial cell membrane.* Circulation Research, 1993. **72**(1): p. 225-231.

172. Mitchell, G.F., et al., *PUlse pressure and risk of new-onset atrial fibrillation.* JAMA, 2007. **297**(7): p. 709-715.

173. Sakuragi, S. and W.P. Abhayaratna, *Arterial stiffness: Methods of measurement, physiologic determinants and prediction of cardiovascular outcomes.* International Journal of Cardiology. **138**(2): p. 112-118.

174. Lau, D.H., et al., *Aortic Stiffness in Lone Atrial Fibrillation: A Novel Risk Factor for Arrhythmia Recurrence.* PLoS ONE, 2013. **8**(10): p. e76776.

175. Lee, S.H., et al., *Effects of atrial fibrillation on arterial stiffness in patients with hypertension.* Angiology, 2008. **59**(4): p. 459-63.

176. Reiffel, J.A., *Is arterial stiffness a contributing factor to atrial fibrillation in patients with hypertension? A preliminary investigation.* American Journal of Hypertension, 2004. **17**(3): p. 213-216.

177. Chamberlain, A.M., et al., *Smoking and incidence of atrial fibrillation: Results from the Atherosclerosis Risk in Communities (ARIC) Study.* Heart Rhythm. **8**(8): p. 1160-1166.

178. Pawar, P.P., et al., *Association between smoking and outcomes in older adults with atrial fibrillation.* Archives of Gerontology and Geriatrics. **55**(1): p. 85-90.

179. Albertsen, I.E., et al., *The impact of smoking on thromboembolism and mortality in patients with incident atrial fibrillation: Insights from the danish diet, cancer, and health study.* Chest, 2014. **145**(3): p. 559-566.

180. Al-Sarraf, N., et al., *The risk of arrhythmias following coronary artery bypass surgery: do smokers have a paradox effect?* Interactive CardioVascular and Thoracic Surgery, 2010. **11**(5): p. 550-555.

181. Larsson, S.C., N. Drca, and A. Wolk, *Alcohol Consumption and Risk of Atrial Fibrillation: A Prospective Study and Dose-Response Meta-Analysis.* Journal of the American College of Cardiology, 2014. **64**(3): p. 281-289.

182. Sano, F., et al., *Heavy Alcohol Consumption and Risk of Atrial Fibrillation*

– The Circulatory Risk in Communities Study (CIRCS) &ndash. Circulation Journal, 2014. **78**(4): p. 955-961.

183. Djoussé, L., et al., *Long-term alcohol consumption and the risk of atrial fibrillation in the Framingham Study.* American journal of Cardiology. **93**(6): p. 710-713.

184. Ariansen, I., et al., *Impact of alcohol habits and smoking on the risk of new-onset atrial fibrillation in hypertensive patients with ECG left ventricular hypertrophy: The LIFE Study.* Blood Pressure, 2012. **21**(1): p. 6-11.

185. Overvad, T.F., et al., *Alcohol intake and prognosis of atrial fibrillation.* Heart, 2013. **99**(15): p. 1093-1099.

186. Mandyam, M.C., et al., *Alcohol and Vagal Tone as Triggers for Paroxysmal Atrial Fibrillation.* American journal of Cardiology. **110**(3): p. 364-368.

187. John, B., et al., *Reverse Remodeling of the Atria After Treatment of Chronic Stretch in Humans: Implications for the Atrial Fibrillation Substrate.* Journal of the American College of Cardiology, 2010. **55**(12): p. 1217-1226.

188. Abed, H.S., et al., *Effect of weight reduction and cardiometabolic risk factor management on symptom burden and severity in patients with atrial fibrillation: A randomized clinical trial.* JAMA, 2013. **310**(19): p. 2050-2060.

189. Li, D., et al., *Effects of Angiotensin-Converting Enzyme Inhibition on the Development of the Atrial Fibrillation Substrate in Dogs With Ventricular Tachypacing–Induced Congestive Heart Failure.* Circulation, 2001. **104**(21): p. 2608-2614.

190. Yamashita, T., et al., *Randomized trial of angiotensin II-receptor blocker vs. dihydropiridine calcium channel blocker in the treatment of paroxysmal atrial fibrillation with hypertension (J-RHYTHM II Study).* Europace, 2011. **13**(4): p. 473-479.

191. Kumagai, K., et al., *Effects of angiotensin II type 1 receptor antagonist on electrical and structural remodeling in atrial fibrillation.* Journal of the American College of Cardiology, 2003. **41**(12): p. 2197-2204.

192. Ausma, J., et al., *Reverse Structural and Gap-Junctional Remodeling After Prolonged Atrial Fibrillation in the Goat.* Circulation, 2003. **107**(15): p. 2051-2058.

193. Everett, T.H., et al., *Electrical, morphological, and ultrastructural remodeling and reverse remodeling in a canine model of chronic atrial fibrillation.* Circulation, 2000. **102**(12): p. 1454-1460.

194. Fan, K., et al., *Internal Cardioversion of Chronic Atrial Fibrillation During Percutaneous Mitral Commissurotomy.* Circulation, 2002. **105**(23): p. 2746-2752.

195. Soylu, M., et al., *Evaluation of atrial refractoriness immediately after percutaneous mitral balloon commissurotomy in patients with mitral stenosis and sinus rhythm.* American Heart Journal, 2004. **147**(4): p. 741-745.

196. Hansson, L., et al., *Randomised trial of old and new antihypertensive drugs in elderly patients: cardiovascular mortality and morbidity the Swedish Trial in Old Patients with Hypertension-2 study.* The Lancet, 1999. **354**(9192): p. 1751-1756.

197. Disertori, M., et al., *Valsartan for prevention of recurrent atrial fibrillation.* N Engl J Med, 2009. **360**(16): p. 1606-17.

198. Murray, K.T., et al., *Inhibition of angiotensin II signaling and recurrence of atrial fibrillation in AFFIRM.* Heart Rhythm, 2004. **1**(6): p. 669-75.

199. Yamashita, T., et al., *Randomized trial of angiotensin II-receptor blocker vs. dihydropiridine calcium channel blocker in the treatment of paroxysmal atrial fibrillation with hypertension (J-RHYTHM II study).* Europace, 2011. **13**(4): p. 473-9.

200. Du, H., et al., *Effect of nifedipine versus telmisartan on prevention of atrial fibrillation recurrence in hypertensive patients.* Hypertension, 2013. **61**(4): p. 786-92.

201. Fogari, R., et al., *Effect of telmisartan on paroxysmal atrial fibrillation recurrence in hypertensive patients with normal or increased left atrial size.* Clin Cardiol, 2012. **35**(6): p. 359-64.

202. Ruknudin, A., F. Sachs, and J.O. Bustamante, *Stretch-activated ion channels in tissue-cultured chick heart.* American Journal of Physiology - Heart and Circulatory Physiology, 1993. **264**(3): p. H960-H972.

203. Hagiwara, N., et al., *Stretch-activated anion currents of rabbit cardiac myocytes.* The Journal of Physiology, 1992. **456**(1): p. 285-302.

204. Kimura, S., et al., *Role of mineralocorticoid receptor on atrial structural remodeling and inducibility of atrial fibrillation in hypertensive rats.* Hypertens Res, 2005. **34**(5): p. 584-591.

205. Ji, X., et al., *Renoprotective mechanisms of pirfenidone in hypertension-induced renal injury: through anti-fibrotic and anti-oxidative stress pathways.* Biomedical Research, 2013. **34**(6): p. 309-319.

206. Wang, Y., et al., *Pirfenidone attenuates cardiac fibrosis in a mouse model of TAC-induced left ventricular remodeling by suppressing NLRP3 inflammasome formation.* Cardiology, 2013. **126**(1): p. 1-11.

207. Yamazaki, T., et al., *The antifibrotic agent pirfenidone inhibits angiotensin II-induced cardiac hypertrophy in mice.* Hypertens Res, 2012. **35**(1): p. 34-40.

208. Mirkovic, S., et al., *Attenuation of cardiac fibrosis by pirfenidone and amiloride in DOCA-salt hypertensive rats.* British Journal of Pharmacology, 2002. **135**(4): p. 961-968.

209. Lee, K.W., et al., *Pirfenidone Prevents the Development of a Vulnerable Substrate for Atrial Fibrillation in a Canine Model of Heart Failure.* Circulation, 2006. **114**(16): p. 1703-1712.

210. Yamazaki, T., et al., *The antifibrotic agent pirfenidone inhibits angiotensin II-induced cardiac hypertrophy in mice.* Hypertens Res, 2011.

211. Adam, O., et al., *Rac1-Induced Connective Tissue Growth Factor Regulates Connexin 43 and N-Cadherin Expression in Atrial Fibrillation.* Journal of the American College of Cardiology, 2010. **55**(5): p. 469-480.

212. Martin, J., et al., *Tranilast attenuates cardiac matrix deposition in experimental diabetes: role of transforming growth factor-Î².* Cardiovascular Research, 2005. **65**(3): p. 694-701.

213. Kelly, D.J., et al., *Tranilast Attenuates Structural and Functional Aspects of Renal Injury in the Remnant Kidney Model.* Journal of the American Society of Nephrology, 2004. **15**(10): p. 2619-2629.

214. Hocher, B., et al., *Inhibition of left ventricular fibrosis by tranilast in rats with renovascular hypertension.* J Hypertens, 2002. **20**(4): p. 745-51.

215. Kagitani, S., et al., *Tranilast attenuates myocardial fibrosis in association with suppression of monocyte/macrophage infiltration in DOCA/salt hypertensive rats.* Journal of Hypertension, 2004. **22**(5): p. 1007-1015.

216. Nakatani, Y., et al., *Tranilast Prevents Atrial Remodeling and Development of Atrial Fibrillation in a Canine Model of Atrial Tachycardia and Left Ventricular Dysfunction.* Journal of the American College of Cardiology, 2013. **61**(5): p. 582-588.

217. Lau, D.H., et al., *Atrial protective effects of n-3 polyunsaturated fatty acids: A long-term study in ovine chronic heart failure.* Heart Rhythm, 2011. **8**(4): p. 575-582.

218. Parikh, A., et al., *Relaxin Suppresses Atrial Fibrillation by Reversing Fibrosis and Myocyte Hypertrophy and Increasing Conduction Velocity and Sodium Current in Spontaneously Hypertensive Rat Hearts.* Circulation Research, 2013. **113**(3): p. 313-321.

219. Fuenmayor A, A.J., et al., *Inter-atrial conduction time shortens after blood pressure control in hypertensive patients with left ventricular hypertrophy.* International Journal of Cardiology, 2005. **102**(3): p. 443-446.

220. Celik, T., et al., *The comparative effects of telmisartan and ramipril on P-wave dispersion in hypertensive patients: A randomized clinical study.* Clinical Cardiology, 2005. **28**(6): p. 298-302.

221. Ehrlich, J.R., S.H. Hohnloser, and S. Nattel, *Role of angiotensin system and effects of its inhibition in atrial fibrillation: clinical and experimental evidence.* European Heart Journal, 2006. **27**(5): p. 512-518.

222. Conen, D., et al., *Influence of Systolic and Diastolic Blood Pressure on the Risk of Incident Atrial Fibrillation in Women.* Circulation, 2009. **119**(16): p. 2146-2152.

223. Chobanian, A.V., *The Hypertension Paradox — More Uncontrolled Disease despite Improved Therapy.* New England Journal of Medicine, 2009. **361**(9): p. 878-887.

224. John, B., et al., *Reverse remodeling of the atria after treatment of chronic stretch in humans: implications for the atrial fibrillation substrate.* J Am Coll Cardiol, 2010. **55**(12): p. 1217-26.

225. Abed, H.S., et al., *Effect of weight reduction and cardiometabolic risk factor management on symptom burden and severity in patients with atrial fibrillation: a randomized clinical trial.* JAMA, 2013. **310**(19): p. 2050-60.

226. Kumagai, K., et al., *Effects of angiotensin II type 1 receptor antagonist on electrical and structural remodeling in atrial fibrillation.* J Am Coll Cardiol, 2003. **41**(12): p. 2197-204.

227. Ausma, J., et al., *Reverse structural and gap-junctional remodeling after prolonged atrial fibrillation in the goat.* Circulation, 2003. **107**(15): p. 2051-8.

228. Anné, W., et al., *Self-terminating AF depends on electrical remodeling while persistent AF depends on additional structural changes in a rapid atrially paced sheep model.* Journal of Molecular and Cellular Cardiology, 2007. **43**(2): p. 148-158.

229. Wang, Z.G., B. Fermini, and S. Nattel, *Repolarization differences between guinea pig atrial endocardium and epicardium: evidence for a role of Ito.* American Journal of Physiology - Heart and Circulatory Physiology, 1991. **260**(5): p. H1501-H1506.

230. Verheule, S., et al., *Loss of Continuity in the Thin Epicardial Layer Because of Endomysial Fibrosis Increases the Complexity of Atrial Fibrillatory Conduction.* Circulation: Arrhythmia and Electrophysiology, 2013. **6**(1): p. 202-211.

231. Lau, D.H., et al., *Short-term hypertension is associated with the development of atrial fibrillation substrate: A study in an ovine hypertensive model.* Heart Rhythm, 2010. **7**(3): p. 396-404.

232. Haefliger, J.-A., et al., *Connexin43-dependent mechanism modulates renin secretion and hypertension.* The Journal of Clinical Investigation, 2006. **116**(2): p. 405-413.

233. Sasano, C., et al., *Internalization and Dephosphorylation of Connexin43 in Hypertrophied Right Ventricles of Rats With Pulmonary Hypertension.* Circulation Journal, 2007. **71**(3): p. 382-389.

234. Morikawa, H., et al., *Expression of connective tissue growth factor in the human liver with idiopathic portal hypertension.* Mol Med, 2007. **13**(5-6): p. 240-5.

235. Recchia, A.G., et al., *Endothelin-1 induces connective tissue growth factor expression in cardiomyocytes.* Journal of Molecular and Cellular Cardiology, 2009. **46**(3): p. 352-59.

236. Liu, X., et al., *Trimetazidine inhibits pressure overload-induced cardiac fibrosis through NADPH oxidase–ROS–CTGF pathway.* Cardiovascular Research, 2010. **88**(1): p. 150-158.

237. L'Allier, P.L., et al., *Angiotensin-converting enzyme inhibition in hypertensive patients is associated with a reduction in the occurrence of atrial fibrillation.* Journal of the American College of Cardiology, 2004. **44**(1): p. 159-164.

238. Healey, J.S., et al., *Prevention of Atrial Fibrillation With Angiotensin-Converting Enzyme Inhibitors and Angiotensin Receptor BlockersA Meta-Analysis.* Journal of the American College of Cardiology, 2005. **45**(11): p. 1832-1839.

239. Bacova, B., et al., *Up-regulation of myocardial connexin-43 in spontaneously hypertensive rats fed red palm oil is most likely implicated in its anti-arrhythmic effects.* Canadian Journal of Physiology and Pharmacology, 2012. **90**(9): p. 1235-1245.

240. *Valsartan for Prevention of Recurrent Atrial Fibrillation.* New England Journal of Medicine, 2009. **360**(16): p. 1606-1617.

241. Murray, K.T., et al., *Inhibition of angiotensin II signaling and recurrence of atrial fibrillation in AFFIRM.* Heart Rhythm. **1**(6): p. 669-675.

242. Du, H., et al., *Effect of Nifedipine Versus Telmisartan on Prevention of Atrial Fibrillation Recurrence in Hypertensive Patients.* Hypertension, 2013. **61**(4): p. 786-792.

243. Fogari, R., et al., *Effect of Telmisartan on Paroxysmal Atrial Fibrillation Recurrence in Hypertensive Patients With Normal or Increased Left Atrial Size.* Clinical Cardiology, 2012. **35**(6): p. 359-364.

244. Silke, B., *Beta-blockade in CHF: pathophysiological considerations.* European Heart Journal Supplements, 2006. **8**(suppl C): p. C13-C18.

245. Udelson, J.E., *Ventricular remodeling in heart failure and the effect of β-blockade.* American journal of Cardiology, 2004. **93**(9): p. 43-48.

246. Lau, D.H., et al., *Characterization of cardiac remodeling in a large animal "one-kidney, one-clip" hypertensive model.* Blood Press, 2010. **19**(2): p. 119-25.

247. Grigioni, F., et al., *Atrial fibrillation complicating the course of degenerative mitral regurgitation: Determinants and long-term outcome.* J Am Coll Cardiol, 2002. **40**(1): p. 84-92.

248. Kanagala, R., et al., *Obstructive Sleep Apnea and the Recurrence of Atrial Fibrillation.* Circulation, 2003. **107**(20): p. 2589-2594.

249. Chalfoun, N., et al., *Reverse Electrical Remodeling of the Atria Post Cardioversion in Patients Who Remain in Sinus Rhythm Assessed by Signal Averaging of the P-Wave.* Pacing and Clinical Electrophysiology, 2007. **30**(4): p. 502-509.

250. Mangrum, J.M., et al., *The effects of reverse atrial electrical remodeling on atrial defibrillation thresholds.* Pacing Clin Electrophysiol, 2002. **25**(4 Pt 1): p. 470-6.

251. Yoshida, K., et al., *Electrogram organization predicts left atrial reverse remodeling after the restoration of sinus rhythm by catheter ablation in patients with persistent*

atrial fibrillation. Heart rhythm : the official journal of the Heart Rhythm Society, 2012. **9**(11): p. 1769-1778.

252. Jahnke, C., et al., *Serial monitoring of reverse left-atrial remodeling after pulmonary vein isolation in patients with atrial fibrillation: A magnetic resonance imaging study.* International Journal of Cardiology, 2011. **153**(1): p. 42-46.

253. Hocini, M., et al., *Reverse Remodeling of Sinus Node Function After Catheter Ablation of Atrial Fibrillation in Patients With Prolonged Sinus Pauses.* Circulation, 2003. **108**(10): p. 1172-1175.

254. Cho, D.-K., et al., *Factors Determining Early Left Atrial Reverse Remodeling After Mitral Valve Surgery.* The American Journal of Cardiology, 2008. **101**(3): p. 374-377.

255. De Bonis, M., et al., *Recurrence of Mitral Regurgitation Parallels the Absence of Left Ventricular Reverse Remodeling After Mitral Repair in Advanced Dilated Cardiomyopathy.* The Annals of thoracic surgery, 2008. **85**(3): p. 932-939.

256. Vieira, M.L., et al., *Left atrium reverse remodeling in patients with mitral valve stenosis after percutaneous valvuloplasty: a 2- and 3-dimensional echocardiographic study.* Rev Esp Cardiol (Engl Ed), 2013. **66**(1): p. 17-23.

257. Goldblatt, H., et al., *Studies on experimental hypertension: The production of persistent elevation of systolic blood pressure by means of renal ischemia.* The Journal of Experimental Medicine, 1934. **59**(3): p. 347-379.

258. Kojodjojo, P., et al., *Age-Related Changes in Human Left and Right Atrial Conduction.* Journal of Cardiovascular Electrophysiology, 2006. **17**(2): p. 120-127.

259. Wijffels, M.C.E.F., et al., *Widening of the Excitable Gap During Pharmacological Cardioversion of Atrial Fibrillation in the Goat: Effects of Cibenzoline, Hydroquinidine, Flecainide, and d-Sotalol.* Circulation, 2000. **102**(2): p. 260-267.

260. Lammers, W.J., et al., *Quantification of spatial inhomogeneity in conduction and initiation of reentrant atrial arrhythmias.* American Journal of Physiology - Heart and Circulatory Physiology, 1990. **259**(4): p. H1254-H1263.

261. Stiles, M.K., et al., *The Effect of Electrogram Duration on Quantification of Complex Fractionated Atrial Electrograms and Dominant Frequency.* Journal of Cardiovascular Electrophysiology, 2008. **19**(3): p. 252-258.

262. Lau, D.H., et al., *Hypertension and atrial fibrillation: evidence of progressive atrial remodeling with electrostructural correlate in a conscious chronically instrumented ovine model.* Heart Rhythm, 2010. **7**(9): p. 1282-90.

263. Choisy, S.C., et al., *Increased susceptibility to atrial tachyarrhythmia in spontaneously hypertensive rat hearts.* Hypertension, 2007. **49**(3): p. 498-505.

264. Marsan, N.A., et al., *Left atrial reverse remodeling and functional improvement after mitral valve repair in degenerative mitral regurgitation: A real-time 3-dimensional echocardiography study.* American Heart Journal, 2011. **161**(2): p. 314-321.

265. Nademanee, K., et al., *A new approach for catheter ablation of atrial fibrillation: mapping of the electrophysiologic substrate.* Journal of the American College of Cardiology, 2004. **43**(11): p. 2044-2053.

266. Rostock, T., et al., *High-density activation mapping of fractionated electrograms in the atria of patients with paroxysmal atrial fibrillation.* Heart rhythm : the official journal of the Heart Rhythm Society, 2006. **3**(1): p. 27-34.

267. Berenfeld, O., et al., *Spatially distributed dominant excitation frequencies reveal hidden organization in atrial fibrillation in the Langendorff-perfused sheep heart.* J Cardiovasc Electrophysiol, 2000. **11**(8): p. 869-79.

268. Sanders, P., et al., *Spectral Analysis Identifies Sites of High-Frequency Activity Maintaining Atrial Fibrillation in Humans.* Circulation, 2005. **112**(6): p. 789-797.

269. Martins, R.P., et al., *Dominant Frequency Increase Rate Predicts Transition from Paroxysmal to Long-Term Persistent Atrial Fibrillation.* Circulation, 2014. **129**(14): p. 1472-1482.

270. Burstein, B. and S. Nattel, *Atrial Fibrosis: Mechanisms and Clinical Relevance in Atrial Fibrillation.* Journal of the American College of Cardiology, 2008. **51**(8): p. 802-809.

271. Boldt, A., et al., *Fibrosis in left atrial tissue of patients with atrial fibrillation with and without underlying mitral valve disease.* Heart, 2004. **90**(4): p. 400-405.

272. Kato, T., et al., *What are Arrhythmogenic Substrates in Diabetic Rat Atria?* Journal of Cardiovascular Electrophysiology, 2006. **17**(8): p. 890-894.

273. Shigeki, S., et al., *Treatment of keloid and hypertrophic scars by iontophoretic transdermal delivery of tranilast.* Scand J Plast Reconstr Surg Hand Surg, 1997. **31**(2): p. 151-8.

274. Taniguchi, S., T. Yorifuji, and T. Hamada, *Treatment of linear localized scleroderma with the anti-allergic drug, tranilast.* Clinical and Experimental Dermatology, 1994. **19**(5): p. 391-393.

275. Suzawa, H., et al., *The Mechanism Involved in the Inhibitory Action of Tranilast on Collagen Biosynthesis of Keloid Fibroblasts.* The Japanese Journal of Pharmacology, 1992. **60**(2): p. 91-96.

276. Shimizu, T., et al., *Suppression of Matrix Metalloproteinase Production in Nasal Fibroblasts by Tranilast, an Antiallergic Agent, In Vitro.* Mediators of Inflammation, 2005. **2005**(3): p. 150-159.

277. Eckstein, J., et al., *Time course and mechanisms of endo-epicardial electrical dissociation during atrial fibrillation in the goat.* Cardiovascular Research, 2011. **89**(4): p. 816-824.

278. Ward, M.R., et al., *Inhibitory effects of tranilast on expression of transforming growth factor-β isoforms and receptors in injured arteries.* Atherosclerosis. **137**(2): p. 267-275.

279. Pinto, Y.M., et al., *Reduction in Left Ventricular Messenger RNA for Transforming Growth Factor β1 Attenuates Left Ventricular Fibrosis and Improves Survival Without Lowering Blood Pressure in the Hypertensive TGR(mRen2)27 Rat.* Hypertension, 2000. **36**(5): p. 747-754.

280. Botto, G.L., et al., *Temporal Variability of Atrial Fibrillation in Pacemaker Recipients for Bradycardia: Implications for Crossover Designed Trials, Study Sample Size, and Identification of Responder Patients by Means of Arrhythmia Burden.* J Cardiovasc Electrophysiol, 2007. **18**(3): p. 250-257.

281. Kabra, R. and J.P. Singh, *Catheter ablation targeting complex fractionated atrial electrograms for the control of atrial fibrillation.* Current Opinion in Cardiology, 2012. **27**(1): p. 49-54 10.1097/HCO.0b013e32834dc3bc.

282. Iriki, Y., et al., *Relationship between clinical outcomes and unintentional pulmonary vein isolation during substrate ablation of atrial fibrillation guided solely by complex*

fractionated atrial electrogram mapping. Journal of cardiology, 2011. **58**(3): p. 278-286.

283. Nademanee, K., et al., *Clinical Outcomes of Catheter Substrate Ablation for High-Risk Patients With Atrial Fibrillation.* Journal of the American College of Cardiology, 2008. **51**(8): p. 843-849.

284. Oral, H., et al., *Radiofrequency Catheter Ablation of Chronic Atrial Fibrillation Guided by Complex Electrograms.* Circulation, 2007. **115**(20): p. 2606-2612.

285. Hayward, R.M., et al., *Pulmonary vein isolation with complex fractionated atrial electrogram ablation for paroxysmal and nonparoxysmal atrial fibrillation: A meta-analysis.* Heart Rhythm. **8**(7): p. 994-1000.

286. Takahashi, Y., et al., *Organization of Frequency Spectra of Atrial Fibrillation: Relevance to Radiofrequency Catheter Ablation.* Journal of Cardiovascular Electrophysiology, 2006. **17**(4): p. 382-388.

287. Verma, A., et al., *Relationship Between Complex Fractionated Electrograms (CFE) and Dominant Frequency (DF) Sites and Prospective Assessment of Adding DF-Guided Ablation to Pulmonary Vein Isolation in Persistent Atrial Fibrillation (AF).* Journal of Cardiovascular Electrophysiology, 2011. **22**(12): p. 1309-1316.

288. Scherr, D., et al., *Automated detection and characterization of complex fractionated atrial electrograms in human left atrium during atrial fibrillation.* Heart rhythm : the official journal of the Heart Rhythm Society, 2007. **4**(8): p. 1013-1020.

289. Aizer, A., et al., *Standardization and validation of an automated algorithm to identify fractionation as a guide for atrial fibrillation ablation.* Heart rhythm : the official journal of the Heart Rhythm Society, 2008. **5**(8): p. 1134-1141.

290. Porter, M., et al., *Prospective study of atrial fibrillation termination during ablation guided by automated detection of fractionated electrograms.* J Cardiovasc Electrophysiol, 2008. **19**(6): p. 613-20.

291. Stiles, M.K., et al., *High-Density Mapping of Atrial Fibrillation in Humans: Relationship Between High-Frequency Activation and Electrogram Fractionation.* J Cardiovasc Electrophysiol, 2008. **19**(12): p. 1245-1253.

292. Lin, Y.-J., et al., *Consistency of complex fractionated atrial electrograms during atrial fibrillation.* Heart rhythm : the official journal of the Heart Rhythm Society, 2008. **5**(3): p. 406-412.

293. Roux, J.-F., et al., *Complex Fractionated Electrogram Distribution and Temporal Stability in Patients Undergoing Atrial Fibrillation Ablation.* J Cardiovasc Electrophysiol, 2008. **19**(8): p. 815-820.

294. Monir, G. and S.J. Pollak, *Consistency of the CFAE Phenomena Using Custom Software for Automated Detection of Complex Fractionated Atrial Electrograms (CFAEs) in the Left Atrium During Atrial Fibrillation.* J Cardiovasc Electrophysiol, 2008. **19**(9): p. 915-919.

295. Calo, L., et al., *Diagnostic Accuracy of a New Software for Complex Fractionated Electrograms Identification in Patients with Persistent and Permanent Atrial Fibrillation.* J Cardiovasc Electrophysiol, 2008. **19**(10): p. 1024-1030.

296. Scherr, D., et al., *Long- and Short-Term Temporal Stability of Complex Fractionated Atrial Electrograms in Human Left Atrium During Atrial Fibrillation.* J Cardiovasc Electrophysiol, 2009. **20**(1): p. 13-21.

297. Verma, A., et al., *Spatial and Temporal Stability of Complex Fractionated Electrograms in Patients with Persistent Atrial Fibrillation over Longer Time Periods: Relationship to Local Electrogram Cycle Length.* Heart rhythm : the official journal of the Heart Rhythm Society, 2008. **5**(8): p. 1127-1133.

298. Habel, N., et al., *The temporal variability of dominant frequency and complex fractionated atrial electrograms constrains the validity of sequential mapping in human atrial fibrillation.* Heart Rhythm, 2010. **7**(5): p. 586-593.

299. Konings, K.T.S., et al., *Configuration of Unipolar Atrial Electrograms During Electrically Induced Atrial Fibrillation in Humans.* Circulation, 1997. **95**(5): p. 1231-1241.

300. Konings, K.T., et al., *High-density mapping of electrically induced atrial fibrillation in humans.* Circulation, 1994. **89**(4): p. 1665-80.

301. Roberts-Thomson, K.C., et al., *The role of chronic atrial stretch and atrial fibrillation on posterior left atrial wall conduction.* Heart Rhythm, 2009. **6**(8): p. 1109-1117.

302. Tanaka, K., et al., *Spatial Distribution of Fibrosis Governs Fibrillation Wave Dynamics in the Posterior Left Atrium During Heart Failure.* Circulation Research, 2007. **101**(8): p. 839-847.

303. Sanders, P., et al., *Spectral analysis identifies sites of high-frequency activity maintaining atrial fibrillation in humans.* Circulation, 2005. **112**(6): p. 789-797.

304. Ryu, K., et al., *Mapping of Atrial Activation During Sustained Atrial Fibrillation in Dogs with Rapid Ventricular Pacing Induced Heart Failure: Evidence for a Role of Driver Regions.* Journal of Cardiovascular Electrophysiology, 2005. **16**(12): p. 1348-1358.

305. Skanes, A.C., et al., *Spatiotemporal periodicity during atrial fibrillation in the isolated sheep heart.* Circulation, 1998. **98**(12): p. 1236-1248.

306. Lee, G., et al., *Relationship among complex signals, short cycle length activity, and dominant frequency in patients with long-lasting persistent AF: a high-density epicardial mapping study in humans.* Heart Rhythm, 2011. **8**(11): p. 1714-9.

307. Stiles, M.K., et al., *High-density mapping of atrial fibrillation in humans: relationship between high-frequency activation and electrogram fractionation.* J Cardiovasc Electrophysiol, 2008. **19**(12): p. 1245-53.

308. Brooks, A.G., et al., *Outcomes of long-standing persistent atrial fibrillation ablation: a systematic review.* Heart Rhythm, 2010. **7**(6): p. 835-46.

309. Verma, A., et al., *Relationship between complex fractionated electrograms (CFE) and dominant frequency (DF) sites and prospective assessment of adding DF-guided ablation to pulmonary vein isolation in persistent atrial fibrillation (AF).* J Cardiovasc Electrophysiol, 2011. **22**(12): p. 1309-16.

310. Li, W.J., et al., *Additional ablation of complex fractionated atrial electrograms after pulmonary vein isolation in patients with atrial fibrillation: a meta-analysis.* Circ Arrhythm Electrophysiol, 2011. **4**(2): p. 143-8.

311. Hayward, R.M., et al., *Pulmonary vein isolation with complex fractionated atrial electrogram ablation for paroxysmal and nonparoxysmal atrial fibrillation: A meta-analysis.* Heart Rhythm, 2011. **8**(7): p. 994-1000.

312. Teh, A.W., et al., *The relationship between complex fractionated electrograms and atrial low-voltage zones during atrial fibrillation and paced rhythm.* Europace, 2011. **13**(12): p. 1709-16.

313. Narayan, S.M., et al., *Classifying fractionated electrograms in human atrial fibrillation using monophasic action potentials and activation mapping: evidence for localized drivers, rate acceleration, and nonlocal signal etiologies.* Heart Rhythm, 2011. **8**(2): p. 244-53.

314. Lau, D.H., et al., *Stability of complex fractionated atrial electrograms: a systematic review.* J Cardiovasc Electrophysiol, 2012. **23**(9): p. 980-7.

315. Lau, D.H., et al., *Catheter Ablation Targeting Complex Fractionated Atrial Electrogram in Atrial Fibrillation.* J Atr Fibrillation, 2013. **6**(3): p. 86-92.

316. de Groot, N.M., et al., *Electropathological substrate of longstanding persistent atrial fibrillation in patients with structural heart disease: epicardial breakthrough.* Circulation, 2010. **122**(17): p. 1674-82.

317. Zlochiver, S., et al., *Rotor meandering contributes to irregularity in electrograms during atrial fibrillation.* Heart Rhythm., 2008. **5**(6): p. 846-854.

318. Holm, M., et al., *Epicardial right atrial free wall mapping in chronic atrial fibrillation. Documentation of repetitive activation with a focal spread--a hitherto unrecognised phenomenon in man.* Eur Heart J, 1997. **18**(2): p. 290-310.